ALMA MATER STUDIORUM - UNIVERSITÀ DI BOLOGNA

SCUOLA DI INGEGNERIA E ARCHITETTURA

DIPARTIMENTO DI INGEGNERIA INDUSTRIALE
DIN

CORSO DI LAUREA IN INGEGNERIA EDILE ARCHITETTURA

TESI DI LAUREA

in
Fisica Tecnica Ambientale

DESIGN AND ACOUSTIC CHARACTERIZATION OF A NEW LISTENING ROOM

Progettazione e caratterizzazione acustica di una nuova sala d'ascolto

CANDIDATO
Francesco Saverio Ciani

RELATORE
Chiar.mo Prof. Massimo Garai

CORRELATORI
Prof. Ing. Luca Barbaresi
Ing. Dario D'Orazio
Ing. Simona De Cesaris

Anno Accademico 2013-2014
Sessione I

A mamma, papá
e a Luca Visani

Sommario

Il presente lavoro tratta la progettazione e caratterizzazione di una nuova *listening room* ad acustica controllata partendo dai requisiti dettati dalle norme tecniche ITU-R BS 1116-1 e EBU/UER Tech. doc. 3276. Ad oggi é presente un'ampia letteratura, che tratta approcci per valutazione acustica delle sale di ascolto. Essa inizialmente era volta a trovare proporzioni ideali tra le dimensioni della camera, poi la ricerca si é spostata sull'elaborazione di modelli previsionali. Purtroppo tali metodi spesso non riescono a garantire le prestazioni desiderate, mentre le prove sperimentali dettate dalle norme risultano essere di comprovata validitá. L'ambiente oggetto di studio é stato progettato all'interno dello spazio dei laboratori CIRI. La tecnologia costruttiva é frutto di uno studio approfondito, in particolare la scelta di fibre di poliestere termolegate, per il rivestimento delle pareti interne, é stata valutata attraverso misure in camera riverberante secondo UNI-EN-ISO 354. Si é poi seguita una metodologia iterativa che coinvolgesse messa in opera, misurazioni *in situ* e valutazione tramite confronto con i parametri consigliati dalle normative tecniche sopra citate. In quest'ottica sono state effettuate acquisizioni di risposte all'impulso monoaurali e dei livelli di pressione sonora per verificare la qualitá di isolamento e il comportamento alle basse frequenze. La validazione restituisce indicazioni positive per gli utilizzi dell'ambiente ipotizzati e risulta compatibile con le stringenti richieste delle norme tecniche.

Abstract

The present study concerns the design and acoustic characterization of a new "listening room" with monitered acoustics, following the requirement of the technical recommentdation ITU-R BS 1116-1 and EBU/UER Tech. doc. 3276. At the current state of art there is a wide literature about evaluation of the listening room acoustic. It was initialy oriented to find "optimum" room ratio, then the research has shifted to the elaboration of previsional models. Unfortunately these methods often cannot ensure the desired performance, while the sperimental measurement proposed in the technical standard proved to be reliable. The case study room was built inside the CIRI laboratories. The building technologies have been chosen after a deep study, *inter alia* the choice of polyester bonded fibers, in order to upholster the inner walls, was evaluated through reverberant chamber measurement, following UNI-EN-ISO 354. An iterative methodology was followed that involves installation, *in situ* measurement and evaluation through the comparison with parameters recommended by the above mentioned standards. In this context tmonoaural impulse responses and sound pressure levels have been measured in order to verify the insulation quality and the low-frequency behavior. The validation gives positive indication concerning the expected use of the environment and meets the strict recommendations of the standards.

Contents

List of Abbreviations **11**

List of Figures **12**

List of Tables **20**

1 Listening room acoustics **23**
1.1 Formal solution of the wave equation 24
1.2 Rectangular room with hard walls 29
1.2.1 Distribution of eigenfrequencies 34
1.2.2 Decay modes and reverberation 38
1.2.3 Critical frequency 42
1.3 "Optimum" room ratio recommendation 44
1.3.1 The Bolt's 'blob' 45
1.3.2 Louden's approach 47
1.3.3 Walker's ratio range 49
1.3.4 Bonello's criterion 51
1.3.5 The Fazenda's of the Modulation Transfer Function based analysis 55
1.4 ITU 1116 and EBU 3276 recommendation 57
1.4.1 Tolerance limits on the reverberation time . . . 59
1.4.2 Background noise in a listening room 64

2 Loudspeakers in room **67**
2.1 Sound power and sound intensity 74
2.2 Sound intensity measurement techniques 78
2.3 UNI EN ISO 9614 81

3 The design of the listening room 83
3.1 Architectural design 84
3.2 Room acoustic design 97
3.3 Plant design 107
3.3.1 Ventilation 107
3.3.2 Artificial lights and Electrical plant 110
3.3.3 Main monitors 113

4 Validation of the room: results and discussions 119
4.1 Room dimension requirements 121
4.2 Background and plant noise evaluation 126
4.3 Reverberation time 129
4.3.1 IR measurements 131
4.3.2 Configurations 134
4.3.3 Results 139
4.4 Sound pressure level measurements 152
4.4.1 Result and interaction with room modes 152
4.5 Directivity of the source 161
4.5.1 Results 167

5 Final consideration and conclusion 171

List of Abbreviations

MTF Modulation transfer function

FFT Fast Fourier Transform

NR Noise rating curve

NC Noise criterion

PNC Preferred noise criterion

T Reverberation time

MLS Maximum Length Sequence

SPL Sound pressure level

T_m Average value of reverberation time

V Volume

V_0 Reference volume

STI Speech transmission index

JND Just noticeable difference

List of Figures

1.1 Different kind of sizes of spaces. 24
1.2 Representation of the model hypothesis of the Rayleigh's wave theory 30
1.3 Resonances illustrated in two isolated, parallel, reflecting wall 33
1.4 Sound-pressure contour plots on a section through a rectangular room. 33
1.5 Distribution of allowed frequencies in 'frequency space'for a rectangular room sides 34
1.6 Comparison of four transmission curves recorded with and without an absorbing sample 37
1.7 Resonance curve for a normal mode of vibration. 39
1.8 Sound-pressure decay curves and logarithmic curves of the envelope. 41
1.9 Decay curves with a double slopes produced by normal modes of vibration with different decay constants . . . 41
1.10 Transition between the region of modal behavior and the region of diffuse behavior. 44
1.11 Bolt's design chart to determine Normal frequency statistics for Rectangular room. 46
1.12 Bolt's frequency spacing index plot contour 46
1.13 Bolt's blob domain that encloses optimum dimension ratios in small rectangular room 47
1.14 Different contour map plotted by Walker of room quality, for different fixed parameter. 50

1.15 Contour map of room "quality" for fixed height and variable volume 51
1.16 Contour map of room "quality" for fixed height of 3.5 and variable volume, overlaid with the Walker's criteria. 52
1.17 Graphic comparison between the Bolt's blob and the walker approach. 52
1.18 Comparsion between two room with different ratio using the Bonello criterion. 54
1.19 Comparative analysis of Bolt's criterion with that proposed by Bonello. 55
1.20 Sound pressure level vs. time graph that shows the decay 60
1.21 Suggested reverberation times for recording studios. . . 60
1.22 Tolerance limits for the reverberation time, relative to the average value, T_m 61
1.23 Test listening arrangement with loudspeakers L and R for stereophonic sound systems with small impairments 63
1.24 NR curves, Noise rating diagram based on the information of the ISO 9568 65

2.1 Cutaway view of a dynamic loudspeaker for the bass register. 68
2.2 Cutaway view of a dynamic tweeter. 68
2.3 Cutaway view of a dynamic midrange speaker. 68
2.4 Bass reflex enclosure schematic cross-section. 70
2.5 Loudspeaker radiation patterns at low frequencies. . . . 70
2.6 Radiation from a sealed box loudspeaker. 72
2.7 Directivity versus frequency in a conventional box loudspeaker 72
2.8 Diffraction on a sharp edge. 73
2.9 Cabinet diffraction. 74
2.10 The thermal analogy with the sound field. 75
2.11 The sound intensity and sound power. 76
2.12 Two closely spaced microphones that are ables to obtain a pressure gradient. 77

2.13 Schematic of the structure of a time based acoustic intensity meter. 80
2.14 Diagram of an acoustic intensity meter based on FFT analysis. 81
2.15 Theoretical sound intensity on measurement surface. . 82
2.16 Best measurement surface shapes 82

3.1 Section of the laboratories. The room in question is in the red circle 84
3.2 Planimetry of the laboratories. 85
3.3 Plan that explain the manufacturing process. 86
3.4 Photos of the progressive manufacturing progress of the wall in masonry plastered. Pictures taken in 26/06/2013. 87
3.5 Listening room plan. 88
3.6 Two trasversal cross-section. The once above show the front wall, the second the rear one. 89
3.7 Two cross-section. The once above show the wall on the right side, the second the left side. 90
3.8 3-D detail of the wall on the left side. 91
3.9 Re-reflexion between layers in a wall detail. 92
3.10 Assembly furniture drawing, plans and elevation and photo of the furniture final realization. 92
3.11 Furniture photo taken after and before be placed in the wall. 93
3.12 3-D detail of the rear wall. 93
3.13 Covering plan of the plasterboard suspended structure. 94
3.14 Progressive picture of the ceiling construction process. Pictures taken in 14/11/2013. 95
3.15 Two test listening arrangement, before and after rotating the panels. 96
3.16 Room reflection system: front view, cross section and details. 98
3.17 Room reflection system details and panels dimension. . 99
3.18 Transmission through real panels. 100
3.19 Assembled plasterboard structure detail. 101

3.20 Absorption coefficients for normal incidence measured with the Kundt's tube. 102
3.21 Plan and two different sections of the room without manufacturing used as reverberant chamber. 104
3.22 Pictures taken in the reverberant chamber during the IR measurements. The absorptive material is laid on the ground in several configurations. Pictures taken in 13/09/2013. 105
3.23 Absorption coefficient graphs per octave bands measured through the backward integrated impulse response method. 107
3.24 Distribution of the absorber panel of polyester fibers. . 108
3.25 3-D detail of the absorptive panel of polyester fibers placed on the metal grid. 108
3.26 Pictures taken during the cirfiber®mounting process. Picture taken in 03/04/2014. 109
3.27 Daikin air conditioning unit placed on the plasterboard wall. 110
3.28 Technical detail of the Daikin RX-JV(GV) inverter unit. 111
3.29 Disano®1130 Punto (Max 500 W) placed on the plasterboard wall. 112
3.30 Disano®1130 Punto (Max 500 W) technical detail. . . 112
3.31 Picture of the electrical cable over the plasterboard ceiling, made during the manufacturing process. 113
3.32 Data and power cables of the electrical plant described in plan. 114
3.33 Audio and electrical plant described in plan. 115
3.34 Description of the Dynaudio acoustic BM15. 116

4.1 Measurement position in the reference case study. . . . 121
4.2 Calculation of resonance modes and application of the Bonello criterion for the case study listening room. . . 124
4.3 Bolt's blob and the red dot that represent the position of the case study listening room. 125
4.4 Microphone and loudspeaker in the two opposite corners of the room in order to have equally energized modes. . 126

4.5 Microphone positions for Noise criteria 127
4.6 One-third octave band background noise level limits noise rating curves, based on the former ISO NR curves. . . 128
4.7 The continuous background noise produced by an air conditioning system (in maximum and medium power) and with air conditioning system turned on. 129
4.8 Reverberation time domain, in the case study room, highlighted in red. 130
4.9 Measurement position in the reference case study. . . . 133
4.10 Optimised measurement position. The measurement positions are identified by circles and the listening positions are identified by squares. 133
4.11 Definition of listening area. 134
4.12 IR measurement positions in the listening room. 135
4.13 The two different set-up of sources position. 135
4.14 Perspective cross-section views representing different set-up analyzed in the IR measurement. Near every perspective cross section view there is the view represented in plan. 137
4.15 Panel stiffening manufacturing process. 138
4.16 Rods placed in the OSB panel, respecting the metal frame constraint 138
4.17 Impulse response of the measurment position number 17 (represented in the right plan as a red dot) at 250 Hz in the first configuration. 140
4.18 Cross-section that show the part of ceiling that as to be considered in order to calculate axial modes. 140
4.19 Interpolation maps of T_{30} from the IR. The room is settled in the first configuration. 142
4.20 Interpolation maps of T_{30} from the IR. The room is settled in the second configuration. 143
4.21 Interpolation maps of T_{30} from the IR. The room is settled in the third configuration. 144
4.22 Interpolation maps of T_{30} from the IR. The room is settled in the fourth configuration. 145

4.23 Comparison of the impulse response of the measurment position number 17 (represented in the right plan as a red dot) at 250 Hz. The first configuration is on the left, the third is on the right. 146

4.24 Trends of the parameter T_{30} (s) as a function of frequency from IR. First and second configuration are compared 149

4.25 Trends of the parameter T_{30} (s) as a function of frequency from IR. First and third configuration are compared 149

4.26 Trends of the parameter T_{30} (s) as a function of frequency from IR. First, third and fourth configuration are compared 149

4.27 Trends of the mean value of the parameter T_{30} (s) in the positions around the listening postion number 23 compared with the listening position JND of the T_{30}. . 151

4.28 Trends of the mean value of the parameter T_{30} (s) in the positions around the listening postion number 11 compared with the listening position JND of the T_{30}. . 153

4.29 Sound pressure level measurement positions in the listening room. 154

4.30 Trend of the parameter SPL as function of one-third octave bands; mean values, max, min. The case study configuration is the first. 155

4.31 Interpolation maps of Sound pressure level. The case study configuration is the first. 155

4.32 Hypothetical standing wave applied to the case study room along the y-axis $n_y = 2$. 157

4.33 Hypothetical standing wave applied to the case study room along the x-axis with $n_x = 2$. 157

4.34 Hypothetical standing waves applied to the case study room. The left one is along the x-axis with $n_y = 3$, the right one is along the x-axis with $n_y = 4$ 157

4.35 Trend of the parameter SPL as function of one-third octave bands; mean values, maxi, min. The case study configuration is the third. 159
4.36 Interpolation maps of Ssound pressure level. Third configuration. 159
4.37 An illustration of how room boundaries that have low frequency absorption, *i.e.* flexure, can improve the uniformity of sound distribution at the modal frequencies. 160
4.38 Trend of the parameter SPL as function of one-third octave bands; mean values, max and min. The case study configuration is the fourth 162
4.39 Interpolation maps of sound pressure level. Fourth configuration. 162
4.40 Interpolation maps of SPL difference between the third configuration and the fourth configuration. 163
4.41 The 50GI-R Sound intensity probe 164
4.42 Frequency ranges coverd by the various spacer lengths. 164
4.43 Picture of the sound intensity measurement, during the placing of the 50GI-R (left picture) and during the data acquisition with $dBfFA©$ (left picture). 166
4.44 Frontal picture of the mesh for the Sound Intensity interpolation maps. Plan with the measurement position. 166
4.45 Frequency response measurements of a loudspeaker showing (top to bottom) a very smooth and flat on-axis response, and increasingly non-flat behavior at increasing angles off axis. 168
4.46 Interpolation maps of sound intensity levels. The measurement surface it is 0.5 m toward the Dynaudio BM15 plane. 169

List of Tables

1.1 Louden's dimension-ratios of the acoustic quality of rectangular rooms. 48
1.2 Resuming table of the ideal room ratio theory scheme. 58

3.1 Summary table of main data of CIRFONIC®. 101
3.2 Summary table of main data of Cirfiber®. 102
3.3 Comparison of the two methods characteristics of methods to measure the sound absorption coefficient. 103
3.4 Resuming table of the BM15 dimensions, weight and volume. 116

4.1 Table that shows the fist 48 modes, using the rectangular room approximation, *i.e.*, using the given equation 1.34. 123
4.2 Spatial position of the microphones. 127
4.3 Octave band sound pressure level values in dB. 128
4.4 Spatial loudspeaker position and panel angles. 136
4.5 Axial modes in z-axis, considering the fist 6 modes. . . 141

Chapter 1

Listening room acoustics

The study of sound in enclosures involves not only a search into how sounds are reflected backward and forward in an enclosure but also on investigation into how to measure sound under such conditions and the effect that various materials have in absorbing and controlling this sound. It is also of great importance the understanding of the personal preferences of listeners, whether listening in the room where the music is produced or listened at a remote point to a microphone pickup.

Different cases to the study of sound in enclosures can be analyzed. The first is the 'large room', where it is assumed that the sound field throughout a large relatively reverberant space is diffuse. In technical terms that means that the sound field is homogeneous (the same everywhere in the space) and isotropic (with sound energy arriving at every point equally from all directions). That theoretical ideal is never achieved because of sound absorption at boundaries, by the audience and in air, but it is an acceptable starting point. Diffuse-field theory may not apply perfectly to concert halls, but it applies even less well to other kinds of rooms. In the acoustical transition from a large performance space to a "small" room, it seems that the significant factors are a reduced ceiling height (relative to length and width), significant areas of absorption on one or more of the boundary surfaces, and proportionally large absorbing and scattering objects distributed throughout the floor area. Sound radiating from a source is either absorbed immediately on its first encounter with a surface or object, or the objects redirect the sound into something else that absorbs it. Thus the late re-

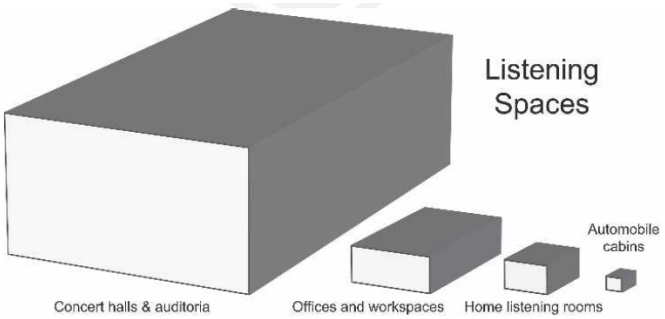

Figure 1.1: Pictorial representation of the range of sizes and shapes of spaces for which it is needed acoustical measurements and rules. After [44].

flected sound field is greatly diminished with distance from the source. These listening rooms are also known as not Sabine spaces, and it is not appropriate to treat them using the same theory[44].

The focus of this work will be on small enclosures because of the dimension of the case study room.

In this cases the interior sound field is describable in precise mathematical terms, with the modal theory although the analysis becomes complicated if the walls of the enclosure are covered on the whole or in part with acoustical absorbing materials [4]. Worth mentioning that room modes are recognized as one of the most noticeable problems in professional audio control rooms. Although this problem is widely acknowledged, efficient solutions are still difficult to implement. In order to understand the implications of room modes on subjective perception, a thorough knowledge of the behavior of sound in the room, and more specifically the factors associated with resonances, is necessary.

1.1 Formal solution of the wave equation

The starting point for a wave theory representation of the sound field in a room is the 3-D wave equation

$$\nabla^2 p = \frac{1}{c^2}\frac{\partial^2 p}{\partial t^2} \tag{1.1}$$

where p is the pressure and t the time. This differential equation governs the propagation of sound waves in any lossless fluid and is

therefore of central importance for almost all acoustical phenomena. It holds not only for sound pressure but also for density and temperature variations. Hence, it is possible to take the time invariant form of the wave equation. If a harmonic time law is assumed for pressure and particle velocity, we can divide the function in a position-dependent term and a time-dependent term:

$$p(\mathbf{r}, t) = R(\mathbf{r})T(t) = R(\mathbf{r})e^{i\omega t} \tag{1.2}$$

Where r is the distance between the source and the receiver point .Applying this in the wave equation we arrive at the Helmholtz equation

$$\nabla^2 p + k^2 p = 0 \tag{1.3}$$

This equation can be seen as a homogeneous differential equation, where k=$\frac{\omega}{c}$. Furthermore, it is assumed that the room assumed in this theory has locally reacting walls and ceiling, the acoustical properties of which are completely charachterised by a wall impedance depending on the coordinates and the frequency but not on the angle of sound incidence. The velocity component normal to any wall or boundary is

$$v_n = -\frac{1}{i\omega\rho_0}(\nabla p)_n = \frac{i}{\omega\rho_0}\frac{\partial p}{\partial n} \tag{1.4}$$

Using the definition of impedance Z it is possible to write the previous equation as:

$$Z\frac{\partial p}{\partial n} + i\omega\rho_0 p = 0 \tag{1.5}$$

Now it can be shown that the wave equation yields non-zero solutions fulfilling the previous boundary condition only for particular discrete values of k, called *eigenvalues*. These quantities need to be distinguished from each other by an index number n or m, though it is often more convenient to use a trio of subscripts because of the three-dimensional nature of the problem. Each eigenvalue k_n is associated with a solution $p_n(\mathbf{r})$, which is known as an eigenfunction or characteristic function ($\mathbf{r}$ is used as an abbreviation for the three spatial coordinates). It represents a three-dimensional standing wave, a so-called

normal mode of the room. As mentioned earlier, for a given enclosure the explicit evaluation of the eigenvalues and eigenfunctions is generally quite difficult and requires the application of numerical methods such as the Finite Element Method (FEM). There are only a few room shapes for which the eigenfunctions can be presented in closed form. An important example will be given in the next section.

One can prove that the the eigenfunctions form a complete and mutually orthogonal set of functions:

$$\iiint_V p_n(\mathbf{r}) p_m(\mathbf{r}) dV = \begin{cases} K_n, & \text{for } n = \text{m} \\ 0, & \text{for } n \neq \text{m} \end{cases} \tag{1.6}$$

where the integration has to be extended over the whole volume V enclosed by the walls. Here K_n is a constant a scalar dependent on room volume. If all the eigenvalues and eigenfunctions, which in general are functions of the frequency, are known, we can in principle evaluate any desired acoustical property of the room; for instance, its steady state response to arbitrary sound sources. Suppose the sound sources are distributed continuously over the room according to a density function q($\mathbf{r}$), where $q(\mathbf{r})$dV is the volume velocity of a volume element dV at $\mathbf{r}$. Here q($\mathbf{r}$) may be a complex function to account of possible phase differences between the various infinitesimal sound sources. Furthermore it is assumed a common driving frequency ω.

By adding $\rho_0 q(\mathbf{r})$ to the right-hand side of equation 1.7

$$\rho_0 \nabla \cdot (\mathbf{r}) = -\frac{\partial p}{\partial n} \tag{1.7}$$

It is easily seen that Helmholtz equation becomes:

$$\nabla^2 p + k^2 p = -i\omega\rho_0 q(\mathbf{r}) \tag{1.8}$$

with the same boundary condition as above. Since the eigenfunctions form a complete and orthogonal set of functions, it is possible to expand the source function in a series of pressures p_n:

$$q(\mathbf{r}) = \sum_n C_n p_n(\mathbf{r}) \tag{1.9}$$

where:

$$C_n = \frac{1}{K_n} \iiint_V p_n(\mathbf{r}) q(\mathbf{r}) dV \tag{1.10}$$

where the summation is extended over all possible combinations of subscripts. In the same way the solution $p_\omega(\mathbf{r})$ can be expanded in eigenfunctions:

$$p_\omega(\mathbf{r}) = \sum_n D_n p_n(\mathbf{r}) \tag{1.11}$$

The problem is solved if the unknown coefficients D_n are expressed by the known coefficients C_n. For this purpose are inserted both series into the equation 1.8:

$$\sum D_n \nabla^2 p_n + k^2 p = -i\omega\rho_0 \sum C_n p_n \tag{1.12}$$

Now $\nabla^2 p_n = -k^2 p_n$. Using this relation and equating term by term in the equation above, it is obtained:

$$D_n = i\omega\rho_0 \frac{C_n}{k^2 - k_n^2} \tag{1.13}$$

The source shall be modeled with the simple case of point source. Whilst infinite small in physical terms, the point source approximation may be considered valid where the dimension of the source are small in comparison to the wavelength of the sound emitted. At low frequency this can be considered true. A dirac delta function is used to represent this source, with the form:

$$q(\mathbf{r}) = Q\delta(\mathbf{r} - \mathbf{r_0}) \tag{1.14}$$

where Q is the volume velocity. When substituted into equation 1.10 this gives:

$$C_n = \frac{1}{K_n} \iiint_V p_n(\mathbf{r}) Q\delta(\mathbf{r} - \mathbf{r_0}) dV \tag{1.15}$$

A special property of the delta function allows us to apply the "sifting property" where by:

$$\int f_x Q\delta(\mathbf{r} - \mathbf{r_0})dV = f(x_0) \tag{1.16}$$

Hence it results:

$$C_n = \frac{1}{K_n} Q_n p_n(\mathbf{r_0}) \tag{1.17}$$

Finally, it is possible to equate 1.11, with a point source excitation at $\mathbf{r}$ and receiver $\mathbf{r_0}$, finding what is known as the "Green function" of the room.

$$p_\omega(\mathbf{r}) = iQ^2 c\omega\rho_0 \sum_n \frac{p_n(\mathbf{r})p_n(\mathbf{r_0})}{K_n(k^2 + k_n^2)} \tag{1.18}$$

It is interesting to note that the equation 1.18 is symmetric in the coordinates of the sound source and of the point of observation. If the sound source is placed at $\mathbf{r}$, it is seen that at point $\mathbf{r_0}$ there is the same sound pressure that it was noticed at $\mathbf{r}$, when the sound source was at $\mathbf{r_0}$. Thus equation 1.18 is the mathematical expression of the well known reciprocity theorem which can be applied sometimes with advantage to measurement in room acoustic.

With complex boundary conditions, the k_n terms are usually complex quantities. Therefore if:

$$k_n = \frac{\omega_n}{c} + i\frac{\delta_n}{c} \tag{1.19}$$

where the δ is a damping constant, the equation 1.18 becomes:

$$p_\omega(\mathbf{r}) = iQ^2 c\omega\rho_0 \sum_n \frac{p_n(\mathbf{r})p_n(\mathbf{r_0})}{K_n(\omega^2 + \omega_n^2 - 2i\delta_n\omega_n)} \tag{1.20}$$

where it is assumed $\delta_n << \omega_n$. Considered as a function of the frequency, this expression is the transfer function of the room between the two points $\mathbf{r}$ and $\mathbf{r_0}$. At the angular frequencies $\omega = \omega_n$, the associated term of this series assumes a particularly high absolute value. The corresponding frequencies $f_n = \frac{\omega_n}{2\pi}$ are called eigenfrequencies of the room; sometimes they are referred to as "resonance frequencies" because of some sort of resonance occurring in the vicinity of those

frequencies [29].

In order to find the transfer function that describes with the highest accuracy the system, the damping constant δ_n has to be found. In the simple case of a rigid with rigid walls and ceilings, with an assumed uniform sound-field, the damping constant can also be assumed uniform, and therefore, reverberation time decreases linearly. In this case, there is a direct relationship between the weighted average δ_0 and the reverberation time T (in s):

$$\delta_0 = \frac{6,91}{T} \tag{1.21}$$

The damping is also affected by the mode type, *i.e.* axial, tangential or oblique. A wave traveling a greater distance in its reflective path is absorbed to a greater extent. The grazing effect (the absorption due to the angle of incidence as a wave travels along a surface) is assumed to be zero here. It follows that modes of the three different types are absorbed by differing amounts. We assume that, on average, each mode type is subject to the same additional absorption. Therefore, constants are introduced. Where n=0 , $\epsilon = 1$ and where $n \leq 0$, $\epsilon = 2$. To further increase the realism of the damping condition, we include the specific values and the absorption coefficients α for the material on each wall. Morse [32] shows that the approximate formula for the damping coefficient in this case is:

$$\delta_0 = \frac{c}{8V}\left(\frac{1}{2}\epsilon_{nx}\alpha_x + \frac{1}{2}\epsilon_{ny}\alpha_y + \frac{1}{2}\epsilon_{nz}\alpha_z\right) \tag{1.22}$$

1.2 Rectangular room with hard walls - modal theory

It is taken in consideration now a room with parallel pairs of walls, the pairs being perpendicular to each other. It will be referred to in the following as a 'rectangular room'[28]. The specific case of a rectangular room with perfectly smooth, rigid walls had a solution already in 19th century by Lord Rayleigh, that found the existence of eigenmodes. He defined an equation for the determining the resonance frequencies in

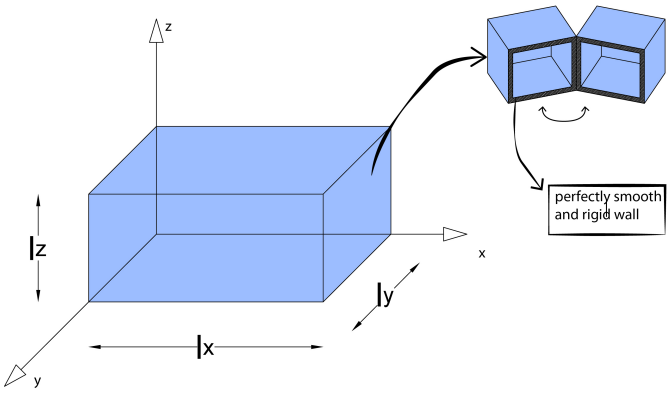

Figure 1.2: Representation of the model hypothesis of the Rayleigh's wave theory

rooms. This theory permits to have an analytic solution only for simple geometries, *i.e.* for a room that has sides l_x, l_y, l_z. Worth mentioning that the boundary condition for a rigid wall is that the air velocity perpendicular to the wall is zero at the wall. This boundary condition avoids to study the materials and this is an other big approximation. In cartesian coordinates the Helmholtz equation may be written as:

$$\frac{\partial^2 p}{\partial x^2} + \frac{\partial^2 p}{\partial y^2} + \frac{\partial^2 p}{\partial z^2} + k^2 p = 0 \tag{1.23}$$

The variables can be separated, which means that we can compose the solution of three factors:

$$p(x, y, z) = p_x(x) p_y(y) p_z(z) \tag{1.24}$$

which depend on respectively x only, on y only and on z only. If this product is inserted into the Helmholtz equation, the latter splits up into three ordinary differential equations. The same is true for the boundary conditions. For instance, p_1 must satisfy the equation

$$\frac{\partial^2 p_x}{\partial x^2} + k_x^2 p_x = 0 \tag{1.25}$$

Since the walls are rigid and hard, the normal component of air particle velocity on the wall surface must be equal to zero, *i.e.* the velocity of air particles near any wall must be parallel to that wall.

$u = 0$ for x=0 and $x = l_x$
$v = 0$ for y=0 and $x = l_y$
$w = 0$ for z=0 and $x = l_z$
where u, v, w are the particle velocities in the three axes. So formally for the single x-axis the boundary condition is

$$\frac{dp_x}{dx} = 0 \; for \; x = l_x \tag{1.26}$$

Analogous equation holds for $p_y(y)$ and $p_z(z)$; also the constants k_x, k_y, k_z must satisfy

$$k_x^2 + k_y^2 + k_z^2 = k^2 \tag{1.27}$$

Where k_x/k, k_y/k, k_z/k represent the direction cosines made by the directions of wave propagation with respect to x, y and z-axes. Remembering that k is the wave number in angular notation, using the relationship:

$$k = \frac{2\pi f}{c} \tag{1.28}$$

where f is frequency in Hertz and c the speed of sound in air in ms^{-1}.

$$k = \frac{\omega}{c} = \sqrt{k_x^2 + k_y^2 + k_z^2} \tag{1.29}$$

The homogeneous differential equation 1.25 has a general solution

$$p_1(x) = A_1 cos(k_x x) + B_1 sin(k_x x) \tag{1.30}$$

The constants A_1 and B_1 are used for adapting this solution to the boundary conditions in 1.26. So it is seen immediately that we must put B_1 since only the cosine function possesses at x = 0 the horizontal tangent required by equation 1.26. For the occurrence of a horizontal tangent too at $x = l_x$, it is to be satisfied the condition $cos(k_x l_x) = \pm 1$ thus $k_x l_x$ must be an integral multiple of π. The costant k_x must therefore assume one of the allowed values:

$$k(x) = \frac{n_x \pi}{l_x} \tag{1.31}$$

n_x being a non-negative integer. Similarly, it is obtained for the allowed

values of k_y, k_z. Inserting these values into equation 1.29 results in the following equation for the eigenvalues of the wave equation:

$$k_{n_x n_y n_z} = \pi \sqrt{\left(\frac{n_x}{l_x}\right)^2 + \left(\frac{n_y}{l_y}\right)^2 + \left(\frac{n_z}{l_z}\right)^2} \tag{1.32}$$

The eigenfunctions associated with these eigenvalues are simply obtained by multiplication of three cosines, each of which describes the dependence of the pressure on one coordinate:

$$p_{n_x n_y n_z} = C cos(k_x x) cos(k_y y) cos(k_z z) \tag{1.33}$$

where C is an arbitrary constant and x, y and z positions within the room. $p_{n_x n_y n_z}$ now represent a three dimensional standing wave at a single point within the room; of course, it is incomplete without the factor $e^{i\omega t}$ describing the time dependence of the sound pressure.

In terms of frequency for the corresponding room modes the equation is expresed as:

$$f = \frac{\omega}{2\pi} = \frac{kc}{2\pi} = \frac{c}{2} \sqrt{\left(\frac{n_x}{l_x}\right)^2 + \left(\frac{n_y}{l_y}\right)^2 + \left(\frac{n_z}{l_z}\right)^2} \tag{1.34}$$

Where n_x, n_y, n_z are the indices of the room modes.

Waves traveling "parallel" to a wall are affected by the wall (are absorbed by it for istance) ta a lesser extent than waves having oblique incidence. Therefore standing waves were separeted in three categories and seven classes:

1. Axial waves (for which two n are zero)
1.1 x-axial waves, parallel to the x-axis (n_y,$n_z = 0$)
1.2 y-axial waves, parallel to the y-axis (n_x,$n_z = 0$)
1.3 z-axial waves, parallel to the z-axis (n_y,$n_x = 0$)
2. Tangential waves (for which one n is zero)
2.1 y,z-tangential waves, parallel to the x-plane ($n_x = 0$)
2.2 x,z-tangential waves, parallel to the y-plane ($n_y = 0$)
2.2 x,y-tangential waves, parallel to the z-plane ($n_z = 0$)
3. Oblique waves (for which no n is zero)

It is possible to see these different kind of modes in figure 1.4.

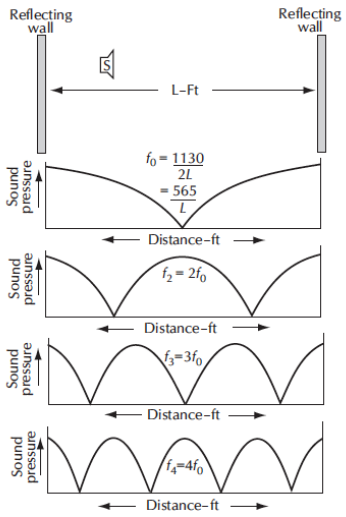

Figure 1.3: The simplest form of room resonance can be illustrated by two isolated, parallel, reflecting wall surfaces. After [3].

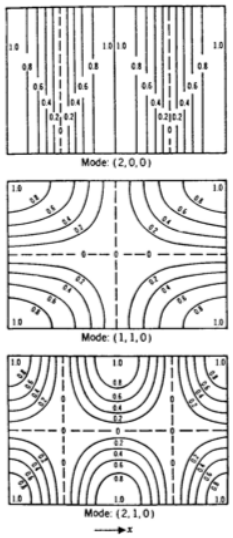

Figure 1.4: Sound-pressure contour plots on a section through a rectangular room. The numbers on the plots indicate the relative sound pressure. After [4].

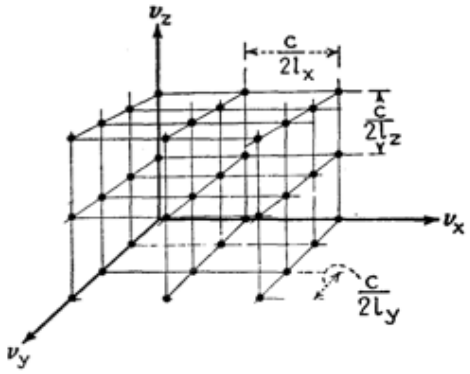

Figure 1.5: Distribution of allowed frequencies in "frequency space" for a rectangular room sides l_x,l_y and l_z The length of the vector gives the direction cosines of the corresponding standing wave in the room. After [32].

It will turn out that, even in the first approximation, waves of different classes have different reverberation time and, waves of the same class have the same reverberation time.

1.2.1 Distribution of eigenfrequencies

Considering the distribution of the modes within the room, it is quite tedious to count the individual allowed frequency below a given frequency band, so it is useful to obtain a "smoothed-out" formula for average values of the counts. The rapresentation in a lattice system is useful here, infact *e.g.* a normal mode of oscillation can be considered as a pont in 'frequency space', whose x component is an integral number of unit length $(c/2l_x)$ etc. like is possible to see in the fig 1.5. Considering that each lattice point "occupies" a rectangular block of dimensions $(c/2l_x)$, $(c/2l_y)$, $(c/2l_z)$ in frequency space, with the actual lattice point at the center of the block. Then the average number of points can be obtained by dividing the volume of frequency space considered by the volume $(c^3/8V)(V = l_x l_y l_z)$ of each block, viz:

$$N_{ax} \approx \left(\frac{fL}{2c}\right) \tag{1.35}$$

where L = $4(l_x+l_y+l_z)$ is the sum of the length of all the edges of the room. The average number of y,z-tangential waves is the number of

blocks in a quarter of a disk of thickness $(c/2l_x)$ and radius f, minus a correction to allow account the axial waves, which have been counted separately. This correction in volume is one-half the space "occupied" by the y and the z axial lattice points. The factor one-half comes in because only one-half of the volume "occupied" by the axial lattice points is inside the angular sector formed between the y- and z- axes, which bounds the quarter disk. Therefore the average number of al the tangential waves with frequencies less than f is

$$N_{ta} \approx \left(\frac{\pi f^2 A}{2c^2}\right) - \left(\frac{fL}{2c}\right) \tag{1.36}$$

where $A = 2(l_x l_y + l_x l_z + l_y l_z)$ is the total wall area. We are neglecting the corrections for the overlapping regions at the origin, f=0, for they are independent of f and are small in magnitude. The volume "occupied" by the lattice points for the oblique waves of frequency less than f is the volume of one-eight sphere minus the volume already counted for the other classes of waves:

$$N_{ob} \approx \left(\frac{4\pi f^3 V}{3c^3}\right) - \left(\frac{\pi f^2 A}{4c^2}\right) + \left(\frac{fL}{8c}\right) \tag{1.37}$$

where $V = l_x l_y l_z$ is the volume of air in the room. Therefore the total number of standing waves of all classes which have frequencies less than f is

$$N \approx \left(\frac{4\pi f^3 V}{3c^3}\right) + \left(\frac{\pi f^2 A}{4c^2}\right) + \left(\frac{fL}{8c}\right) \tag{1.38}$$

The correct value for N fluctuates above and below this average value but is seldom more than on or two units away.

It is always stated that it is quite tedious to calculate or even count the individual eigentones less the counts are given. So we have for the average number of eigentones δN with frequencies in a band of width δf the following approximate formula

$$\frac{\delta N}{\delta f} = \left(\frac{4\pi f^2 V}{c^3}\right) + \left(\frac{\pi f A}{2c^2}\right) + \left(\frac{L}{8c}\right) \tag{1.39}$$

The right hand side of the equation gives the number of eigentones

per bandwidth of one Hz. The reciprocal of it, $\frac{\delta N}{\delta f}$, gives the frequency interval between two neighbor eigentones. It gives only an approximate average value which does not depend on the ratio between the room dimensions. Exact values for the eigentones interspacing can only be obtained by calculating the individual eigentones and subtracting each frequency from its neighbor's one [32].

For large rooms, the last two summand on the equation 1.38 could be neglected because of the predominant effect of axial modes. Hence the given value of N is:

$$N \approx \left(\frac{4\pi f^3 V}{3c^3} \right) \tag{1.40}$$

The equation 1.40 was proved to be worth for the practice also for small enclosures that have different shapes [42].

Worth mentioning the work of Hunt in 1939 [23] that makes a validation of the modal theory. The curves in figure 1.6 were obtained by slowly varying the frequency (a pure tone) of the loudspeaker and simultaneously recording the output of the microphone. The eightfold increase in the number of modes of vibration which were excited with the source at the corner overt that with the source at the center is apparent. It seems also that the addition of sound-absorbing material decreases the height of resonance peaks and smooths the transmission curve, particularly at the higher frequencies, where the sound-absorbing material is most effective. The figure 1.6 illustrates a comparison of four transmission curves recorded with and without an absorbing sample on a 0.76x0.61 m^2 wall on a model chamber with dimension (0.76x0.61x0.41) m^3. In transmission curves in figure 1.6**a** and 1.6**b** the microphone was in one corner, and the source was diagonally opposite. The dashed line shows the relative response of the small loudspeaker ($\frac{3}{8}$ in diameter) measured at 2 in. in free space. Zero decibel for the source curve is about 50 dB. In the curves in thfigure 1.6**b** and 1.6**c**, the source was in the center of the room and the zero decibel reference for the source characteristic is about 71 dB. Regarding the material of this chamber in figure 1.6**a** and 1.6**a** the curves have with a good approximation infinite impedance, in figure 1.6**b** and 1.6**d** one of the surfaces (0.76x0.41)

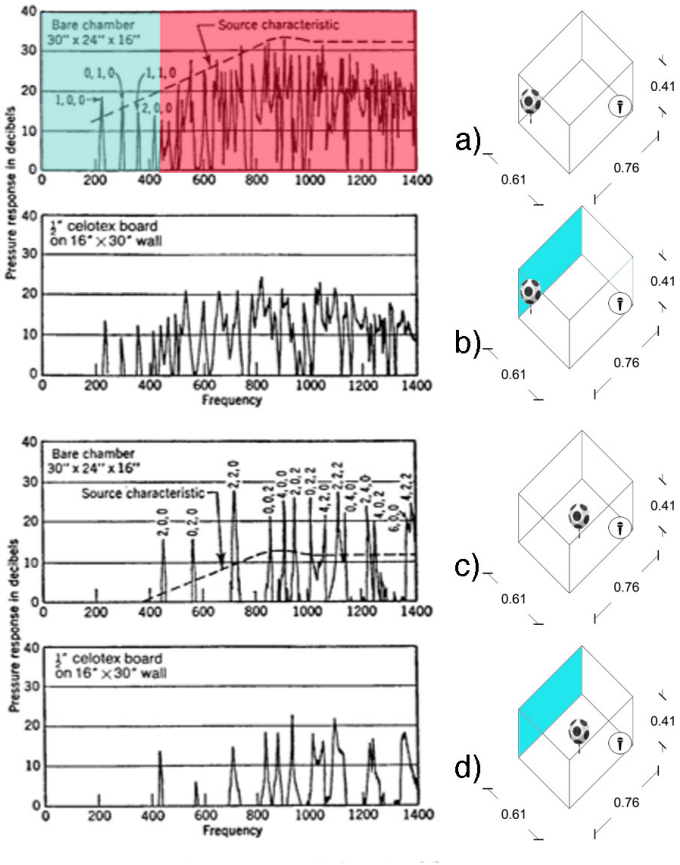

Figure 1.6: Comparison of four transmission curves recorded with and without an absorbing sample on a 0.76x0.61 wall on a model chamber with dimension (0.76x0.61x0.41) m^3. After [4].

m^2 is finished with a porous material of 13 mm. In the blue part in the a) curve it is possible to recognize very well the mode peaks of the first four modes. In the red part, increasing the frequency, the modal density increases and the resonance curves of modes start to overlap and it is very difficult to identify the specific mode. This overlapping effect is quantified by the indicator M, called modal overlapping:

$$M = \Delta f \frac{dN}{df} \tag{1.41}$$

In the 1.6**b** curve, the dissipation effect of the material is clear. In fact mode peaks appear to be with a smaller width, and the increasing of the width of resonance bands produce an increasing of modal overlapping. The 1.6**c** curve represents a validation of the reciprocity principle. In this case the source is placed in the center of the parallelepiped and it is clear that it misses the contribution of the modes that have one of the three modal number odd. Hence the modal overlapping decreases and the modes appear to be more isolate. At least the 1.6**d** curves shows the dissipation effect for the 1.6**c** configuration.

Hence it is clear that the sound pressure is dominated by few modes, when the frequency of the source is low according to the room dimensions. This can be called "small room" behavior. Instead, when the modal density increases with the frequency, the sound pressure is the result of excited resonance modes overlapping.

1.2.2 Decay modes and reverberation

When a source of sound is turned on in a small enclosure, it will excite one or more of the stationary waves. Let us assume that the source is constant in strength and is of a single frequency and that its frequency coincides with one of the normal frequencies of the enclosure. The sound pressure for that normal mode of vibration will build up until the magnitude of its rms value (averaged in time and also in space by moving the microphone backward and forward over a wavelength) equals:

$$|p_n| = \frac{K}{\delta_n} \tag{1.42}$$

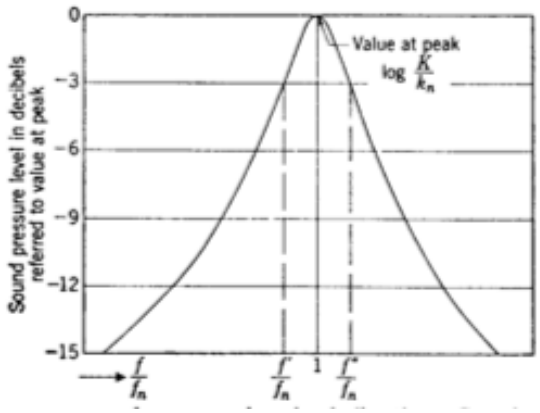

Figure 1.7: Resonance curve for a normal mode of vibration. Sound pressure level vs. the ratio of the frequency to f_n. In this image Beranek [4] write the damping constant k_n[4].

K is the source constant determined principally by the strength and location of the source and by the volume of the room. δ_n is the damping constant determined principally by the amount of absorption in the room and by the volume of the room. The more absorbing material that is introduced into the room, the greater δ_n, and the smaller the value of the average pressure. When the driving frequency does not coincide with the normal frequency, the pressure for that particular mode of vibration builds up according to a standard resonance curve as shown in equation1.7. The width of the resonance curve at half power (3 dB down) points is equal to:

$$f'' - f' = \frac{\delta_n}{\pi} \tag{1.43}$$

The magnitude of the sound pressure p_n is given by:

$$|p_n| = \frac{2K\omega}{\sqrt{4{\omega_n}^2{\delta_n}^2 + (\omega^2 - {\omega^2}_n)^2}} \tag{1.44}$$

where ω is the angular driving frequency and ω_n is the angular normal frequency given approximately by the equation 1.34. Obviously, if the driving frequency lies between to normal frequencies, or if k_n is large so that the resonance curve is broad, more than one normal mode of vibration will be excited significantly, each to the extent shown by

equation 1.45. When the source of sound is turned off, each normal mode of vibration behaves like an electrical parallel-resonance circuit in which energy has been stored initially. The pressure for each normal mode of vibration will decay exponentially at its own normal frequency as shown in figure 1.8.

If only one mode of vibration is excited, the decay is as shown in figure 1.8 **a** and as given by:

$$p_n = \frac{K}{\delta_n} e^{-\delta_n t} cos\omega_n t \tag{1.45}$$

Stated differently, on a $log(p_n)$ scale vs. time, the magnitude of the rms sound pressure level decays linearly with time. If two or more modes of vibration are decaying simultaneously, beats will occur because each has its own normal frequency (fig. 1.9). In summary, we see that when a sound source of a given frequency is placed in a rectangular enclosure, it will excite one or more of the infinity of resonance conditions, called normal modes of vibration. Each of those normal modes of vibration has a different distribution of sound pressures in the enclosure. The normal frequency, and the damping constant, related to the normal modes, determines the maximum height and the width of the steady-state sound-pressure resonance curve. The room is thus an assemblage of resonators that act independently of each other when the sound source is turned off. The larger the room and the higher the frequency, the nearer together will be the normal frequencies and the larger will be the number of modes of vibration excited by a single-frequency source or by a source with a narrow band of frequencies [4]. It is interesting to relate the coefficient δ_n to the reverberation time T. From equation 1.45 the time required for the pressure to drop by 60 dB is $T = 6.91/\delta_n$ which, when substitutet into equation 1.43 yields

$$\Delta f = \frac{6,91}{\pi T} = \frac{2.2}{T} \tag{1.46}$$

showing that the bandwidth of the resonance modes is constant and independent of frequency if the reverberation time is also constant. The T measured in a room is the average of the individual T for each

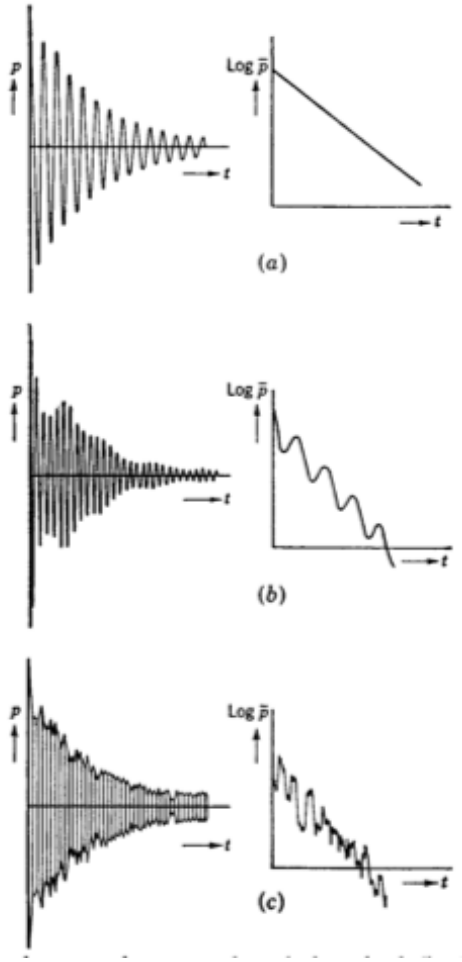

Figure 1.8: a) Sound-pressure decay curve for a single mode of vibration. b) Sound-pressure decay curve for two closely spaced modes of vibration with the same decay constant. c) Sound-pressure decay curve for a number of closely spaced modes of vibration with the same decay constant. The graph on the left shows the curve of the envelope of the left graph, plotted in a *log(p)* vs. t coordinate system. After [4].

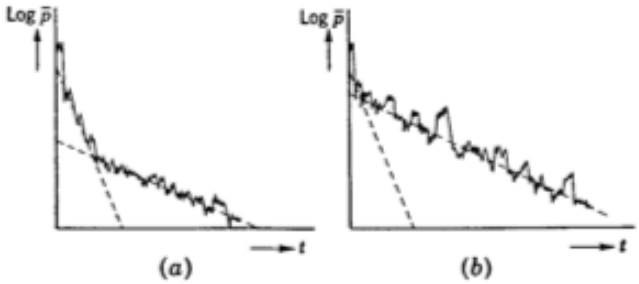

Figure 1.9: a) Decay curves with a double slopes produced by normal modes of vibration with different decay constants. After [4].

of the modes, but for practical purposes the T used in equation 1.46 is the same measured with pink noise. For the rooms normally used as studios, the modal T are approximately constant with frequency. This constancy implies that the bandwidth given by equation 1.46 is between 3 and 10 Hz. In terms of relative bandwidth, measured in fractions of an octave and commonly used in electroacoustics, we have:

$$\frac{\Delta f}{f} = 2^{\frac{1}{2n}} - 2^{-\frac{1}{2n}} \tag{1.47}$$

where 1/n is the bandwidth in octave. Taking into account eqs. 1.46 and 1.47, we see that as T increases, the bandwidth decreases. Rooms built with low T in the bass will have wider bandwidths, advantageous for a larger number of responsive modes. On the other hand, for constant T, the selectivity of the modes increases with frequency; the bandwidth in octaves decreases. This is not important at high frequencies since the number of modes increases rapidly; but conversely the bass end is enhanced, since the octave bandwidth becomes large [7].

1.2.3 Critical frequency

Because all rooms have modes in their lower frequency ranges, there will always be a frequency below which the modal effects dominate and the room can no longer be treated as diffuse. Even anechoic rooms have lower frequency limits to their operation. One of the effects of room modes is to cause variations in the frequency response of the room, due to its effect on the reverberant field. The frequency response due to modal behavior will also be dependent on the room position, due to the spatial variation of standing waves. An important consequence of this is that the room no longer supports a diffuse field in the modal region and so the reverberation time concept is invalid in this frequency region. Instead an approach based on modal decay should be used. The transition thresholds between the region of modal behavior and the region of diffuse behavior is known as the critical frequency. As is usual in these situations, although the critical frequency is a single frequency it is not a sharp boundary: it represents some defined point in a transition region between the two regions. The concept of crit-

ical frequency (also known as the 'Schroeder frequency'or large room frequency) allows us to define the difference between rooms which are large and small in acoustical terms. In an acoustically large room the critical frequency is below the lowest frequency of the sound that will be generated in the room whereas in an acoustically small room the critical frequency will occur within the frequency range of the sounds being produced in it. Examples of acoustically large rooms would be concert halls, cathedrals and large recording studios. Most of us listen to and produce music in acoustically small rooms, such as bedrooms, bathrooms and living rooms, and there is an increasing trend due to the effect of computer recording and editing technology and because it is cheaper to perform more and more music and sound production tasks in small rooms [22].

Now it is important to quantify this critical frequency. In order to calculate it several assumptions have to be done. First of all, if the mean spacing of resonance frequencies is substantially larger than the average half-width, found in 1.46, most of the room resonances are well separated, and each of them can be individually excited and detected. In a tiled bathroom, for example, the resonances are usually weakly damped, and thus one can often find one or several resonances by singing or humming. If, on the contrary, the average half-width of the resonances is much larger than the average spacing of the eigenfrequencies, there will be strong overlap of resonance peaks and the latter cannot be separated. According to Schroeder [38] a limiting frequency separating both cases can be defined by the requirement that on average three eigenfrequencies fall into one resonance half-width, or, with equation 1.39.

$$\langle \Delta f_n \rangle = 3\frac{c^3}{4\pi V f^2} \tag{1.48}$$

Where the angle brackets indicate averages. Solving for the frequency yields the limiting frequency, the so-called Schroeder frequency [38]:

$$f_s = \frac{5400}{\sqrt{(V\langle \delta_n \rangle)}} \approx 2000\left(\frac{T}{V}\right)^{\frac{1}{2}} \tag{1.49}$$

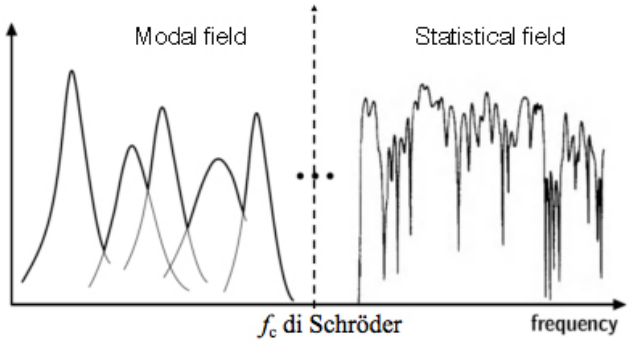

Figure 1.10: It is highlighted the transition boundary between the region of modal behavior and the region of diffuse behavior. This boundary corresponds to a frequency called 'Schroeder frequency'. After [18].

Where the room volume V is expressed in cubic meters and T in seconds. For large halls the Schroeder frequency is typically about 20 or 30 Hz, hence there is strong modal overlap in the whole frequency range of interest, and there is no point in evaluating any eigenfrequencies. It is only in small rooms that a part of the important frequency range lies below f_s and in this range the acoustic properties are determined largely by the values of individual eigenfrequencies.

1.3 "Optimum" room ratio recommendation

The problems related to the eigenmodes and the distribution of modes, e.g coloration of the sound and instability of the sound image, are known for a long time. In the past several author have tried to find an optimum ratio which the room dimensions should meet. The very first who prescribed optimum room ratios was Sabine [53]. In 1900 he already recommended an ideal ratio of 2:3:5. This suggestion is probably based on the ratios of the harmonic intervals in music [37]. The works that are presented in this section are intended to find quick and simple rules for the room ratios in order to permit to evaluate, with simple calculation, if the room has or not an optimum modal distribution. The main scope is to avoid clustering of modes near certain frequencies and excessive gaps between adjacent frequencies. The theory behind the most of these approaches uses the approximation

of the rectangular room with hard walls. Recently several authors are trying to give a better approximation of the room beahvior introducing more parameters, and using the calculation power of the computer simulation.

1.3.1 The Bolt's 'blob'

Richard Bolt [6] in 1946 produced a design chart (fig.1.11) that may be used to determine the average number N of normal frequencies, up to a frequencies ν in a rectangular room of volume V having dimension L, pL, qL where L is the longest dimension of the room and the dimension ratios p and q are equal to or less than unity. The design chart may also be used to determine the average spacing between adjacent normal frequencies in a rectangular room at a given frequency. Defining spacing index ψ as follows:

$$\psi = \frac{1}{\mu_b - \mu_a} \sum_{a}^{b} \left(\frac{\delta^2}{\bar{\delta}} \right) \tag{1.50}$$

where δ is an actual normal frequency space, $\bar{\delta}$ is the average space (as obtained from figure 1.11) at the mean normal frequency of the space δ. μ_b and μ_a are the limiting frequency between which the summation in the above equation is taken.

The index ψ has the properties of a mean squared ratio of actual to average spacing over the band μ_a to μ_b. This quantity is directly a measure of statistical fluctuation in frequency spacing. The figure 1.12 is a plot of the *low frequency space index* ψ. The so-called blob in the chart 3.28 encloses an area of good room proportions given smoothest frequency response at low frequencies in small rectangular rooms, here the dimension ratios of the rectangular room are given as 1:X:Y. Ratios of 2:3:5 and $1 : 2^{1/3} : 4^{1/3}$(1:1,26:1,59) are suggested, by Bolt also notes that there is a broad area over which the average modal spacing criterion is acceptable. This later ratio is often rounded to the commonly quoted figure of 1:1,25:1,6.

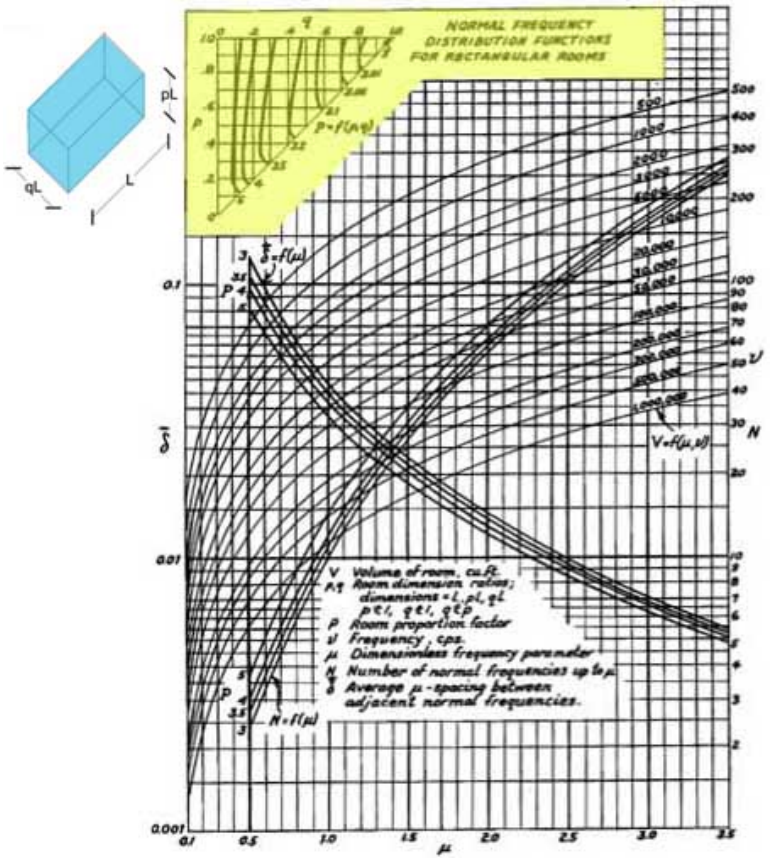

Figure 1.11: Bolt's design chart to determine Normal frequency statistics for Rectangular room. After [6]

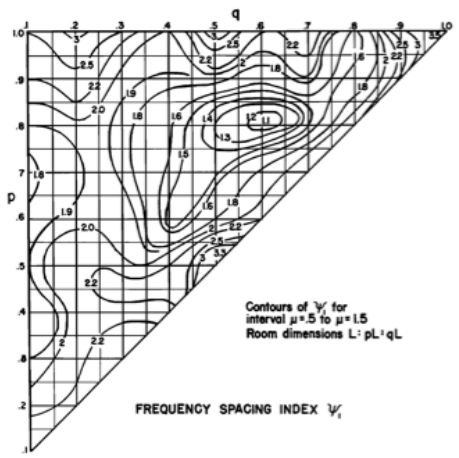

Figure 1.12: Bolt's frequency spacing index plot contour[6].

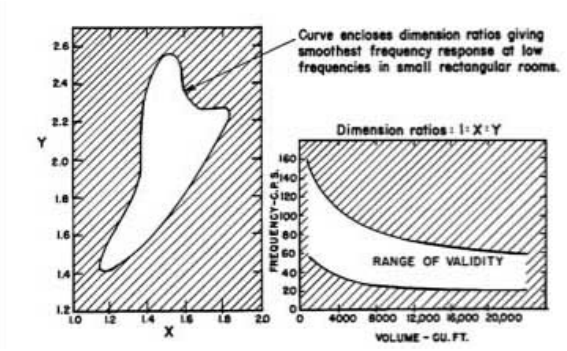

Figure 1.13: Curve domain that encloses dimension ratios given smoothest frequency response at low frequencies in small rectangular room[6].

1.3.2 Louden’s approach

In 1971 Louden [30] proposed a different approach to investigate modal distribution. Initially he calculated 216 eigentones for which room, using the equation 1.34. This number is obtained by allowing n_x, n_y, n_z, separately to take the values 0,1,2,3,4,5. The 216 frequencies are sorted in ascending order to enable the subtraction of each two neighbor frequencies. Up to a limit frequency equal to six times the lowest frequency thus obtained, no eigentone can have a lower frequency than this limit. This frequency limit frequency will be called f_6. In the literature [32, 46] a minimum frequency is given by:

$$f_{min} = \frac{555}{V^{\frac{5}{12}}} \tag{1.51}$$

The problem is to find ratios of rooms dimensions which have evenly distributed eigentones. An ideal room would be a one which the frequency intervals between each tow eigentones follow the curve of $\frac{\delta F}{\delta N}$ as can be obtained from equation 1.38. The greater the deviation between the actual interspacing and $\frac{\delta F}{\delta N}$, the worse will be the acoustic quality of the room. Louden used, as figure of merit to judge room ratio, the standard deviation of the intermode spacing, so again this is a regime to achieve evenly spaced modes. The method produces the well known room ratio of 1:1.4:1.9 [30].

Table 1.1: Louden's dimension-ratios listed in descending order of the acoustic quality of rectangular rooms built according to them [30].

Order	X	Y	SS	Order	X	Y	SS
1	1.9	1.4	1.1445	64	1.9	2.2	1.8097
2	1.9	1.3	1.1542	65	1.3	1.5	1.8173
3	1.5	2.1	1.1677	66	1.6	2.6	1.8262
4	1.5	2.2	1.2064	67	1.1	1.7	1.8352
5	1.2	1.5	1.2158	68	1.6	1.4	1.8392
6	1.4	2.1	1.2213	69	1.8	2.1	1.8492
7	1.1	1.4	1.2260	70	1.5	1.4	1.8668
8	1.8	1.4	1.2311	71	1.7	1.9	1.8768
9	1.6	2.1	1.2488	72	1.3	2.4	1.8798
10	1.2	1.4	1.2612	73	1.4	2.6	1.8949
11	1.6	1.2	1.2623	74	1.5	2.5	1.9060
12	1.6	2.3	1.2771	75	1.1	1.8	1.9216
13	1.6	2.2	1.3178	76	1.4	2.4	1.9286
14	1.8	1.3	1.3335	77	1.2	2.5	1.9298
15	1.1	1.5	1.3503	78	1.7	1.6	1.9379
16	1.6	2.4	1.3841	79	1.4	2.5	1.9665
17	1.6	1.3	1.4028	80	1.6	2.7	2.0019
18	1.9	1.5	1.4139	81	1.9	2.1	2.0158
19	1.1	1.6	1.4285	82	1.3	2.3	2.0213
20	1.3	1.7	1.4352	83	1.2	2.6	2.0260
21	1.8	2.3	1.4404	84	1.1	2.8	2.0352
22	1.9	2.4	1.4527	85	1.7	1.8	2.0586
23	1.4	2.2	1.4592	86	1.3	2.8	2.0735
24	1.7	2.3	1.4747	87	1.2	2.8	2.0766
25	1.7	2.2	1.4839	88	1.2	2.7	2.0972
26	1.9	2.6	1.4956	89	1.5	2.7	2.1003
27	1.4	2.0	1.4969	90	1.1	2.7	2.1045
28	1.3	2.1	1.5038	91	1.3	2.5	2.1193
29	1.5	2.4	1.5172	92	1.7	2.8	2.1211
30	1.9	2.3	1.5209	93	1.5	2.8	2.1341
31	1.9	2.5	1.5233	94	1.7	2.0	2.1409
32	1.9	2.7	1.5268	95	1.1	2.6	2.1556
33	1.8	2.5	1.5285	96	1.1	1.9	2.1576
34	1.5	2.3	1.5291	97	1.2	2.2	2.1585
35	1.8	2.4	1.5318	98	1.3	2.7	2.1680
36	1.8	1.5	1.5504	99	1.8	1.9	2.1731
37	1.7	1.4	1.5598	100	1.6	2.8	2.1772
38	1.7	2.4	1.5598	101	1.2	2.1	2.1948
39	1.2	1.9	1.5630	102	1.1	2.4	2.1988
40	1.5	2.0	1.5761	103	1.2	2.0	2.2080
41	1.7	2.5	1.5785	104	1.4	2.7	2.2367
42	1.8	2.2	1.5785	105	1.5	2.6	2.2431
43	1.9	2.8	1.5824	106	1.8	2.0	2.2670
44	1.6	1.8	1.5896	107	1.2	2.3	2.2848
45	1.6	2.0	1.5963	108	1.2	2.4	2.2892
46	1.8	2.6	1.5966	109	1.1	2.5	2.2986
47	1.1	1.3	1.6011	110	1.2	1.2	2.3225
48	1.7	1.2	1.6133	111	1.3	2.6	2.4083
49	1.2	1.3	1.6145	112	1.6	1.6	2.4259
50	1.8	2.8	1.6277	113	1.1	2.3	2.4298
51	1.6	2.5	1.6289	114	1.1	2.1	2.4594
52	1.4	1.3	1.6479	115	1.1	2.0	2.4622
53	1.8	2.7	1.6541	116	1.9	2.0	2.5013
54	1.1	1.2	1.6588	117	1.3	1.3	2.5252
55	1.2	1.8	1.6692	118	1.5	1.5	2.5639
56	1.9	1.6	1.6813	119	1.8	1.8	2.6452
57	1.7	2.1	1.6938	120	1.9	1.9	2.7124
58	1.3	2.0	1.7038	121	1.7	1.7	2.7300
59	1.4	2.3	1.7116	122	1.1	2.2	2.7453
60	1.5	1.6	1.7414	123	1.4	1.4	2.8161
61	1.7	2.7	1.7693	124	1.4	2.8	2.8288
62	1.7	2.6	1.7909	125	1.7	1.5	1.8004
63	1.3	2.2	1.7944				

1.3.3 Walker's ratio range

The purpose of the Walker's work [54] was to derive a relatively simple criterion for room proportions, to encompass the majority of the area of "good quality" rooms and exclude all of the "poor" rooms and to be accepted as a uniform standard for high quality listing environments. First of all Walker [55] investigated several different room quality indices and he recognized the "mean square spacing of mode frequencies" as the most important factor. In general, a rectangular room has four principal characteristic dimensional parameters: length, width, height and volume (any three of which are independent). A fully general plot of the quality would therefore be four dimensional and difficult to portray on paper. By fixing one or more of these four parameters, the number of independent axes can be reduced. Subsequently Bolt investigated several plot contour[8] with a fixed parameter (fig. 1.14).

Walker [54] proposed a criterion in order to modify the Draft Technical Recommendations for the Nordic Public Broadcasting Corporations [12] (fig.1.15). He improved the criterion shifting the permissible $\frac{l}{w}$ ratios from 1.25-1.45 towards about 1.1-1.35 in order to permit to smaller room to fit in the criteria as well. Figure 1.16 shows a much better basis for a criterion. The lower limit for $\frac{l}{w}$ is of the same form as previously, that is, a simple multiplier. In the figure 1.16 $\frac{l}{w}$ has the value of 1.1. This is indicated by the line **a-a**. The upper limit for $\frac{l}{h}$ has been altered to the line marked **b-b**. It clearly includes much more of the usable range of "better" rooms. On the axes of $\frac{l}{h}$ and $\frac{w}{h}$, the equation of line **b-b** is:

$$\frac{l}{h} = 4.5\frac{w}{h} - 4 \tag{1.52}$$

(The exact position of the line **b-b** has been chosen to make coefficients numerically relatively simple.) So the proposed new criterion for acceptable room proportion is [54]:

$$1.1\left(\frac{w}{h} \leq \frac{l}{h}\right) \leq \left(4.5\frac{w}{h} - 4\right) \tag{1.53}$$

Now it is possible to evaluate, through this formula, the behavior of the room. The effectiveness and the success of this formula is the fact that

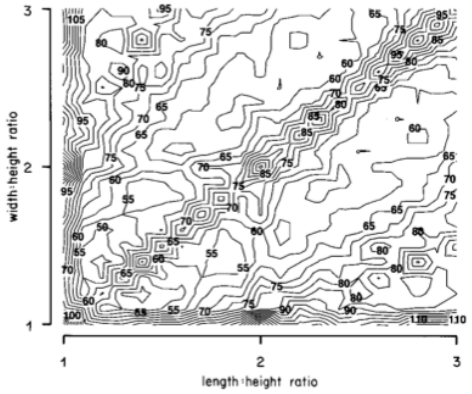

(a) Contour map of room quality for $200m^3$ room, using mean square mode spacing for modes up to 120 Hz[54].

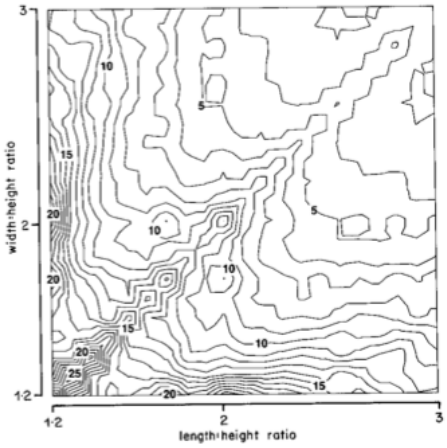

(b) Contour map of room quality for fixed height of 3.5 m and variable volume.

Figure 1.14: Different contour map plotted by Walker of room quality, for different fixed parameter. After [54].

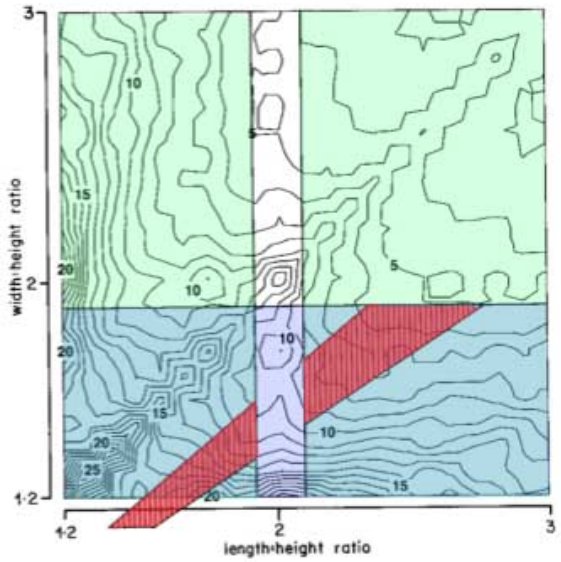

Figure 1.15: Contour map of room "quality" for fixed height of 3.5 m and variable volume, overlaid with room proportion design criteria from the Nordic Public Broadcasting Corporation. After [54].

there is not complex calculation to do or theory to know. Because of this conciseness it was selected as criteria in the ITU-R BS 1116-1 [26] and EBU document Tech 3276-1966 [14]. Despite the fact that Bolt [6] and Walker [54] used different method to arrive to a valid area of room ratio, it is possible to see in figure 1.17 that the solutions overlap in some areas.

1.3.4 Bonello's criterion

Proof that modal resonances in rooms are an international problem, this method of evaluating their effect comes from Buenos Aires. The goal of the Bonello criterion [7] was to inform the designer whether or not the three dimensions for a given room are correct. If they are not, one or more of them should be changed, and the criterion applied once again. It should also inform the designer about the frequency band in which there will be coloring of sound in case the dimensions cannot be corrected. The first step consists of calculating, by means of a minicomputer or a programmable calculator program, each of the lower resonance modes of the room. Equation 1.34 is used for this calculation.

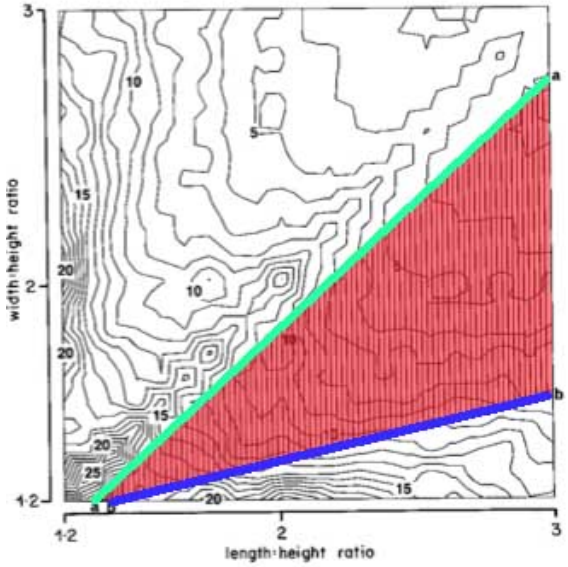

Figure 1.16: Contour map of room "quality" for fixed height of 3.5 m and variable volume, overlaid with the Walker's criteria. After [54].

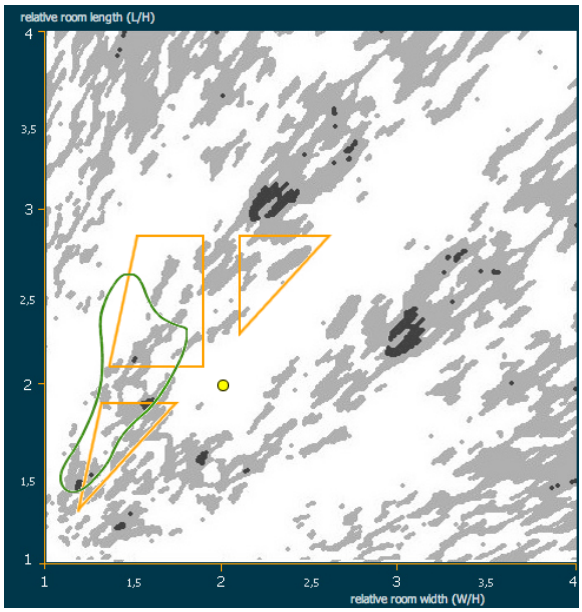

Figure 1.17: The Green contour is the Bolt's blob, the orange one is the Walker contour. The canvas comes from a Cox publication [11]. Dark areas on diagram background correspond to room sizes with the smoothest modal characteristics; consequently, these corresponding proportions are more acceptable while building music-rooms and control rooms. Best proportions areas are shown in black color, gray color is given to areas of acceptable proportions, and others are shown in white. After [40].

It is not necessary to exceed a certain frequency or a certain order, due to considerations already noted and based on equations 1.39 and 1.40. In the programs, which will be discussed later, the calculation is limited to the first 48 modes. Once the eigenfrequencies of the room are known, we analyze how many modes fall within each interval into which we divide the frequency spectrum. If we use the simplifying hypothesis that the ear is unable to discriminate modes within the interval, but only the sum of their contributions to the sound energy received within that band, it is necessary to know only the number of modes to obtain the total sound pressure. This implies that each mode is considered, taking in account its response to sound pressure given by equation 1.45. In the Bonello's opinion [7], it is this concept of energy instead of frequency spacing that makes the criterion plausible.

One of the main point for the Bonello criterion is what bandwidth shall we choose. The value finally adopted is one-third octave. It is used a relative bandwidth, not an absolute one, taking into account the logarithmic characteristic of auditory perception and the ear's response to musical intervals. We are also influenced by electroacoustical experience which indicates the usefulness of one-third octave as a minimum unit of bandwidth. According to these concepts, the number of eigentones falling within each one-third octave between 10 Hz and 200 Hz is calculated; this number gives the modal density function per one-third octave, $D = F(f)$. The program plots modal density as ordinates and frequencies as logarithmic abscissas (the center frequencies of the one-third-octave bands). To analyze this curve, is important know that for optimum room dimensions the following conditions should be met:

1. The curve $D = F(f)$ should increase monotonically. Each one-third octave should have more modes than the preceding one (or, at least, an equal number if $D = 1$).

2. There should be no double modes. Or, at most, double modes will be tolerated only in one-third-octave bands with densities equal to or greater than 5.

Bonello assumed the condition that two successive bands can have the same number of modes with D greater than 1. This condition simplifies

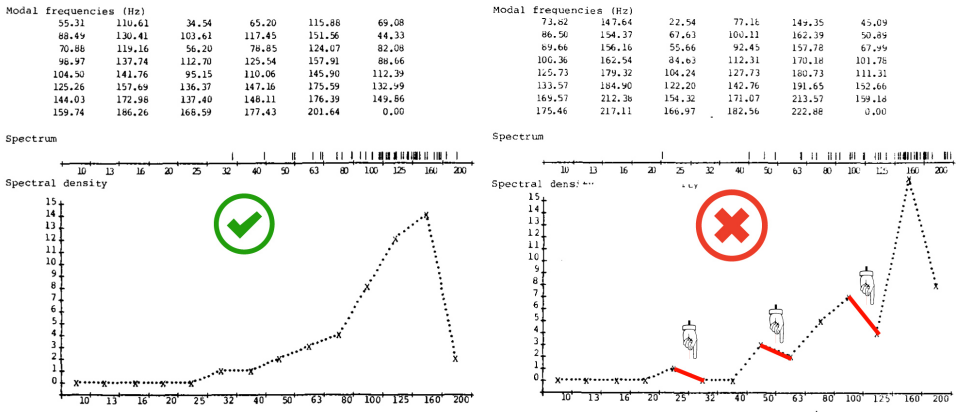

Figure 1.18: Calculation of resonance modes and application of the Bonello criterion for a studio of 60 m^3. Comparsion between the relatioship 1:1.25:1.6 and 7.63:3.36:2.33. After [7].

the requirements, even though conditions 1) and 2) of the criterion are to be preferred in the design stage. In figure 1.18 two computer plots of curve $D = F(f)$ are proposed. The first one shows a room that complies satisfactorily with the criterion, while the other room does not, and its dimensions are not recommended for this room volume. Because of the limited number of calculated modes, the density curve increases up to a certain frequency and then begins to decrease. Accordingly, condition 1) should be applied only up to that frequency.

One of the most interesting part of the Bonello's work was the comparison between different criteria. First he analyzes the ratio recommended by Knudsen [27] for small studios, 1:1.25:1.6. This same ratio was recommended by Olson [35] and others. He [7] validates this ratio, like it is possible to see in figure 1.18. He standardized all ratios for 60 m^3. Some comply with both criteria (such as F and I). The lack of correspondence for some values has been noted by other authors and is due, besides other factors, to the room volume, an important parameter which Bonello criterion takes into account. Thus the same relationship can be acceptable for one size of room and acceptable for another.

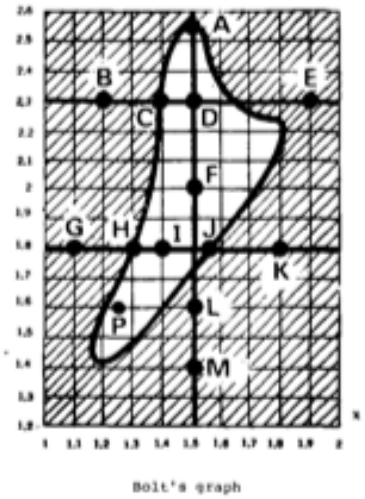

Figure 1.19: Comparative analysis of Bolt’s criterion with that proposed by Bonello. The ratios have been standardized for $60m^3$. After [7].

1.3.5 The Fazenda’s of the Modulation Transfer Function based analysis

Recently the approach to the small room acoustic is changing. Thanks to the higher computational power given by new computer it is possible to use new kinds of models that avoid the approximation of the theories discussed above. Fazenda et al. [16] concentrated on the use of the MTF as an objective measure of reproduction quality of audio system at low frequencies. The MTF incorporates both time and frequency domain information and it has been suggested that it can be a useful measure of the accuracy with which details in the low frequency sounds are perceived. The MTF measures the ability of a system to preserve depth of modulation from an input signal at specified frequency bands. This can be obtained directly from the following expression:

$$m(F) \approx \frac{\sum_0^N h_f^2(n) e^{-j2\pi \frac{Fn}{Fs}}}{\sum_0^N h_f^2(n)} \tag{1.54}$$

Where F is the modulation frequency and $h_f(n)$ is the discrete impulse response of the system, band-pass filtered with centre frequency *f*. Ten modulation frequencies are used in the range 3.15 Hz to 12.14 Hz. The

results are then averaged over all modulation frequencies and a figure is obtained for each of the frequency bands. The MTF response then describes the performance of the system over the frequency range under test. Result are bound between 0 and 1, with 1 corresponding to full modulation preservation. A single figure score may be obtained by further averaging all frequency bands. The Green function (eq. 1.20) has been used as a model to generate discrete room responses at sampling frequency Fs (512 Hz). This technique is known to perform well at low levels of damping and has been used successfully for similar work. At high damping levels the result from the model start to diverge from the exact conditions found in a specific room. As the model is used here to represent generic condition found in a room rather than a specific room response, the Fazenda approach is considered appropriate and is not deemed to affect the overall trend of result. The length of these digital filters has a direct consequence on the MTF results, restricting a maximum score obtained for the MTF and, in extreme cases (500+points), dominating the result such that what is being measured is the response of the filters themselves. Care has been taken to ensure that the results obtained relate to the corresponding room responses rather than the digital filtering effects. The maximum value of the MTF has been calibrated using the response of a delta function.

The modulation transfer function has been the basis for speech intelligibility systems such as the Speech Transmission Index (STI), and therefore closely associated with assessing the subjective performance in conveying audio information to listeners. Rating scales have been previously defined for intelligibility scores and these are also applied here to quantify the subjective performance of room responses.

Different room characteristics have been frequently regarded as relevant factors affecting the reproduction quality at low frequencies:

Volume affecting the modal density at the very low frequencies;

Aspect ratios affecting the modal distribution;

Effective absorption affecting low frequency damping;

MTF plots of listening rooms describing their low frequency performance correlate well to the subjective perception of quality and detail

at low frequencies. In order to attain high MTF scores, any excessive modal activity must be controlled and the MTF plot is therefore a useful indicator of which frequency range may be the most problematic in any given listening room. An added advantage of using the MTF to measure room performance is that, when applied to room measurements, the results will also include the performance of the loudspeakers used, so combined MTF scores can assess different loudspeaker/room combinations, including position-related effects. Furthermore, these factors have a clear effect on measurements of frequency and time responses in rooms. The relative changes produced on the scores of the MTF for each of these factors is investigated. The influence of source/receiver location is another important factor. However, although this has not been included in the investigation, it is nevertheless an important factor and a possible subject of further investigations. The results suggest that volume and aspect ratio of rooms appear to have a peripheral effect on subjective performance of rooms used for audio monitoring, with variation of these factors not affecting significantly the MTF scores. Investigations presented here have shown that changing the room dimensions or sizes, despite having considerable effect on the modal distribution and range, do not significantly affect the MTF figure as long as the damping in the room remains typically low. In contrast, a reduction of the decay time of room responses is mirrored by an increase in the MTF score suggesting that lower decays afford more precise monitoring conditions. This result is in accordance with other works that show how any resonant low frequencies can mask the details in other low frequency sounds, and hence can reduce the overall bass definition in the perception of a musical signal.

1.4 ITU 1116 and EBU 3276 recommendation

The most important standard in room acoustic is the ISO standard 3382 [50]. This standard concerns the measurement calculation methods for room acoustical parameters in large rooms such as concert halls and theatres. As this standard only concerns large rooms with a statistical sound field, it is not applicable in small rooms, *i.e.* critical listening

Table 1.2: Resuming table of the ideal room ratio theory scheme.

	Approach 1	Approach 2
Room shape	Rectangular	Rectangular
Wall	rigid and smooth	Considering damping
Source	X	Point source
Equation	$\nabla^2 p + k^2 p = 0$	$\nabla^2 p + k^2 p = -i\omega\rho_0 q(\mathbf{r})$
Authors	Bolt[6] (1946), Louden[30] (1971), Bonello[7] (1981), Walker[54] (1992)	Fazenda[16](2006)

environments, with their distinct characteristic of a non-diffuse sound field.

Contrary to large room acoustics, there is no standard for small room acoustics. For the benefit of the designers as well as the users it is convenient to have some kind of frame to refer to. To achieve a uniform discrete multichannel system, the International Telecommunication Union (ITU) and the European Broadcasting Union (EBU) have edited recommendations. These recommendations are intended for the use in the assessment of systems which introduce impairments so small as to be undetectable without rigorous control of experimental conditions and appropriate statistical analyses [26].

Concerning the design of control rooms the most important recommendation is the ITU-R BS 1116-1, that concerns the listening condition. Among others recommendation this implies room acoustical design issues such as room shape, proportions, reverberation time, sound field conditions etc.. Based on the ITU recommendations the EBU has made three important recommendations regarding the listening conditions. The listening conditions for monophonic and two-channel stereophonic presentations are given in the EBU document Tech 3276-1966 [14]. It has to be noted all the above mentioned documents are recommendations. Therefore all of the documents cannot restrict the designer or client. Nevertheless the documents can be used as a tool for the designer as well as for the client in defining their demands for the designer of a control room.

ITU-R BS 1116-1 describe the listening conditions and arrangement

recommended. "listening conditions" consist of the complex acoustic requirements for a reference sound field affecting a listener in a listening room at the reference listening point, for sound reproduced by loudspeakers. This includes:

- the acoustical and geometric characteristics of the listening room;
- the arrangement of the loudspeakers in the listening room;
- the location of the reference listening point or area;

The above cited factors are producing the resulting sound field characteristics at that point or area. Since the state of the art does not yet allow the description of the reference sound field completely and uniquely by acoustical parameters, some geometric and room acoustic requirements for a reference listening room are given to ensure the viability of the listening conditions described.

Hence every parameter below described has a tolerance limit, that is the recommendation for a listening room.

1.4.1 Tolerance limits on the reverberation time

Until the Fifties, reverberation time was regarded as the most significant parameter for the description of the acoustical properties of a room. Reverberation time T is defined as the duration required for the space-averaged sound energy density in an enclosure to decrease by 60 dB after the source emission has stopped [50]. Worth mentioning that reverberation time is more commonly evaluated on a range smaller than 60 dB on the linear regression fit of the decay curve and extrapolated to a decay of 60 dB. The amount of overall absorbance in a listening room is still important in establishing the general listening conditions. If the room is excessively dead or too live and reverberant, listener fatigue might develop and music quality may deteriorate. Technically, the term reverberation time should not be associated with relatively small spaces in which random sound fields do not exist. However, some first step must be taken to calculate the amount of absorbent needed to bring the general acoustical character of a room up to an acceptable level. While reverberation time is useful for this purpose, it would be

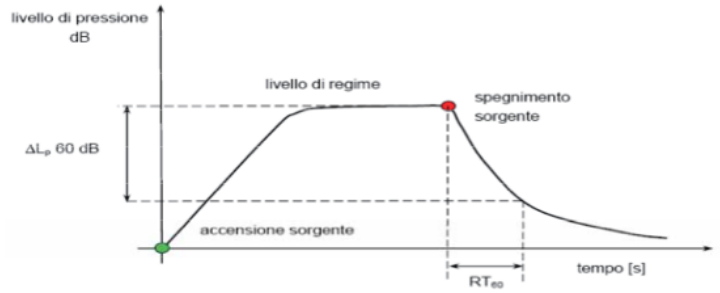

Figure 1.20: Sound pressure level vs. time graph that shows the decay

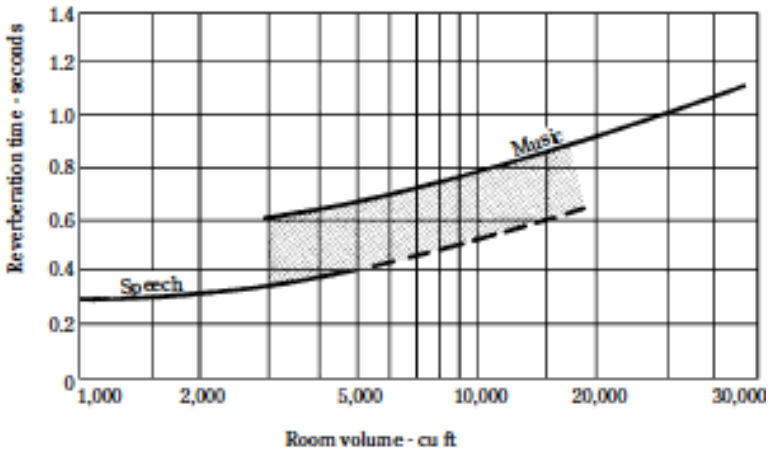

Figure 1.21: Suggested reverberation times for recording studios. The shaded area is a compromise region for studios in which both music and speech are recorded. After [13].

unfortunate to convey the impression that the values of reverberation time so obtained have the same meaning as that in a large space. If the reverberation time is too long (sound decays too slowly), speech syllables and music phrases are slurred and a definite deterioration of speech intelligibility and music quality results. If rooms are too dead (reverberation time too short), music and speech lose character and suffer in quality, with music suffering more. These effects are not so definite and precise as to encourage thinking that there is a specific optimum reverberation time, because many other factors are involved. In spite of so many variables, readers need guidance, and there is a body of experience from which we can extract helpful information. Figure 1.21 is an approximation rather than a true optimum but following it will result in reasonable, usable conditions [13].

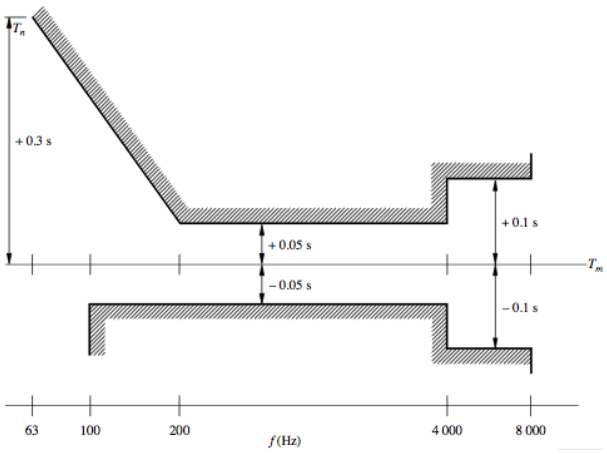

Figure 1.22: Tolerance limits for the reverberation time, relative to the average value, T_m [26].

The ITU-R BS 1116-1 [26] requires a reverberation field sufficiently diffuse over the listening area to avoid perceptible acoustical effects such as flutter echoes. The average value of reverberation time T_m measured over the frequency range from 200 Hz to 4 kHz should be:

$$T_m = 0,25(V/V_0)^{\frac{1}{3}} \tag{1.55}$$

where V is the volume of room in m^3, V_0 is the reference volume of 100 m^3. The tolerances to be applied to T_m over the frequency range from 63 Hz to 8 kHz are given in Fig. 1.22. The tolerance limits based on the room volume gives for standard studio a medium result of 0,3 s, that it is assumed also from Everest [13] as a good value for a listening room. During the past century several formulae for predicting reverberation time were developed empirically and theoretically, based on the assumption of homogeneous repartition of sound energy within the room, and consequently uniformly distributed sound absorption. The prediction of the reverberation time is very useful for the design of listening rooms. The first and most remarkable approach to describe the reverberation characteristics of an enclosure was found by W.C. Sabine [37] around 1900. Sabine established his theory on the basis of practical results. This parameter, found by Sabine, is given by equation:

$$T = 0,16\frac{V}{A} \tag{1.56}$$

where V is the volume in m^3 and A (m^2) is the equivalent absorbing area. The equivalent absorbing area is proportional to the absorption coefficient of the materials and the total surface. It was discovered by Eyring that the classical formula given by Sabine is not fulfilled when there is considerable room absorption. Eyring pointed out in his paper that Sabines formula is essentially a formula for a live room ($\overline{\alpha} \leq 0,253$) and that the reverberation time is shape dependent[4]. He presented the revised theory thoroughly and derived a form of the reverberation time equation, which is more general than Sabines formula.

The Eyring formula is given by equation:

$$T = 0,16\frac{V}{-Sln(1-\overline{\alpha})} \tag{1.57}$$

Where $\overline{\alpha}$ is the mean absorption coefficient value:

$$\overline{\alpha} = \frac{1}{S}(\sum_i S_i\alpha_i) \tag{1.58}$$

Subsequently that formula was revisited by Millington [31] and Sette [39] and other recently by other author.

In order to characterize the room it is important to take measurement of the reverberation time in all the room, but mainly in the listening position. The distance between the loudspeakers is defined in the ITU 1116 [26] as D (see figure 1.23) and the distance between the loudspeakers is defined as B.

The recommendation explains that preferred limits are D = 2-3 m, but values of B up to 5 m may be acceptable in suitably designed rooms. The limits of the distance between the loudspeaker and the listener ranges from 2 to 1.7 B (m). The reference base angle should be equal to 60.

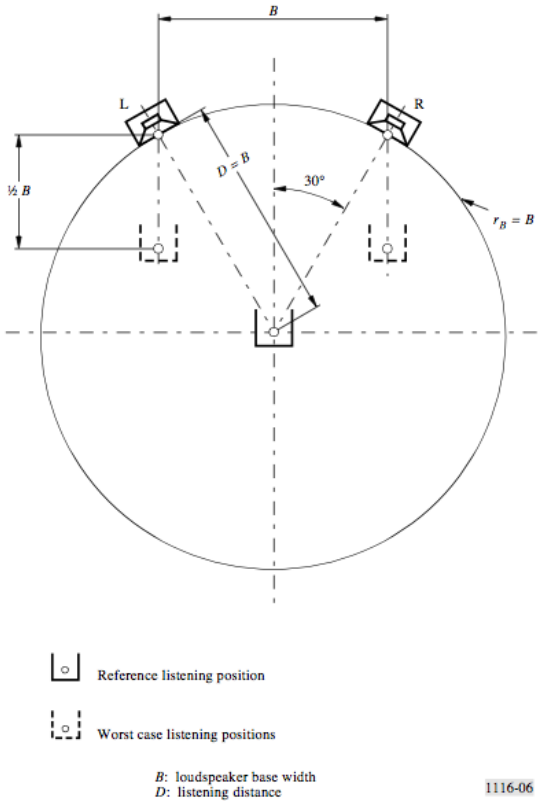

Figure 1.23: Test listening arrangement with loudspeakers L and R for stereophonic sound systems with small impairments

1.4.2 Background noise in a listening room

The background noise levels in recording studios, control rooms, and listening rooms must be kept under control if these rooms are to be of maximum use in their intended way. Hums, buzzes, rumbles, aircraft noises, tooting auto horns, dogs barking, or typewriter sounds are most incongruous if audible during a lull in a program. Such sounds might not be noticed outside the studio when they are a natural part of the situation, but during a pause or a quiet musical or speech passage, they stand out like the proverbial sore pollex. In a studio, interfering sounds can come from control-room monitors operating at high level or from equipment, in adjacent areas. Control rooms have their own noise problems, some intruding from the outside, some generated by recorders, equipment cooling fans, etc. There is one source of noise, however, that is common to all sound sensitive rooms, and that is the noise coming from the air-conditioning diffusors or grilles. A certain feeling of helplessness in approaching air-conditioning noise problems is widespread and quite understandable. The control of air-conditioning noise can be expensive. A noise specification in an air-conditioning contract for a new structure can escalate the price. Alterations of an existing air-conditioning system to correct high noise levels can be even more expensive. It is important for studio designers to have a basic understanding of potential noise problems in air-conditioning systems so that adequate control and supervision can be exercised during planning stages and installation [13]. The single most important decision having to do with background noise is the selection of a noise-level goal. The recommendations [26, 14] use the NR-Rating that is commonly used in Europe, whereas the the Noise Criterion (NC) is more common in USA. The selection of one of these contours establishes the goal of maximum allowable noise-pressure level in each octave band. Putting the noise goal in this form makes it easily checkable by instruments. The downward slope of these contours reflects both the lower sensitivity of the human ear at low frequencies and the fact that most noises with distributed energy drop off with frequency. To determine whether the noise in a given room meets the contour goal selected, sound-pressure

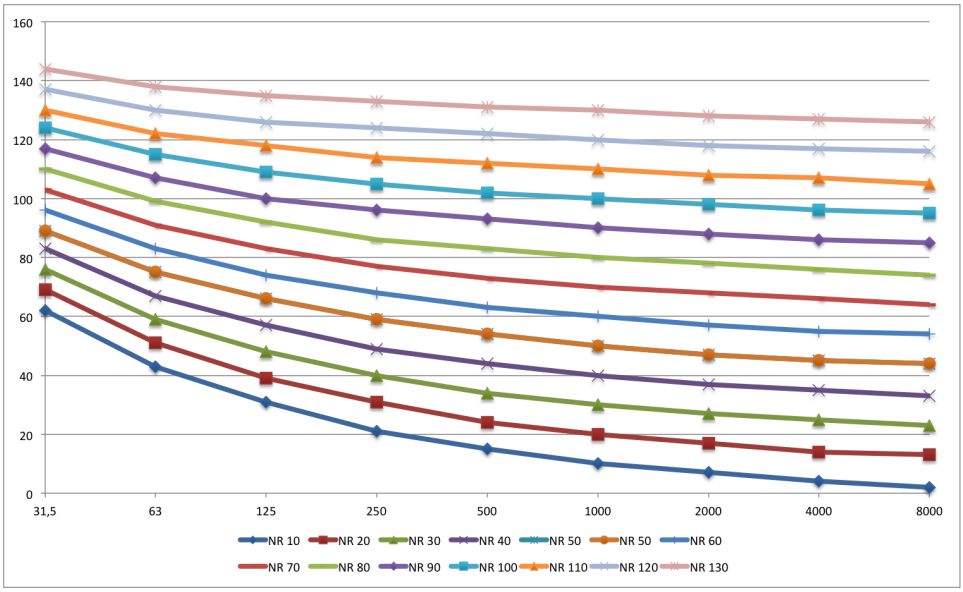

Figure 1.24: NR curves, Noise rating diagram based on the information of the ISO 9568 [25].

level readings are made in each octave and plotted as in figure 1.24.

The recommendations [26, 14] fix a limit for continuous background noise (produced by an air conditioning system, internal equipment or other external sources), measured in the listening area at a height of 1.2 m above the floor that should preferably not exceed NR 10. This recommendation comes from the Beranek's work [5], made in the 1971 and it was included in the ISO Recommendation R1996, but it was withdrawn. Despite in the recommendation there are not so much informations about measurements it is possible to use the ISO 9568 [25].

Chapter 2

Loudspeakers in room

A loudspeaker is an electroacoustic transducer that produces sound in response to an electrical audio signal input. To adequately reproduce a wide range of frequencies, most loudspeaker systems employ more than one driver, in particular to reach higher sound pressure level or maximum accuracy. Individual drivers are used to reproduce different frequency ranges. The drivers are named subwoofers, for very low frequencies; woofers for low frequencies (see figure 2.1); mid-range speakers for middle frequencies (see figure 2.3); tweeters for high frequencies (see figure 2.1); and sometimes supertweeters, optimized for the highest audible frequencies. The terms for different speaker drivers differ, depending on the application. In two-way systems there is no mid-range driver, so the task of reproducing the mid-range sounds falls upon the woofer and tweeter. When multiple drivers are used in a system, a "filter network", called crossover, separates the incoming signal into different frequency ranges and routes them to the appropriate driver. A loudspeaker system with n separate frequency bands is described as "n-way speakers": a two-way system will have a woofer and a tweeter; a three-way system employs a woofer, a mid-range, and a tweeter.

Most loudspeaker systems consist of drivers mounted in an enclosure, or cabinet. The role of the enclosure is to provide a place to physically mount the drivers and to prevent sound waves emanating from the back of a driver from interfering destructively with those from the front; these typically cause cancellations (*e.g.* comb filtering) and significantly alter the level and quality of sound at low frequencies.

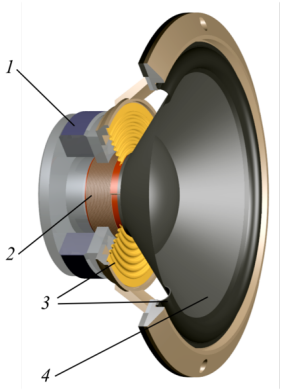

Figure 2.1: Cutaway view of a dynamic loudspeaker for the bass register. 1. Magnet 2. Voicecoil 3. Suspension 4. Diaphragm.

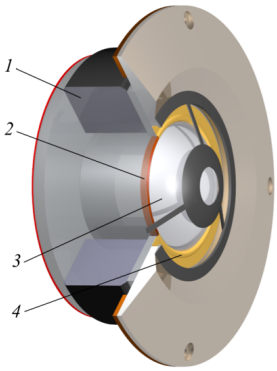

Figure 2.2: Cutaway view of a dynamic tweeter with acoustic lens and a dome-shaped membrane. 1. Magnet 2. Voicecoil 3. Membrane 4. Suspension.

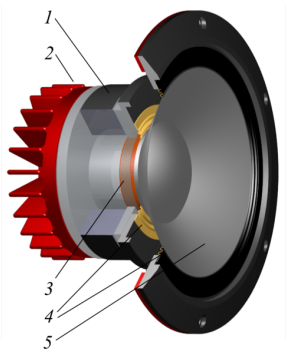

Figure 2.3: Cutaway view of a dynamic midrange speaker.1. Magnet 2. Cooler (sometimes present) 3. Voicecoil 4. Suspension 5. Membrane.

The simplest driver mount is a flat panel (*i.e.* baffle) with the drivers mounted in holes in it. However, in this approach, sound frequencies with a wavelength longer than the baffle dimensions are canceled out, because the anti-phase radiation from the rear of the cone interferes with the radiation from the front. With an infinitely large panel, this interference could be entirely prevented. A sufficiently large sealed box can perform this behavior. Since panels of infinite dimensions are not feasible, most enclosures function by containing the rear radiation from the moving diaphragm. A sealed enclosure prevents the transmission of the sound emitted from the rear of the loudspeaker by confining the sound in a rigid and airtight box. Techniques used to reduce transmission of sound through the walls of the cabinet include thicker cabinet walls, lossy wall material, internal bracing, curved cabinet walls or more rarely, visco-elastic materials (*e.g.* mineral-loaded bitumen) or thin lead sheeting applied to the interior enclosure walls. However, a rigid enclosure reflects sound internally, which can then be transmitted back through the loudspeaker diaphragm resulting in degradation of sound quality. This effect can be reduced by filling the enclosure with absorptive materials, such as glass wool, wool, or synthetic fiber batting. The internal shape of the enclosure can also be designed to reduce this effect by reflecting sounds away from the loudspeaker diaphragm, where they may then be absorbed. Other enclosure types alter the rear sound radiation so that it can interfere constructively with the output from the front of the cone. This kinds of enclosures (including bass reflex, passive radiator, transmission line, *etc.*) are often used to extend the effective low-frequency response and increase low-frequency output of the driver.

The radiation pattern a plot graph of an index that indicate how much of the total energy from the source is radiating in a particular direction. It is important to know the typical radiation pattern of conventional loudspeaker in order to understand the result of the measurements.

Figure 2.5 shows three polar plots of low frequency loudspeaker radiation. The first pattern (a) is that of a dipole source. This is the typical radiation pattern of a conventional woofer on a simple open

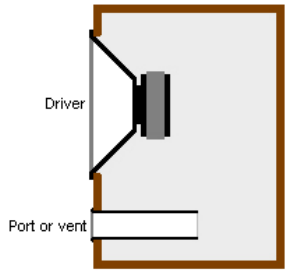

Figure 2.4: Bass reflex enclosure schematic cross-section.

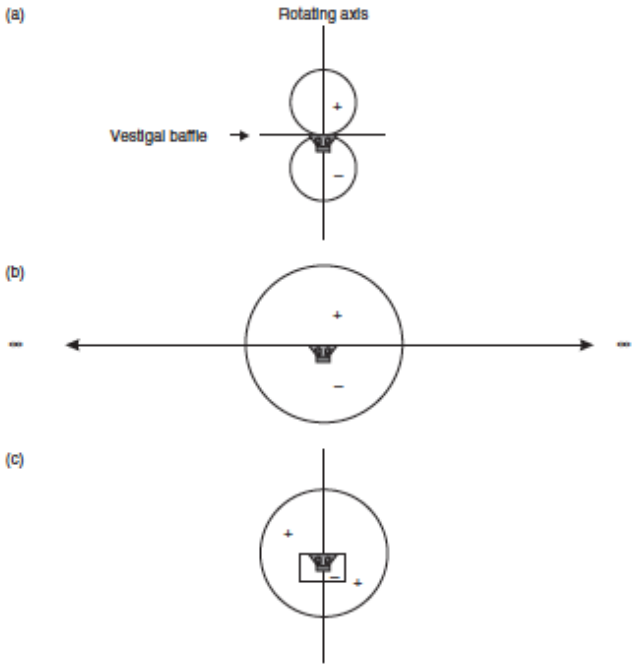

Figure 2.5: Loudspeaker radiation patterns at low frequencies: (a) Dipole source; (b) True infinite baffle; (c) Monopole source (such as a sealed box). After [33].

baffle board. The effect is also typical of the flat electrostatic loudspeakers with open backs. When the diaphragm is driven forwards, a positive pressure is generated in front of the diaphragm and a negative pressure is generated behind it. The lack of enclosure behind the loudspeaker allows the pressure to equalize at the sides, simply by traveling around the edges of the baffle. The size of the baffle board on which the loudspeaker is mounted determines the frequency below which the cancellation will be effective.

Assuming a perfect source, for a listener seated directly in front of the loudspeaker, the perceived frequency response will be down to the frequency where the cancellation begins due to the finite size of the baffle. Below the cancellation a roll-off will begin, which will finally reach 18 dB-octave. For a listener on the extended line of the baffle, *i.e.* listening from side-on, the pressure radiated at the front and rear of the loudspeaker diaphragm will be equal and opposite, and hence they will cancel. This explains the null that appears on both sides of the source in figure 2.5 **a**. If the baffle could be extended to infinity in all directions of its plane, such cancellation would not exist. Hence, for the same drive conditions as shown in **a** the radiation pattern would be as shown in figure 2.5 **b**. Here the areas of positive and negative pressure still exist at the front and rear of the driver, but the truly infinite baffle has prevented the cancellation from occurring around the sides. The radiation pattern becomes a sphere, with the baffle dividing the region of positive and negative pressure. The term infinite baffle is often wrongly used to describe a sealed box loudspeaker. Figure 2.5 (**c** shows how the sealed box in fact resembles more a monopole source. A monopole source describes the radiation pattern of a small pulsating sphere (compared with the wavelength involved). As the sphere cabinet is completely enclosed and in free space, a positive pressure in front of the diaphragm would also radiate in all directions at low frequencies, with the negative pressure being trapped inside the box as the diaphragm moves outwards. As the frequencies rise to a point where the wavelength begins to equal the circumference of the radiating diaphragm, the radiation angle begins to narrow. This is shown in figure 2.6. Here it can be seen that, at positions off-axis, the dis-

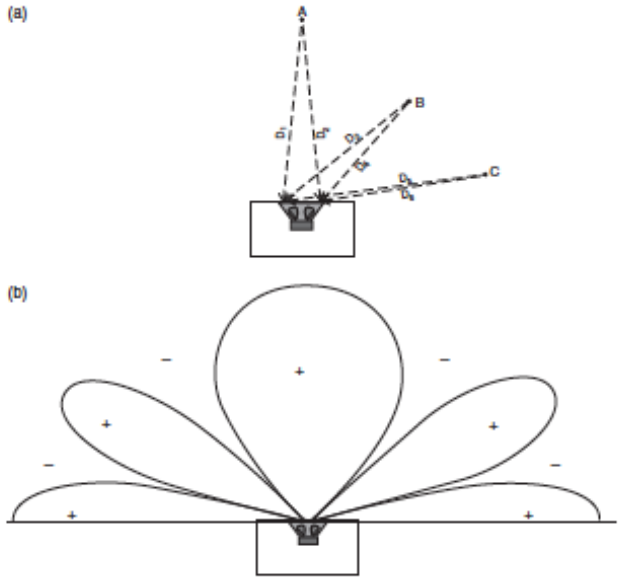

Figure 2.6: Radiation from a sealed box loudspeaker. After [33].

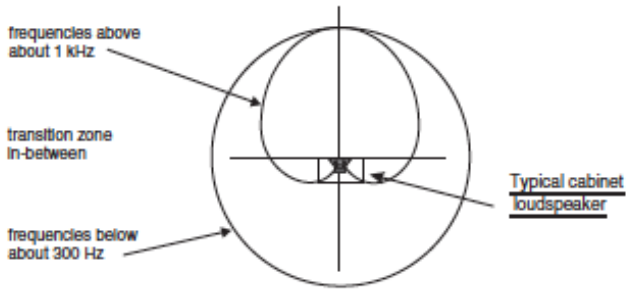

Figure 2.7: Directivity versus frequency in a conventional box loudspeaker. After [33].

tance to the nearest and farthest points on the radiating diaphragm are such that the path length difference to the listening position becomes out of step by half a wavelength, and hence the radiation from these points cancel. When this point is approached, *i.e.* where the uniform forward radiating angle becomes too narrow, it is customary to cross over to a smaller loudspeaker, in order to avoid the forward beaming of high frequencies. In most full range loudspeaker designs there is a gradual narrowing of the response towards the mid frequencies and then, by means of selecting drivers of the appropriate source sizes, that response angle would be maintained until the highest frequencies.

The typical radiation pattern of a conventional box loudspeaker is

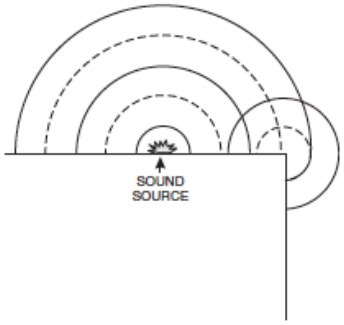

Figure 2.8: Diffraction sources. Representation of the sudden increase in the rate of expansion of a wavefront at a sharp edge. The diffracted wave in the region round the corner has the same phase as the incident wave on the edge, but the diffracted wave, traveling back from the edge towards the source, is phase-reversed. After [33].

shown in figure 2.7.

The diffraction plays a key role when considering the shape of the loudspeaker. Figure 2.8 shows the diffraction caused by the edges of loudspeaker cabinets. Effectively what happens is that the expanding radiated wave travels along the front surface of the loudspeaker cabinet until it arrives at a discontinuity, such as the cabinet edge. From this point on it suddenly has to expand more rapidly around the corner, but the same pressure cannot be sustained in the new, larger volume into which it expands. This sudden increase in expansion rate is due to a change in acoustic impedance, and any change in impedance will send back a reflected wave. The radiation that turns the corner is in-phase with the source, but the reflected wave, due to the sudden drop in pressure, radiates back to the source out of phase. This gives the effect of a spherical type of wave expansion that appears to emanate from the corner discontinuity, giving to the listener the effect shown in figure 2.9. The total effect may be considered as though the loudspeaker were mounted on an infinite baffle, but with additional sources mounted at the positions of the cabinet edges. Objects in any room in which a loudspeaker may be positioned, and especially objects close to a loudspeaker can all act as diffraction sources, disturbing in yet another way the free-field response of a loudspeaker.

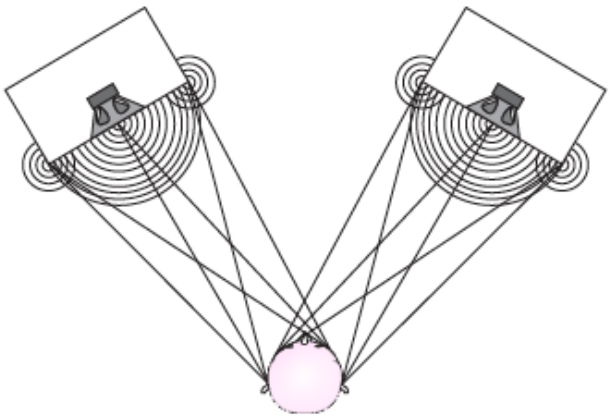

Figure 2.9: Cabinet diffraction. The sharp edges of loudspeaker boxes, mixing console meter bridges, and any other abrupt cross-sectional changes between the loudspeakers and the listener will form secondary diffraction sources that can smear the stereo imaging. It is to help to avoid this problem that many loudspeaker cabinets have rounded or bevelled edges. After [33].

2.1 Sound power and sound intensity

A sound source radiates power and this results in a sound pressure. Sound power is the cause, whereas sound pressure is the effect. It is possible to make the following analogy: an electric heater radiates heat into a room and temperature is the effect. Temperature is also the physical quantity that makes feel hot or cold. The temperature in the room is, first of all, dependent on the room itself, the insulation, and whether other sources of heat are present. But for the same electrical power input, the heater radiates the same power, no matter what environment it is in. The relationship between sound power and sound pressure is similar. What it is possible to hear is the sound pressure but it is caused by the sound power emitted from the source.

A too high sound pressure may cause hearing damage. So when trying to quantify human response to sound, such as noise annoyance or the risk of hearing loss, pressure is the obvious quantity to measure. It is also relatively easy to measure: the pressure variations on the eardrum we perceive as sound are the same pressure variations which are detected on the diaphragm of a condenser microphone.

The sound pressure that it is possible to hear, or measure with

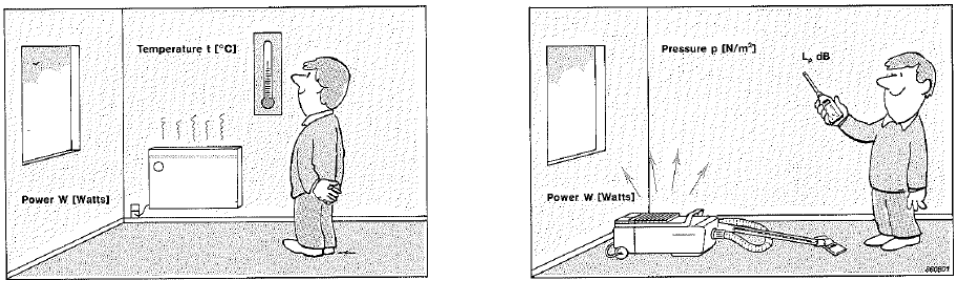

Figure 2.10: Images that explain the thermal analogy with the sound field. After [9]

a microphone, is dependent on the distance from the source and the acoustic environment (or sound field) in which sound waves propagate. This in turn depends on the size of the room and the absorbency of the surfaces. So by measuring sound pressure we cannot necessarily quantify how much noise a machine makes. We have to find the sound power because this quantity is more or less independent of the environment and is the unique descriptor of the noisiness of a sound source.

Any piece of machinery that vibrates radiates acoustical energy. Sound power is the rate at which energy is radiated. Sound intensity describes the rate of energy flow at a point, that is, through a unit area. In the SI system the unit area is 1 m^2 and hence the units for the sound intensity are Watts per square meter. Sound intensity also gives a measure of direction as there will be energy flow in some directions but not in others. Therefore sound intensity is a vector quantity as it has both magnitude and direction. On the other hand pressure is a scalar quantity as it has magnitude only. Usually we measure the intensity in a direction normal to specified unit area through which the sound energy is flowing.

It is also to be stated that sound intensity is the time-averaged rate of energy flow per unit area.

In mathematical terms sound intensity is the time-averaged of the vector $\mathbf{I}(\mathbf{t})$ instantaneous sound intensity in time-stable sound field:

$$\mathbf{I} = \lim_{T\to\infty} \frac{1}{T} \int_{-0}^{T} \mathbf{I}(t)dt \tag{2.1}$$

T in this case is the integration period and $\mathbf{I}(\mathbf{t})$ is the instantaneous

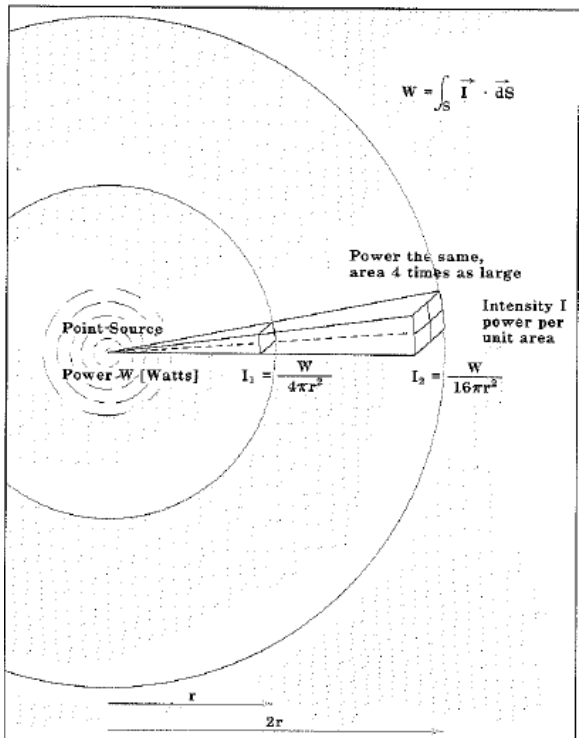

Figure 2.11: Schematic explanation of the sound intensity and sound power. After [9].

sound intensity that is defined as:

$$\mathbf{I(t)} = p(t) \times \mathbf{u}(t) \tag{2.2}$$

where p(t) is the istantaneaous sound pressure in a point, $\mathbf{u}(t)$ is the local instantaneous sound velocity in the same point and t is the time in second.

While pressure can be measured with a single microphone, to measure the particle velocity it is necessary to measure pressure gradient (the rate at which the instantaneous pressure changes with distance) with the linearized Euler equation.

Euler's equation is essentially Newton's Second law applied to a fluid. Newton's Second law relates the acceleration given to a mass to the force acting on it. If we know the force excited and the mass, we can find the acceleration and then integrate it with respect to time to find the velocity.

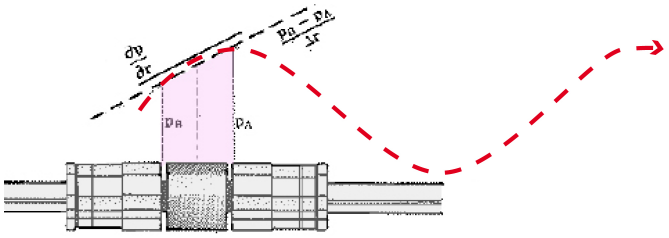

Figure 2.12: Two closely spaced microphones that are ables to obtain a pressure gradient by taking the difference in pressure and dividing by distance between them. After [1].

$$\mathbf{a} = \frac{\mathbf{F}}{m} \tag{2.3}$$

$$\mathbf{v} = \int \frac{\mathbf{F}}{m} dt \tag{2.4}$$

In Euler's equation the pressure gradient accelerates a fluid of density ρ. Given the pressure gradient and the density of the fluid, the particle acceleration can be calculated. Its integration then gives the particle velocity.

$$\mathbf{a} = -\frac{1}{\rho}\nabla p \tag{2.5}$$

in one direction

$$\frac{\partial \mathbf{u}}{\partial t} = -\frac{1}{\rho}\frac{\partial p}{\partial \mathbf{r}} \tag{2.6}$$

$$\mathbf{u} = -\int \frac{1}{\rho}\frac{\partial p}{\partial \mathbf{r}} dt \tag{2.7}$$

The pressure gradient is a continuous function. With two closely spaced microphones it is possible to obtain a straight line approximation to the pressure gradient by taking the difference in pressure and dividing by the distance between them. This is called a finite difference approximation. It can be thought of as an attempt to draw the tangent of a circle by drawing a straight line between two points on the circumference.

The pressure gradient signal must now be integrated to give the particle velocity. The estimate of particle velocity is made at a position in the acoustic centre of the probe, between the two microphones. The pressure is also approximated at this point by taking the average pressure of the two microphones. The pressure and particle velocity signals

are then multiplied together and time averaging gives the intensity. So the particle velocity is:

$$\mathbf{u} = -\frac{1}{\rho}\int \frac{p_B - p_A}{\Delta \mathbf{r}} dt \tag{2.8}$$

where $\Delta \mathbf{r}$ is the distance between the two microphones. The pressure is:

$$p = \frac{p_A + p_B}{2} \tag{2.9}$$

Hence the sound intensity is:

$$\mathbf{I} = p\mathbf{u} = -\frac{p_A + p_B}{2\rho\Delta \mathbf{r}} \int (p_B - p_A) dt \tag{2.10}$$

2.2 Sound intensity measurement techniques

This section deals with the theoretical and practical aspects of sound intensity and sound power measuring instruments. Developments in acoustic measurement instrumentation have not accompanied the general development of acoustic theory. It was not until 1932 that the first acoustic intensity meter was patented by Olson [34]. He developed a system that calculated the average product of signals originating from a pressure microphone and a ribbon microphone sensitive to the pressure gradient. Subsequently a lot of authors investigated on the whole two types of intensity level meters using the two microphone principle. The sound intensity analyzing system, using the two microphone principle, consists of a probe and an analyzer. The probe simply measures the pressure at the two microphones separated by a distance $\Delta \mathbf{r}$. Sound intensity can be computed equivalently using two main techniques: either directly using integrators and filters to implement the equation step by step, or by using a FFT analyzer, that relates the intensity to the imaginary part of the cross spectrum of the two microphone signals.

Usually the probe has two microphones mounted face to face with a solid spacer in between. This arrangement has been found to have better frequency response and directivity characteristics than side-by-side, back-to-back or face-to-face without solid spacers arrangements. Three solid spacers define the effective microphone separation: 6, 12

or 0 mm; The choice of spacer depends on the frequency range to be covered. Half-inch microphones are used for lower frequencies. While quarter-inch microphones are used at high frequencies to reduce interference effects. The directivity characteristic for the sound intensity analyzing system looks like a figure-of-eight pattern- known as a cosine characteristic. This is due to the probe and the calculation within the analyzer. Since pressure is a scalar quantity, a pressure transducer should have an equal response, no matter what the direction of sound incidence. In contrast, sound intensity is a vector quantity. With a two-microphone probe, we do not measure the vector; we measure the component in one direction, along the probe axis. So it is possible to measure the normal sound intensity, that is defined as the component of sound intensity in the perpendicular direction to the measurement surface, defined from the normal unity vector **n**.

$$I_n = \mathbf{I} \times \mathbf{n} \tag{2.11}$$

where **n** is the normal vector directed out to the volume surrounded by the measurement surface. The full vector is made up of three mutually perpendicular components (at 90 to each other)–one for each coordinate direction.

For sound incident at 90 °to the axis there is no component along the probe axis, as there will be no difference in the pressure signal. Hence there will be zero particle velocity and zero intensity. For sound incident at an arbitrary angle θ to the axis, the intensity component along the axis will be reduced by the factor $\cos\theta$. This reduction produces the cosine directivity characteristic. The value approaching the component of the acoustic intensity is, according to equation 2.7:

$$I_n = \frac{1}{2\rho_0 \Delta \mathbf{r}} \langle (p_1 + p_2) \int (p_1 - p_2) dt \rangle \tag{2.12}$$

This formula is derived from the sound pressure signals captured from two microphones as a function of time. The schematic representation in figure 2.13 shows the structure of a measurement instrument that uses analogue electronic circuits.

The most in important development in this measurement is due by

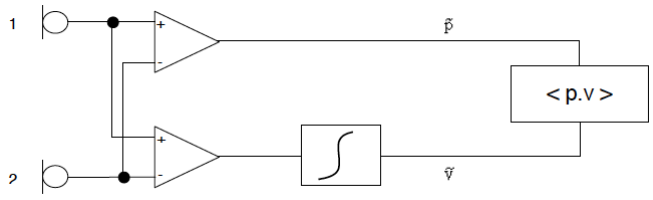

Figure 2.13: Schematic of the structure of a time based acoustic intensity meter[1].

the use of the numerical algorithm fast Fourier transform (FFT). If some filters (one-third octave for example) were included in the circuit, one would obtain a spectral analysis of the acoustic intensity. For stationary signal, one notes an equivalent spectral representation according to equation 2.7:

$$I_n = \int_{-\infty}^{+\infty} I_n(\omega) \frac{d\omega}{2\Pi} \tag{2.13}$$

Where $I_n(\omega)$ is the spectral density of the intensity represented by the real part of the cross spectrum between pressure and velocity (Parseval theory):

$$I_n = Re\{S_{pv}\} \tag{2.14}$$

By using Euler's relationship in terms of the Fourier transform and approximation for $\frac{\partial p}{\partial \mathbf{r}}$ and p, it is possible to reach an expression of the spectral intensity using the imaginary part of the cross spectra of the pressure signals obtained from the two microphones.

$$I_n = \frac{1}{\rho_0 \Delta \mathbf{r}} Re\{S_{21}\} \tag{2.15}$$

This formula is a significant development in the two-microphone method as it offers a simple measurement system for acoustic intensity using FFT spectra for 2 channels: the principle is illustrated in figure 2.14

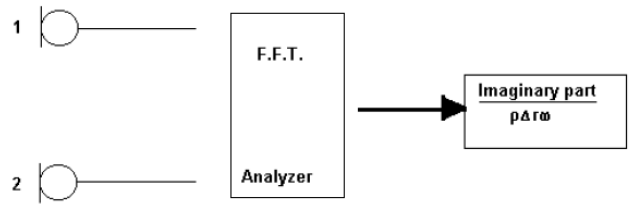

Figure 2.14: Diagram of an acoustic intensity meter based on FFT analysis [1].

2.3 Radiation pattern measurement using the UNI EN ISO 9614

The measurement of sound power using sound intensity would not be possible without a strict definition of the measuring equipment. These requirements are grouped in the international standard IEC1045 [10], the North American equivalent being named ANSI S1-12 [2]. This standard classifies the measurement instruments into two categories: Type 1 and Type 2. Amongst other requirements, it specifies a minimum pressure-residual intensity index δPl_0 of the intensity measurement system at each frequency, and for every probe configuration used. The ISO 9614-1 [52] is the international standard that defines and specifies how to measure the power level of a fixed sound source, measuring the sound intensity on a surface that surrounds the source. The measurements standards are classified according to the methodology used: measurements at discrete points and measurement by scanning.

The discrete points technique is described in the international standard ISO 9614 part 1 [52] and their national equivalents. The North Americans have adopted the standard ANSI S1-12 [2], which is greatly different from the ISO9614-1 [52] standard, especially for the number of field indicators to validate the measurement results. The scanning technique is more recent. It is described in the international standard ISO 9614 part 2 and their national equivalents. This technique aims at lightening the measurement process in order to obtain results faster, but at the expense of a lower grade of accuracy.

The UNI EN ISO 9614 [52] requires that the choice of the positions and of the shapes be made avoiding to take measurement on the re-

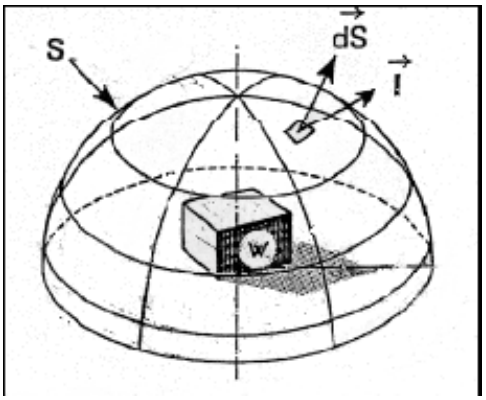

Figure 2.15: Theoretical sound intensity on measurement surface. [1].

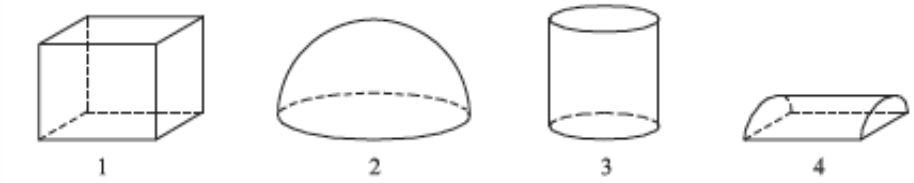

Figure 2.16: Best measurement surface shapes. 1. Parallelepiped 2. Hemisphere 3. Cylinder 4. Hemicylinder [52].

flective or absorptive surfaces. Furthermore in the annex are listed the parameters that should be respected in order to have a representative result. In fact, the sound power radiated by a source is defined by the surface integral of the normal component of the intensity vector I_n. The surface S is a closed surface that englobes the sound source under investigation. In practice the surface is consituted of N smaller discrete surfaces. The surface surrounds that the sound source it could assume different shapes (see fig. 2.16)

The time integration required from the instruments, that use white noise filter with a gaussian distribution, should be:

$$BT \geq 400 \tag{2.16}$$

where B is the filter bandwidth expressed in Hz and T is the integration time expressed in s. This limit ensures a maximum error of 5%.

Chapter 3

The design of the listening room

In order to build a professional listening room, there are many issues to be satisfied that sometimes go beyond acoustics. First of all, it is very important that the room can be used in the working time without disturbing, or being disturbed by, anything or anybody in the local community. It is very rare to have the possibility of choosing an isolate area where to build a listening room. The awareness of how much space can be consumed by acoustic insulation, plant and structures can be very important.

Old buildings often lack of adequate plans and the acoustic properties of the materials used are often unknown. So in most of the cases, in order to ensure the result, the listening room has to be completely re-built. Concrete, steel and plasterboard are relatively cheap materials, but it is necessary to control if structures can cope with supporting a lot extra weight, provided that the design of the room matches with architectural and plants constraints.

The studio should always provide an adequate supply of clean, fresh air, in a temperature and humidity-controlled environment. General comfort is an important issue, as comfortable musicians are inclined to play better than uncomfortable ones, and comfortable listener are inclined to judge better than uncomfortable ones.

Last but not least the everlasting financial problems, in recording

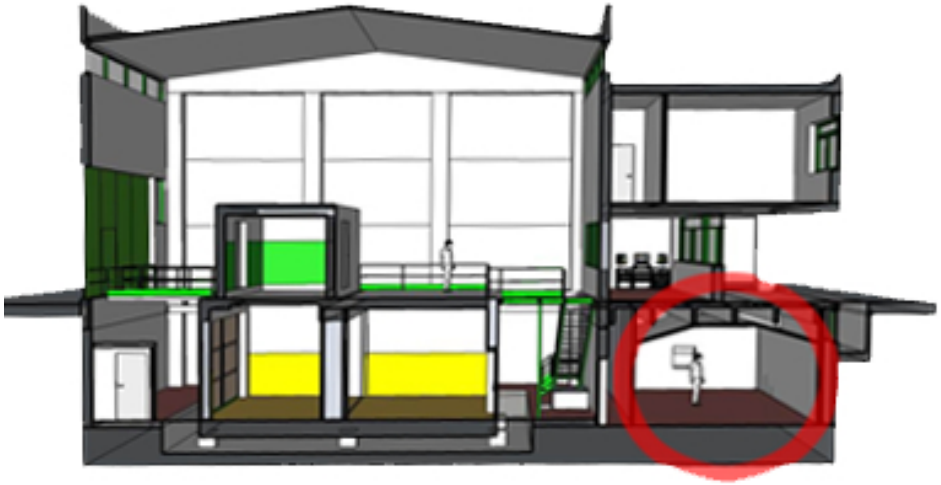

Figure 3.1: Section of the laboratories. The room in question is in the red circle

studios and in listening room. The acoustic engineer has to deal with the financial problem in every aspect of the design.

In the present chapter financial problem will be ignored and the main aspects of the listening room design will be discussed applied to the case study room. In particular, the focus will be on:

1. Architectural design
2. Room acoustic design
3. Plant design

3.1 Architectural design

The case study room is located in the laboratory of environmental physics in the Department of Industrial Engineering.

In order to create the room it was realized an aperture 2.05x1.20 m with a lintel and there was installed a REI 120 door. Subsequently it was built a masonry wall in thermal hollow bricks. Considering plaster on both sides, the total width is 22 cm.

The new available space is a room in the industrial building of the laboratory. The floor area measures 52.5 m^2 and it is made in quartz

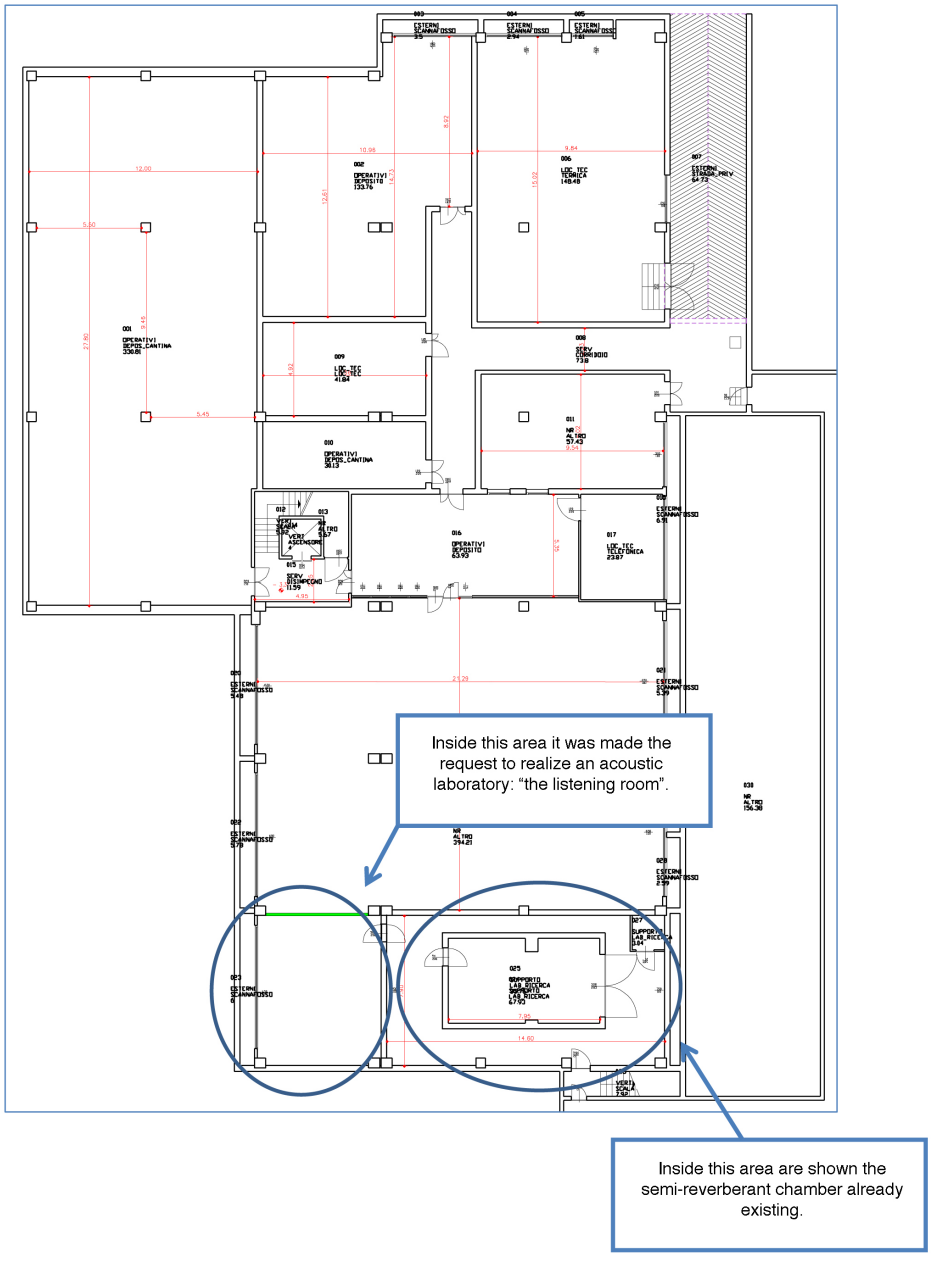

Figure 3.2: Planimetry of the laboratories in via Terracini 34 EX-Dienca. The listening room in question is in the blue circle. The other room in the blue circle are the already existing measurement laboratories of sound insulation of building elements.

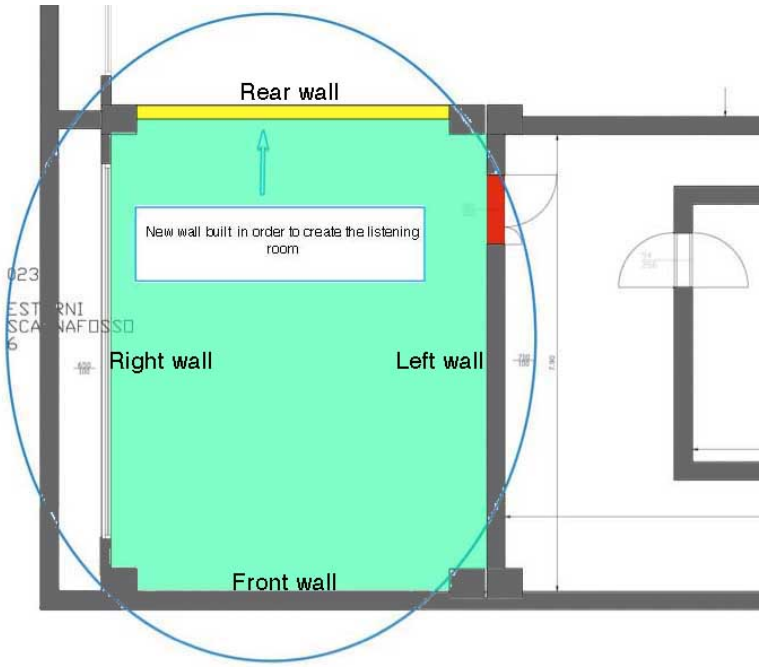

Figure 3.3: An area of the department plan: the yellow wall is new, the red part is the new aperture, the green area is the room

floor hardener. The ceiling is a TT roofing beam. Because of this ceiling, the room height varies from 3.5 m to 2.9 m. The total volume is 182.7 m^3. The front wall was in reinforced concreate, the wall on the right was made in hollow brick with a layer of plaster, placed on this wall at the height of 2.5 m there is a ribbon window. The wall on the left side, where it is placed the outer door is made in hollow brick as well, with two layers of plaster. The regular rectangular plan shape is interrupted at the corner by the reinforced concreate pillars, as seen in figure 3.3. The term left, right, rear and front is the same used in the chapter for the listening room.

A "room within a room" construction stops noise getting in, that means that an inner shell was build. In order to use the maximum available space of the existing installation area, the room is designed using plasterboard, which ensures a maximum flexibility.

Hence the lightweight partition wall and the entire structure consists of an aluminum stud frame construction. This frame creates the supporting structure for the plasterboard sandwich panels.

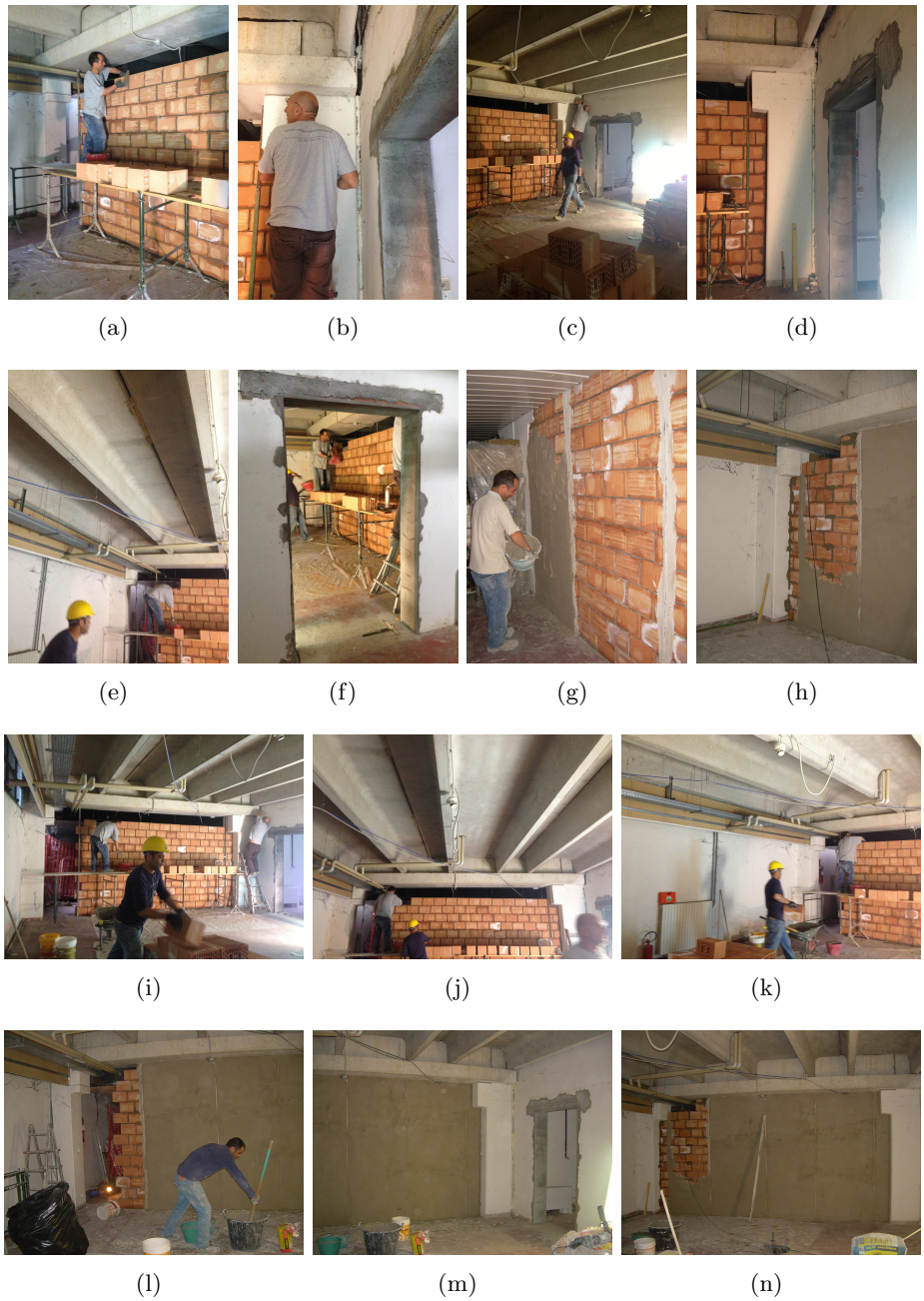

(a) (b) (c) (d)

(e) (f) (g) (h)

(i) (j) (k)

(l) (m) (n)

Figure 3.4: Photos of the progressive manufacturing progress of the wall in masonry plastered. Pictures taken in 26/06/2013.

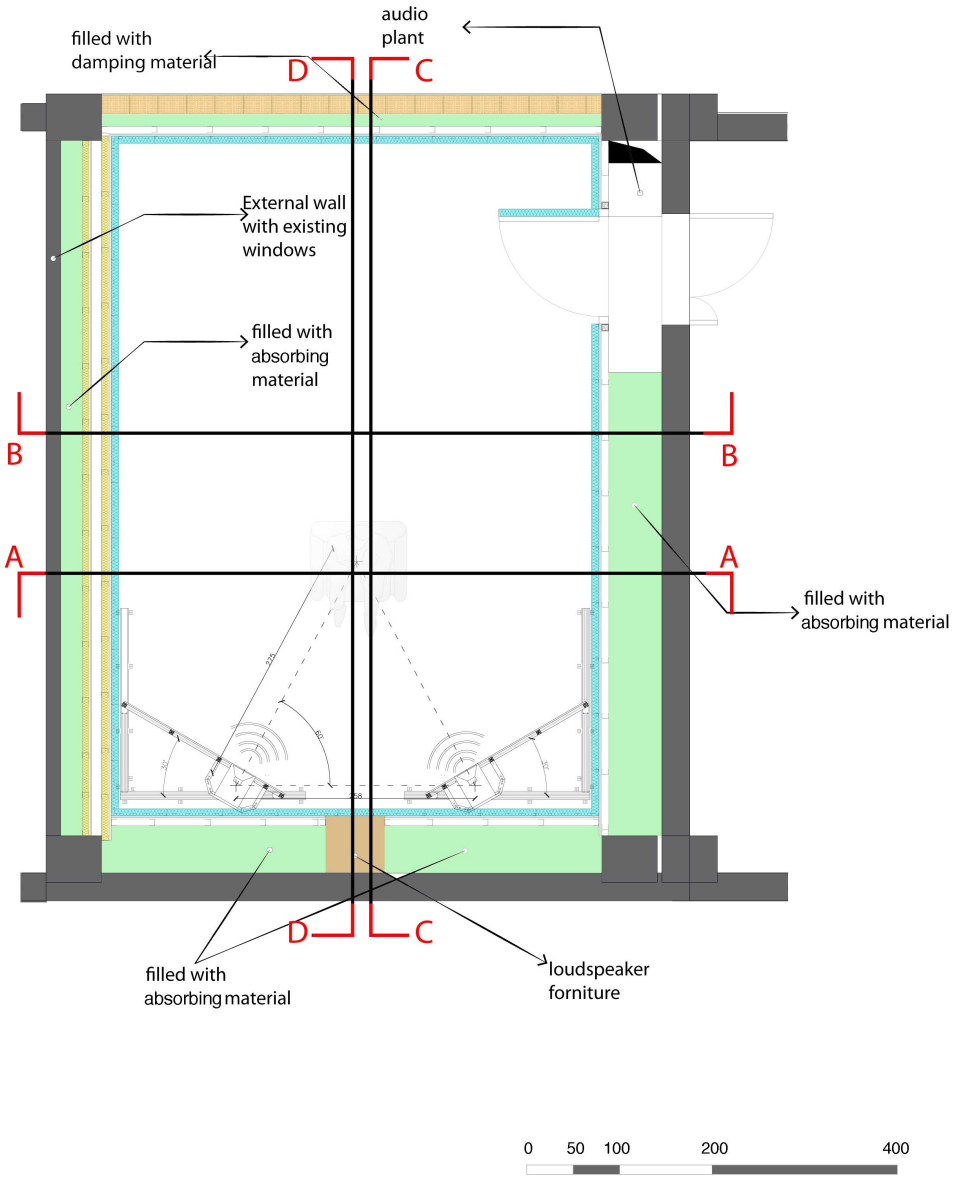

Figure 3.5: Listening room plan.

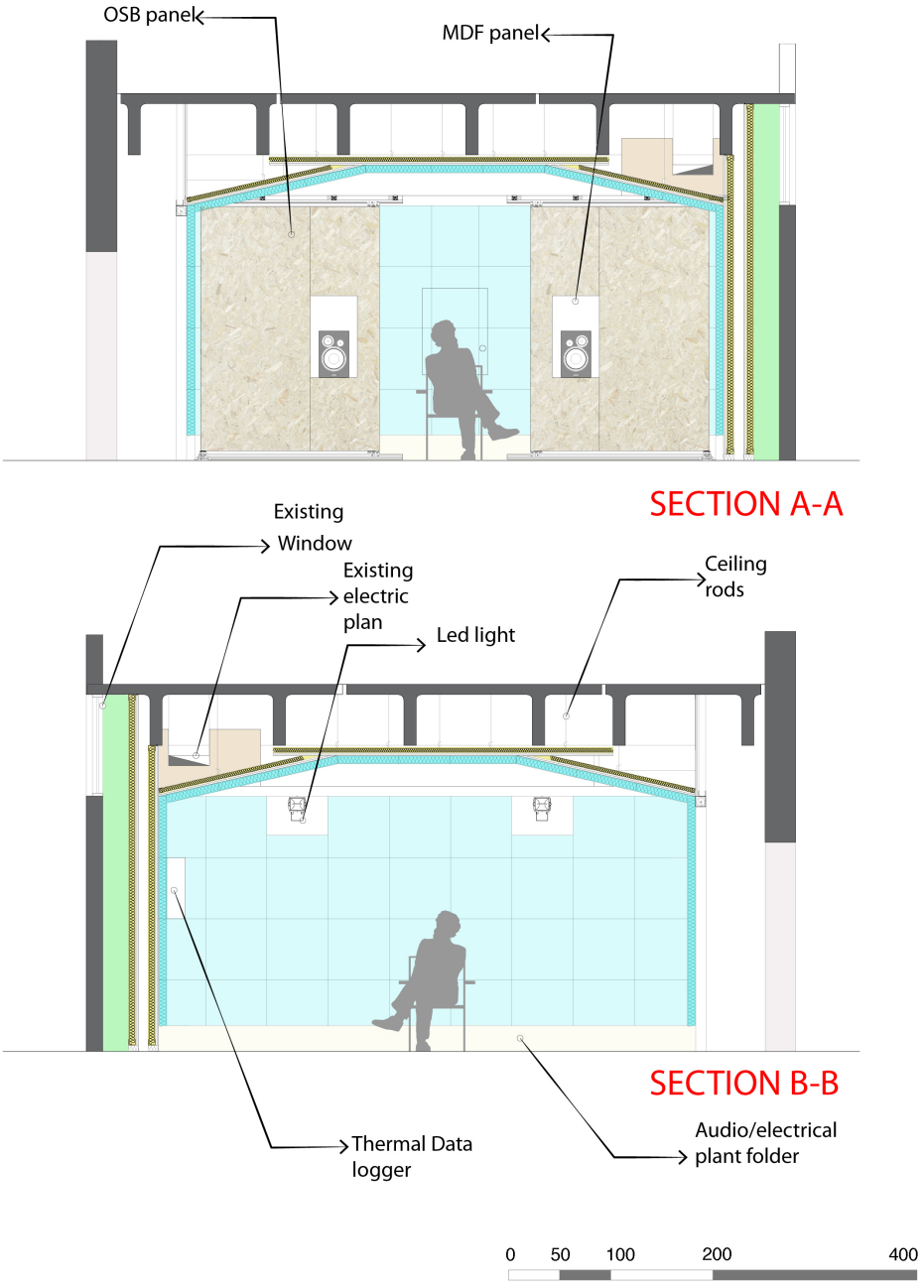

Figure 3.6: Two trasversal cross-section. The once above show the front wall, the second the rear one.

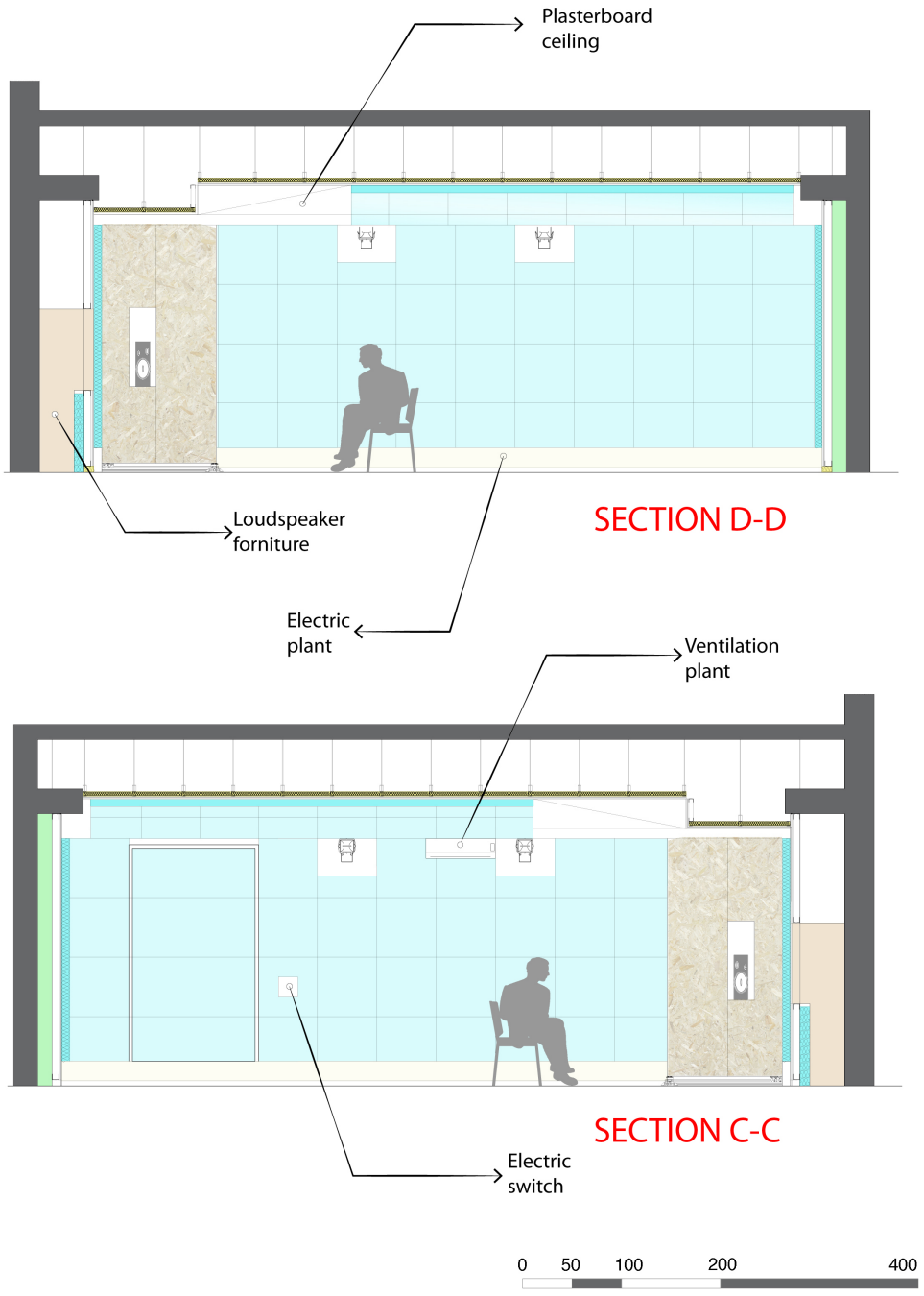

Figure 3.7: Two cross-section. The once above show the wall on the right side, the second the left side.

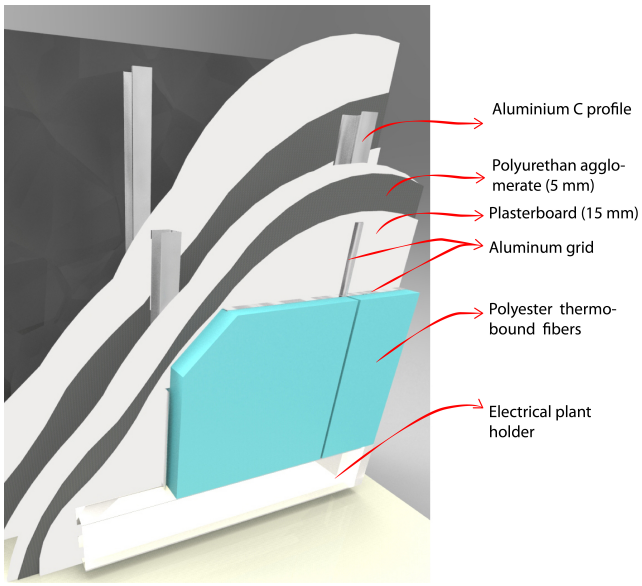

Figure 3.8: 3-D detail of the wall on the left side.

In figure 3.7 is possible to see that the plasterboard on frame system is built respecting an offset to the old unfinished area, in particular the wall are placed reconstituting the rectangular shape. The inner shell has a door as well, that permits to avoid weak point in the insulation system. With the same aim the walls are extended to the intrados of the TT roofing beam. The wall on the left side, as seen in figure 3.8, shows that two assembled plasterboard panel were used to reduce noise, worth mentioning that in that side there is a window that communicates with the outdoor part of the building. The main problem in the wall on the left side is the cavity. Here the simple summation of the calculated isolation provided by each individual section of the complete structure cannot be relied upon to give the isolation of the whole system. It is that internal reflexions can be set up between the layers, which can add re-reflected energy to the forward-going propagation. This is shown diagrammatically in figure 3.9.

The reduction of this effect requires fibrous layers in the various air spaces. Because of that every cavity was filled with porous absorptive material, highlighted also in plan.

In the front wall a cavity was left in order to locate the furniture for an extra sound source and to guarantee the de-coupling between

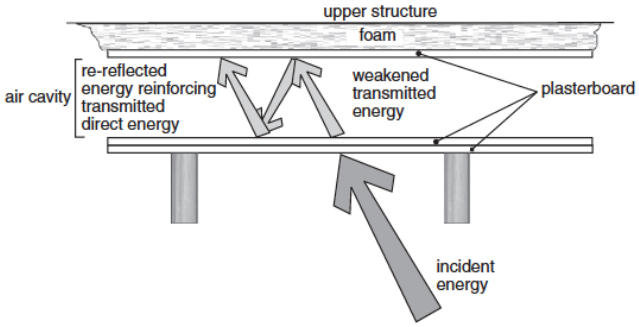

Figure 3.9: Re-reflexion between layers. Resonant build up in air cavity can reduce isolation in a similar way to which the build up of reverberant energy in a space can make a source louder than it would be in free-field conditions [33].

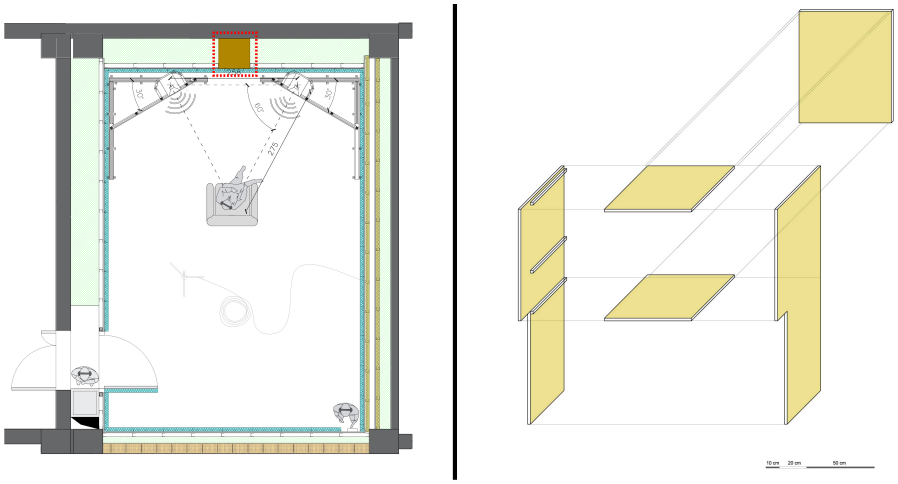

Figure 3.10: Assembly furniture drawing, plans and elevation and photo of the furniture final realization.

source and structure.

That particular furniture was manufactured customized and was assembled as shown in figure 3.10. In order to avoid undesired contacts between plasterboard and the customized furniture, there is a layer of neoprene gasket, whereas in the matter to prevent the cavity resonance it was used polyurethane aggregate.

The rear wall has a similar plasterboard detail but the most external layer is a brick wall (as seen in fig. 3.12).

The plasterboard structure creates a sort of shell and it was chosen to use plasterboard also for the ceiling system. The ceiling is the more

Figure 3.11: Furniture photo taken after and before be placed in the wall. In the second one it is possible to see that is filled of damping material. In the third one is possible to see the final solution.

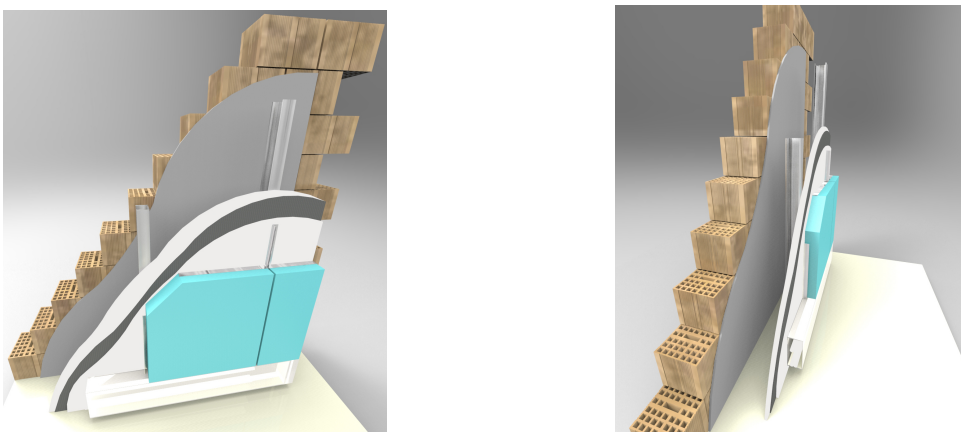

Figure 3.12: 3-D detail of the rear wall.

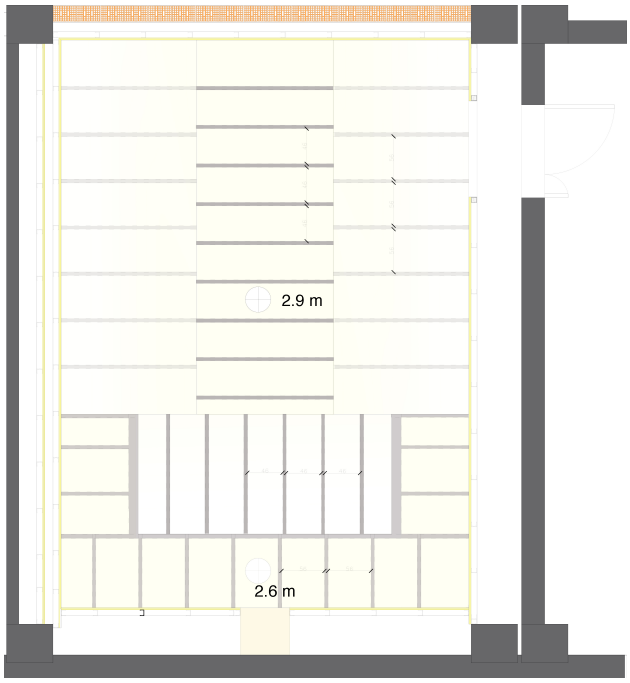

Figure 3.13: Covering plan of the plasterboard suspended structure.

complicated structure of the entire project. The ceiling shape has to satisfy several requirement:

- To exploit the maximum height;
- To avoid parallelism between ceiling and pavement, where it is possible;
- To take in account the plant design;
- To permit the placing of the air conditioning split.

The ceiling plasterboard system is suspended, using suspension rods fixed every 50 cm to structural support.

In the figure 3.13 is shown the ceiling plan. The ceiling shape is due to the necessity to fix the metal rail and to the fact that is important exploit the height of the room.

Obviously the doors ensure a good fireproof quality, and respect the standard of UNI 9177 [47]. It is very important for listening rooms the characteristic to be flexible. Because of that it was designed a

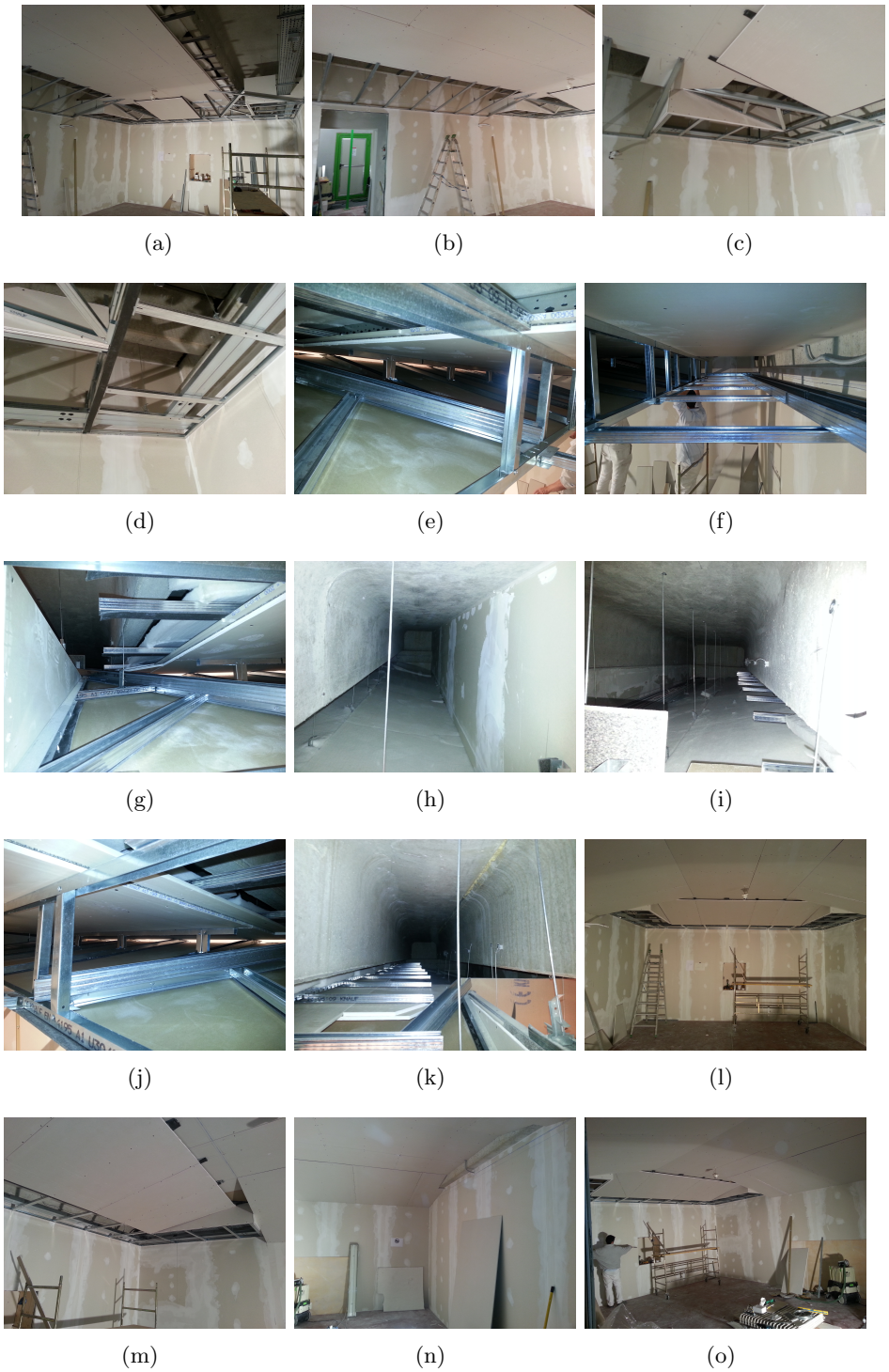

Figure 3.14: Progressive picture of the ceiling construction process. Pictures taken in 14/11/2013.

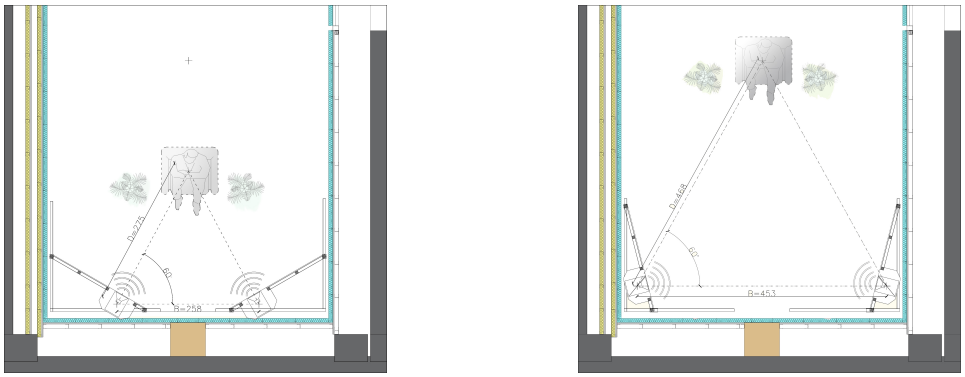

Figure 3.15: Two test listening arrangement, before and after rotating the panels.

mechanical element (fig. 3.17) that allows to change the orientation of panels, thus changing the reflection zone. The innovation of this panel is to ensure a good acoustic quality in more then one position. Hence these tilting panels are able to change the boundary condition, giving more shape option. As shown in figure 3.15 the room can perform two listening positions: the first one is coincident with $\frac{1}{3}$ of the chamber length (square in figure 4.10) and the second one is coincident with $\frac{2}{3}$ of the chamber length. These two positions were chosen in order to avoid maximum or minimum peaks of an hypothetical stationary wave. The main listening position according to the ITU recommendations [26] is the one coincident with $\frac{1}{3}$ of the chamber length. Depending on these two positions the tilting frame for the loudspeaker was designed.

As it is possible to see in figure 3.17, this mechanical system is bonded to the ceiling and to the pavement by metal guides. This metal guides allow to have a sliding. On this mechanical system panels in OSB are mounted with 1.5 cm of thickness and 600 $\frac{kg}{m^3}$ of density, leaving only a window on the loudspeaker support. These panel were mounted in order to avoid undesired modes related to the constraints and boundary condition. Hence angle plates were linked with the mechanical system and connected with the OSB panels with screws. The angle plates were placed randomly in order to avoid symmetries and modes. Finally a frame was placed in order to plug the loudspeaker support. The material of these frame is MDF with wood filler. Medium-density fiberboard (MDF) is an engineered wood product made by

breaking down hardwood or softwood residuals into wood fibers, often in a defibrator, combining it with wax and a resin binder, and forming panels by applying high temperature and pressure. The density of these panel is about 800 $\frac{Kg}{m^3}$.

The height of all the monitor loudspeakers, measured to the acoustical centre of the tweeter, should be about 1.2 m above floor level. This represents the ear height of a seated listener. The orientation of the loudspeakers should be such that their reference axes should pass through the reference position at a height of 1.2 m.

3.2 Room acoustic design

The room acoustic design is not a perfect science, sometimes different choices depend on the professional listening room designer. The acoustical design of listening rooms has come of age during the past decade. Fazenda et al. [17] recently carried out a study in order to identify common languages, views and preferences of professionals using audio listening rooms. Preferences and views regarding reverberance, stereo image, envelopment, positioning of monitors and other parameters are discussed. In this work, as in the most of the listening room, the frequency response, especially at low frequencies, and the spatial distribution of sound levels and spectrum in the room are still difficult problems for control room users. Further investigation should concentrate on the equalization of the listening area in such a way that this could be designed to be larger than it is usually found in contemporary control rooms. One other factor that has been identified is the extensive use of near field monitoring: the problems arising from this are widely discussed in the work mentioned above. Design considerations could include acoustic control for the radiation from near field speakers as well as main monitors.

The room has to be as isolated as possible to avoid structure-borne external noise as well as airborne sound. In order to prevent this kinds of noise, the room has to be uncoupled from the other rooms of the building. In our case, the adjacent test chambers have embedded damping system. The stair could have transmitted vibration, but the struc-

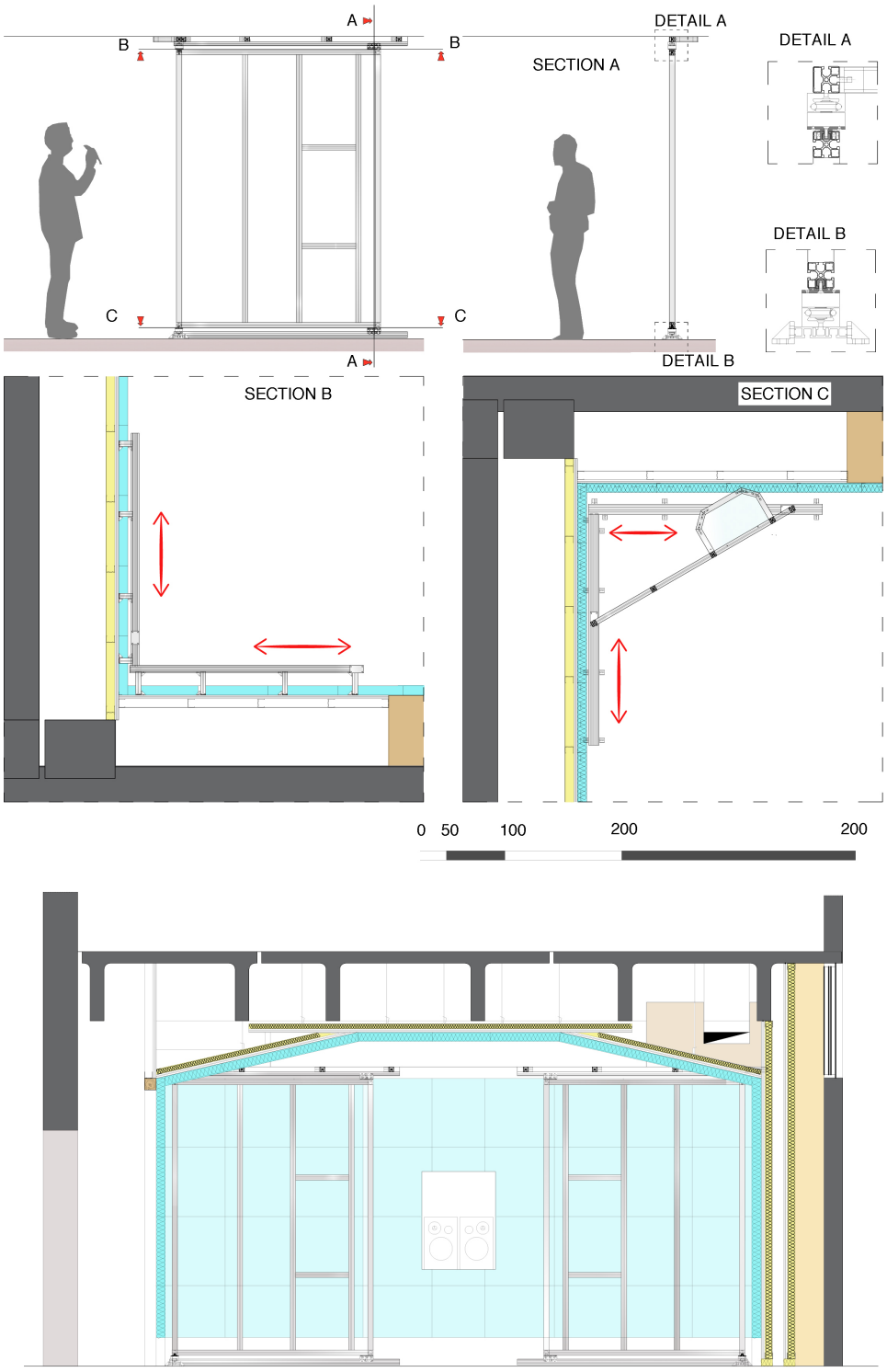

Figure 3.16: Room reflection system: front view, cross section and details.

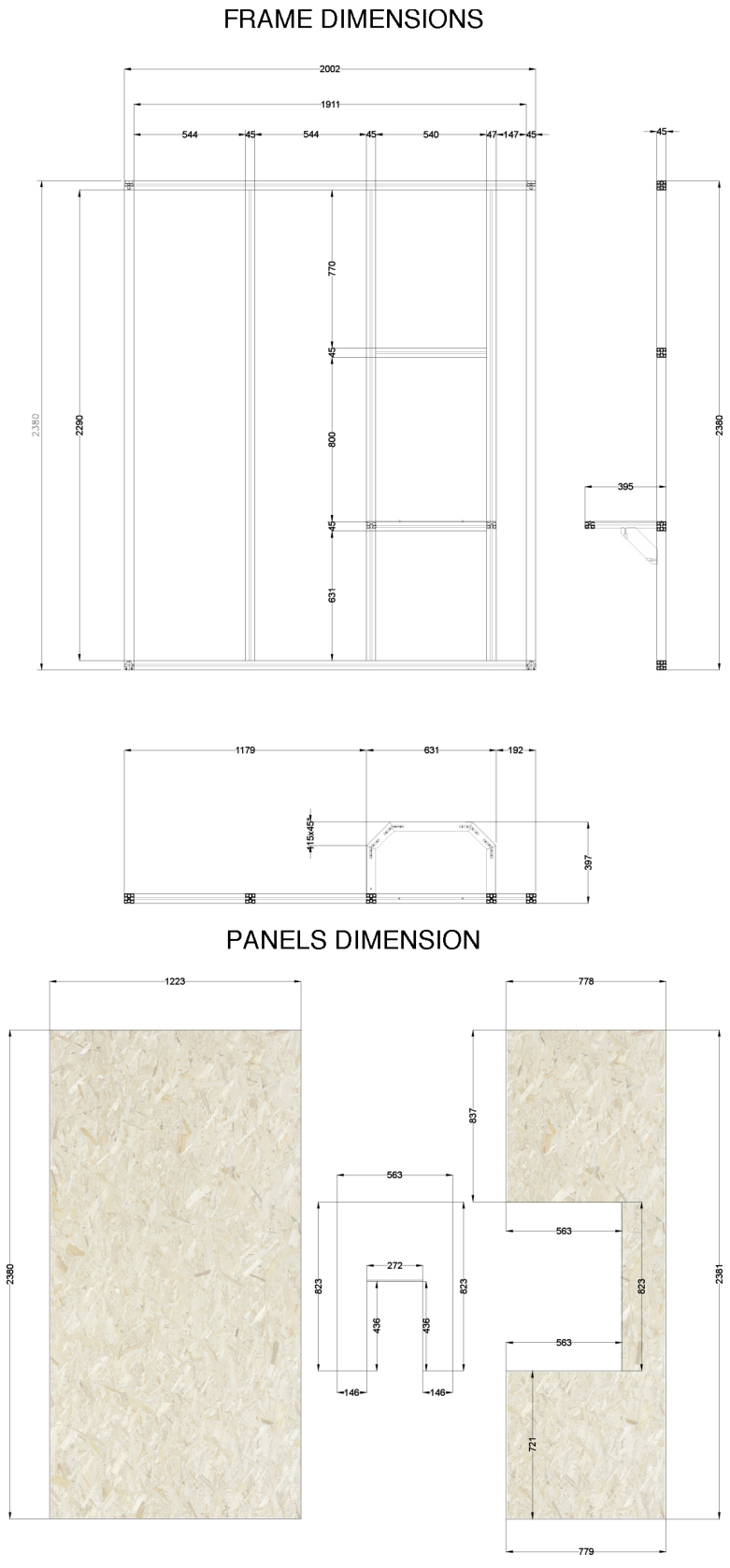

Figure 3.17: Room reflection system details and panels dimension.

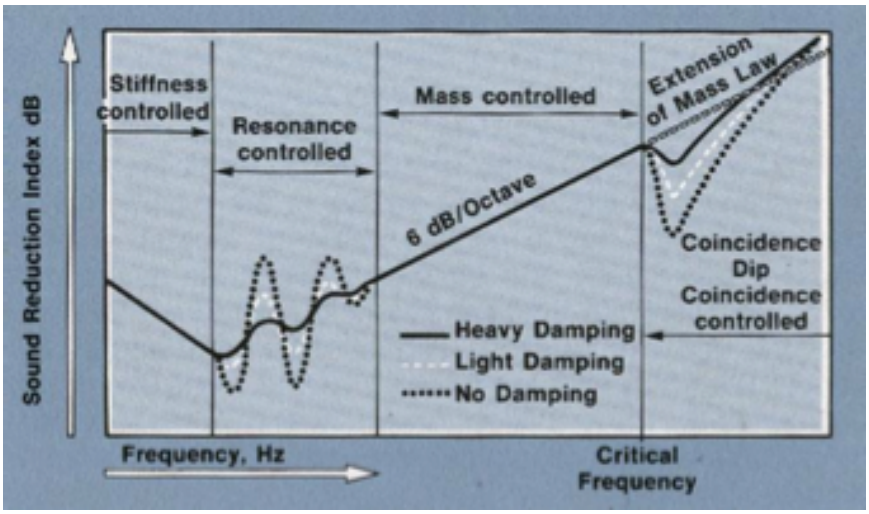

Figure 3.18: Transmission through real panels [18].

tural system is not coupled with the room. So the pavement does not have any insulation problem.

Using this construction technology it is important follow the main goal with awareness of the insulation phenomena. It is known [42] that a great influence on the ability of any structure to provide sound insulation is that of damping. Damping is the degree to which a propagating wave within a material or structure is internally absorbed, normally by the conversion of the vibrational energy into heat [33]. Furthermore the scientific literature [42] illustrates which laws are used for the insulation phenomena (fig. 3.18).

The plasterboard panels are assembled as a sandwich, and the medium material is agglomerated polyurethane foam flexible open cell structure density of 340 kg/m^3 and thickness 4.0 mm and the commercial name is CIRFONIC®. This assembled panel works as a mass - spring - mass system (fig. 3.19). Thanks to the damping capacity of the medium material the system is highly efficient in noise reduction.

For noise control, the focus of attention is naturally on absorbers to remove energy. However, in architectural acoustics, both absorbers and diffusers have a role in creating a good acoustics. Acoustic absorption is the property which a material possesses of preventing sound from being reflected back. In this sense the absorption coefficient refers not only to

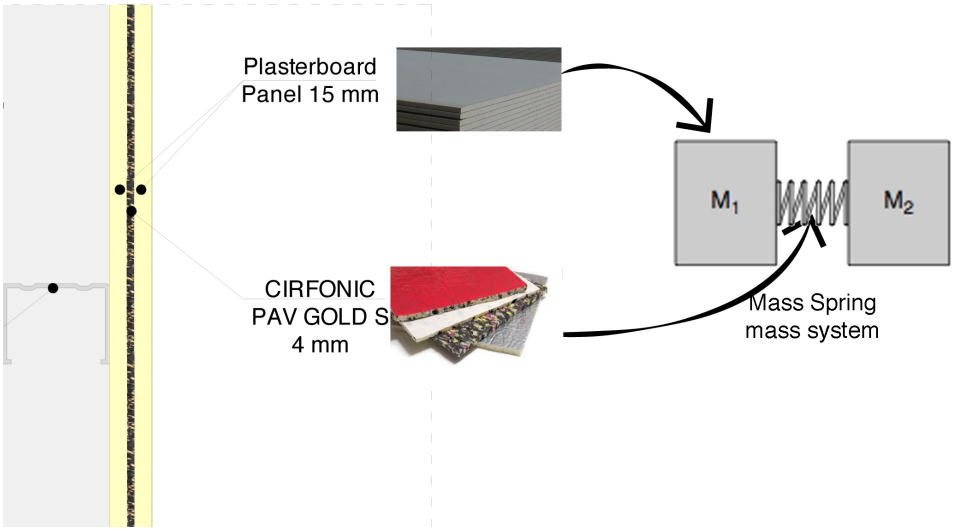

Figure 3.19: Assembled plasterboard structure detail.

Table 3.1: Summary table of main data of CIRFONIC®.

Main data	Unity	Value	Tolerance	Reference standard
Thikness	mm	5	3%	UNI EN ISO 13163
Width	m	1,5	1%	-
Length	m	10	1%	-
Density ρ	$\frac{kg}{m^3}$	70	20%	UNI EN ISO 854
Coloration	-	variable	-	-
Thermal Conductivity λ	$\frac{W}{mK}$	0.033	-	UNI EN ISO 12667

the sound internally absorbed, but also to that which is allowed to pass through. For the selection of the absorber material several things must be considered; the frequency range that has to be covered (including the requirements regarding chamber performance), the size of the place of installation as well as the respective costs.

There are several ways to absorb sound using porous absorptive material or resonant absorbers.

The main work of absorption is made by the polyester fibers. This material can be considered a porous absorptive material because of its open cell on the external surface. Cirfiber®is a sound-absorbing panel in polyester fibers bonded, produced by CIREDILIZIA. It is a a specific product for sound absorption of walls and ceilings. The summary of

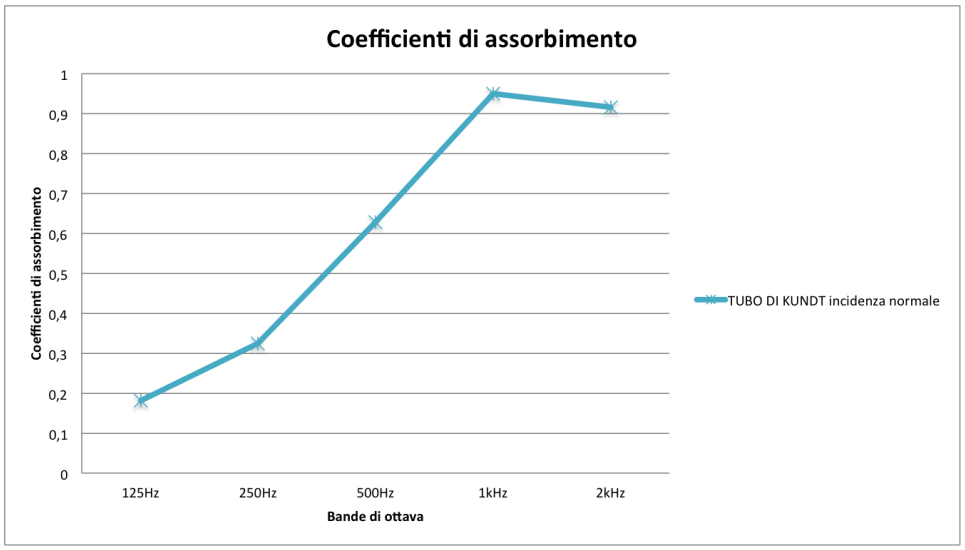

Figure 3.20: Absorption coefficients for normal incidence measured with the Kundt's tube.

the main characteristics is in the table 3.1.

Table 3.2: Summary table of main data of Cirfiber®.

Main data	Unity	Value	Tolerance	Reference standard
Thickness	mm	80	3%	UNI EN ISO 13163
Width	m	0.6	1%	-
Length	m	1.2	1%	-
Density ρ	$\frac{kg}{m^3}$	9,89	20%	UNI EN ISO 854
Recycled content	%	100	-	UNI EN ISO 14021
Coloration	-	variable	-	-
Class of smoke	-	F1	-	AFNOR F 16-101
Reaction to fire	-	I	-	UNI 9177
Thermal Conductivity λ	$\frac{W}{mK}$	0.0377	-	UNI EN ISO 12667
Class sound absorption	-	C	-	UNI EN ISO 354:2003 [51]

In attachment is available the absorption coefficients (see fig. **??**), for normal incidence. In order to obtain this result there were make measurement using the department Kundt's tube, following the ISO 10534-2[48].

Hence, when sound propagates in small spaces, such as the interconnected pores of a porous absorber, energy is lost. This is primarily due to viscous boundary layer effects. Air is a viscous fluid, and con-

Table 3.3: Comparison of the two methods characteristics of methods to measure the sound absorption coefficient.

Method:	Reverberant chamber	Reverberant chamber
Standard:	UNI EN ISO 354	UNI EN ISO 10543-2
		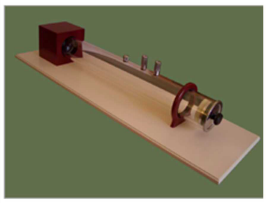
Incidence	Diffuse	Normal incidence
	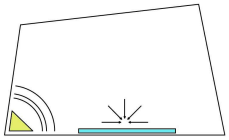	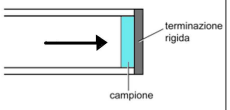

sequently sound energy is dissipated via friction with the pore walls. There is also a loss in momentum due to changes in flow as the sound moves through the irregular pores. The boundary layer in air at audible frequencies is submillimeter. in size, and consequently viscous losses occur in a small air layer adjacent to the pore walls. As well as viscous effects, there will be losses due to thermal conduction from the air to the absorber material; this is more significant at low frequency. For the absorption to be effective there must be interconnected air paths through the material; so an open pore structure is needed.

During the design process a study on the absorptive properties of the cirfiber®was carried out. It was used the method of the reverberant chamber, following the UNI EN ISO 354:2003 [51], for a random incidence and using the Kundt's tube, described in the international standard UNI EN ISO 10534-2 [48] for normal incidence. The result of the two methods were compared. Absorption coefficients depend on several factors and also the angle incidence is very important. Hence it is possible to say that the absorption coefficient measured in the reverberant chamber has a value bigger then the one measured with the Kundt's tube. So we compared this two obtained values using graphic

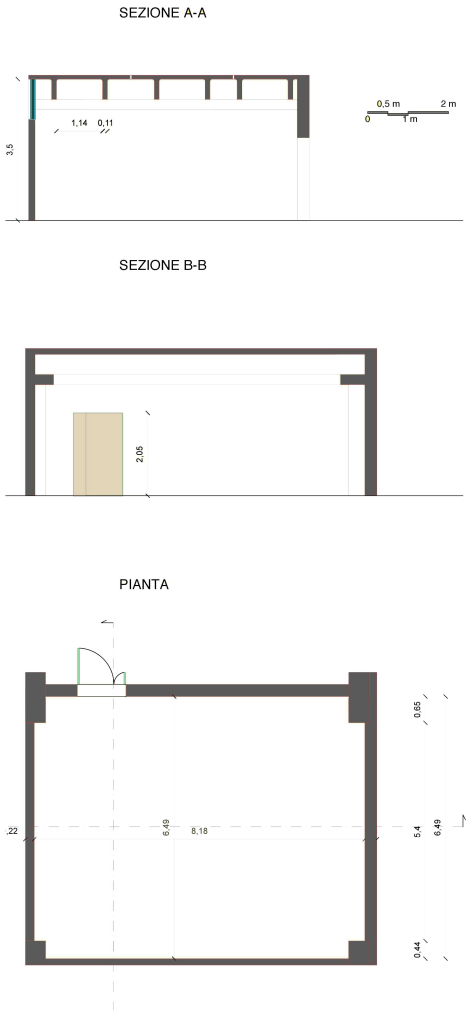

Figure 3.21: Plan and two different sections of the room without manufacturing used as reverberant chamber.

conversion tables. The comparison showed that, though conversion coefficients were used to have the same kind of incidence, this two methods don't match each other. In order to have a significant value of the phenomena in the room, the best choice is to use the results obtained through the reverberant chamber because it give the values of the absorption coefficients for a random incidence, *i.e.* the incidence of the real behavior. Worth mentioning that the reverberant chamber used for the measurements was the listening room itself but without any manufacturing (see fig. 3.21).

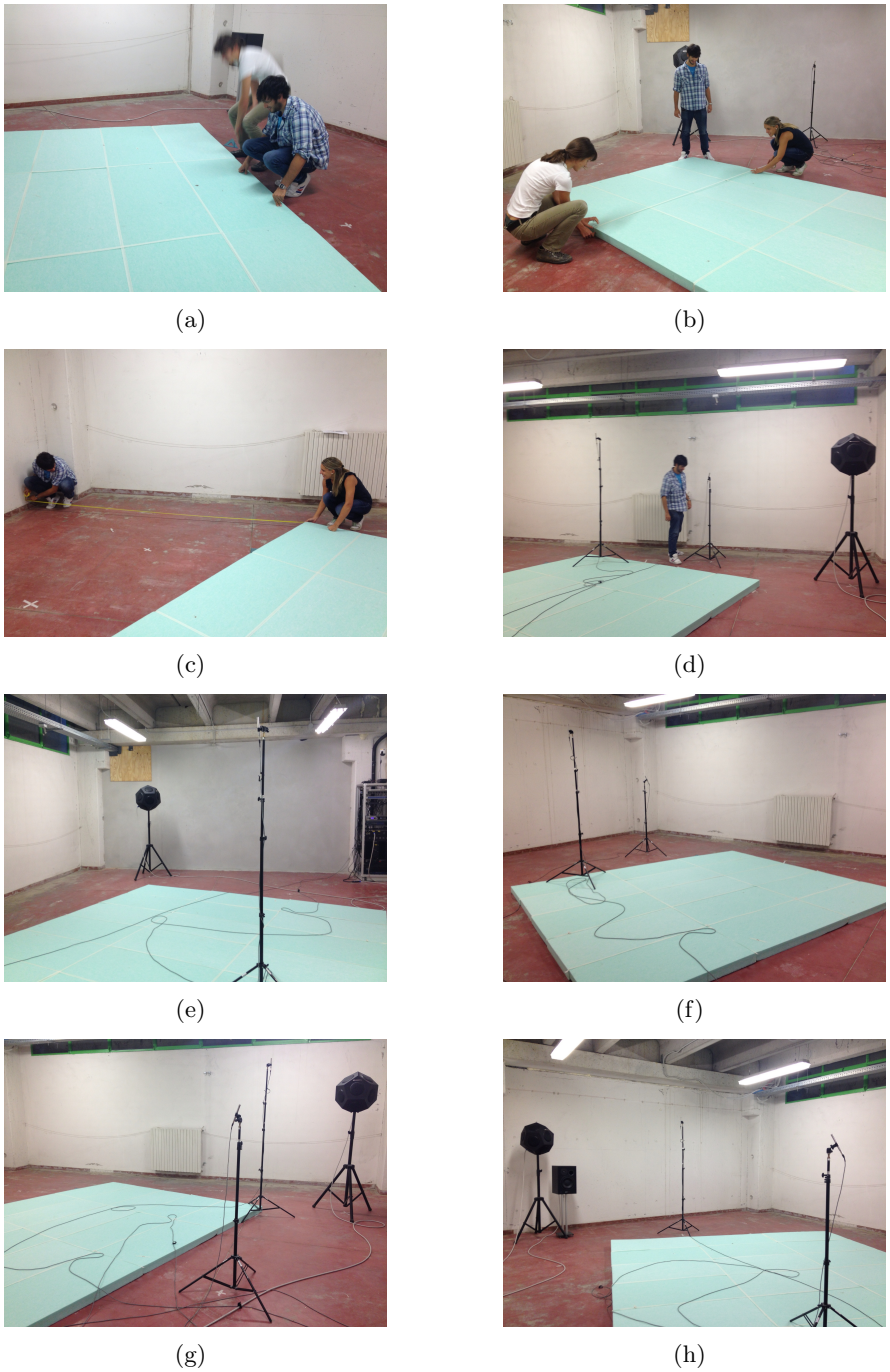

(a) (b) (c) (d) (e) (f) (g) (h)

Figure 3.22: Pictures taken in the reverberant chamber during the IR measurements. The absorptive material is laid on the ground in several configurations. Pictures taken in 13/09/2013.

The results show three different absorption coefficients curves depending on the area of the sample. Theoretically this value should be the same in each area configuration, but it is possible to hypothesize that the coefficient changes because of the perimetric area that has a different impedance and creates a diffraction phenomena that influences the measurement.

Worth outlining that in test specimens the method reports sound absorption coefficients greater than 1.00. This seems at first counter-intuitive because it is impossible for a surface to absorb more than 100 % of the energy striking it. To properly interpret this result, note the units of the sound absorption coefficient: metric sabins per square meter. In cases where the absorption footprint is larger than the area of the specimen, the sound absorption coefficient is greater than 1.00. This is called the edge effect or diffraction effect because it results from wave diffraction at the edges of the specimen. The specimen appears to be larger than its plan area by a perimeter stripe with width proportional to the wavelength where α is the sound absorption coefficient that results from testing an infinite area. The effect increases with decreasing frequency, decreasing specimen size, increasing aspect ratio, and increasing sound absorption coefficient. Although the effect is most noticeable when values exceed 1.00, most low-frequency results for highly absorptive specimens are affected to some degree. One should note that this calculation of the sound absorption is correct for the object in that configuration, that is, in the given size, aspect ratio and mounting, in a diffuse sound field. The corresponding sound absorption coefficient is correct in that configuration for the area used in the computation. Furthermore laboratory measurement of sound absorption is based on the effect of a patch of material on a diffuse sound field in a reverberation chamber. The mathematics used in the analysis presumes that sound travels with equal probability in all directions. This is more or less true throughout the room, except over the sample. For a highly absorptive sample sound travels into the specimen, but very little is reflected back. The discontinuity in the wave field at the edge of the specimen creates a diffraction effect that warps the sound field to make the specimen appear as much as a quarter-wavelength larger

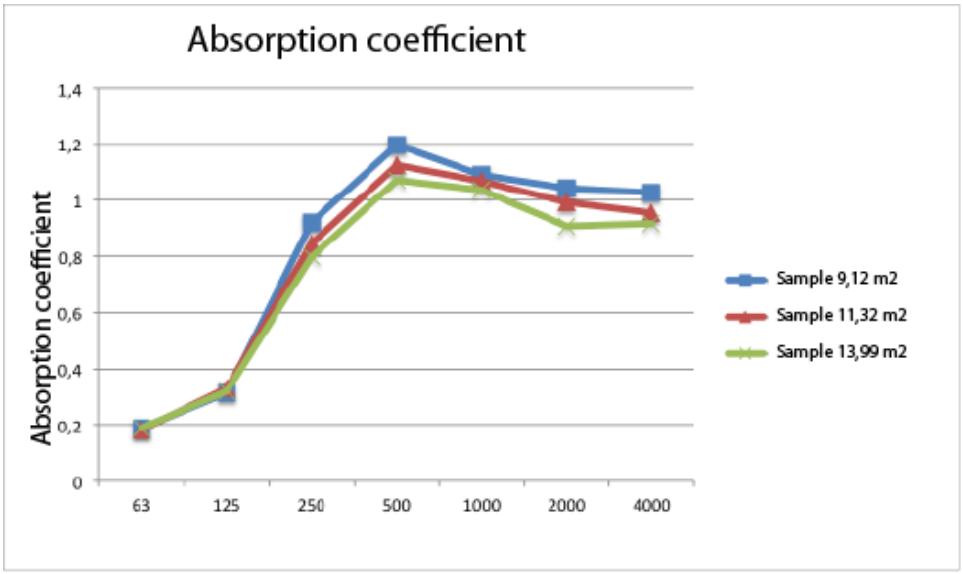

Figure 3.23: Absorption coefficient graphs per octave bands measured through the backward integrated impulse response method.

in each direction. This increases the sound absorption coefficient to such a degree that it often exceeds the theoretical limit of 1.00 [20].

It is important also where and how these absorber panels are placed. The distribution scheme of the polyester fibers is represented in the figure 3.24.

The building system and the placing of the panels is essential, because absorption is building system dependent. In fact the building system represent the boundary condition and can influence resonant modes. In this case it was chosen to have the polyester fibers as exposed face of the inner shell, in order to have a direct absorption for the porosity, avoiding useless material and time wasting. Hence, panels were placed in metal guides in order to permit to the lateral friction to hold the panels like it is possible to see in figure 3.25

3.3 Plant design

3.3.1 Ventilation

In general it is important to tend to create less oppressive atmospheres in which to spend long periods of time. Unfortunately, since sound

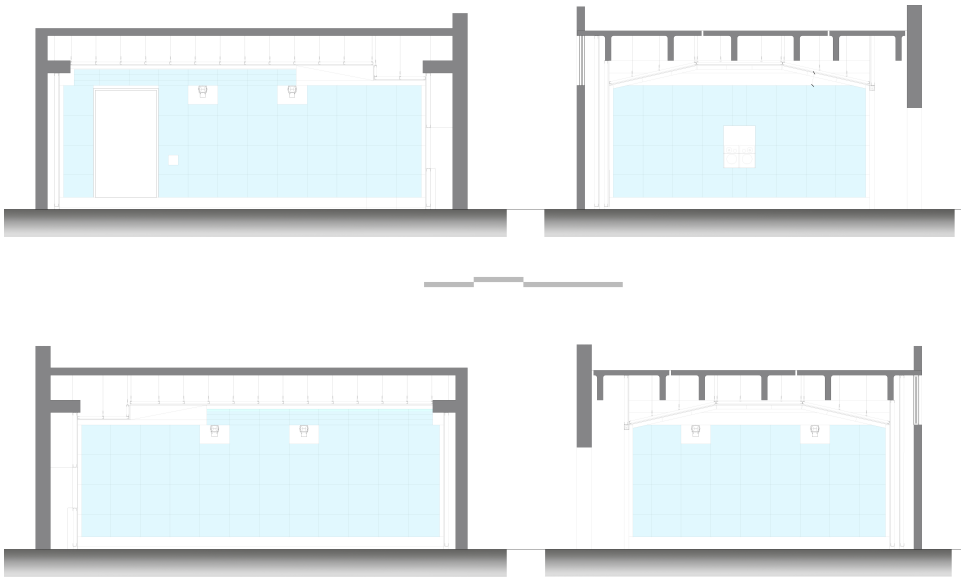

Figure 3.24: Distribution of the absorber panel of polyester fibers.

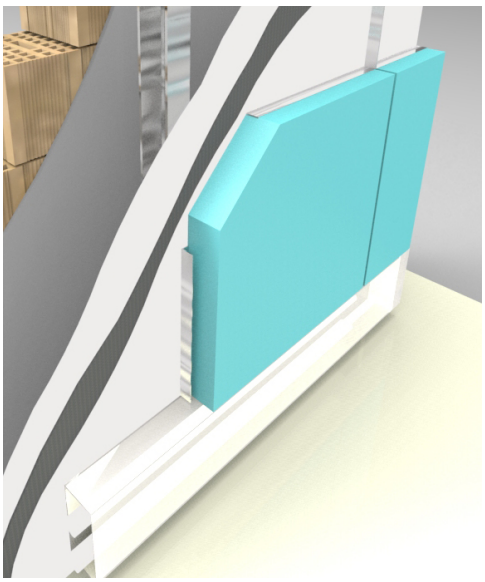

Figure 3.25: 3-D detail of the absorptive panel of polyester fibers placed on the metal grid.

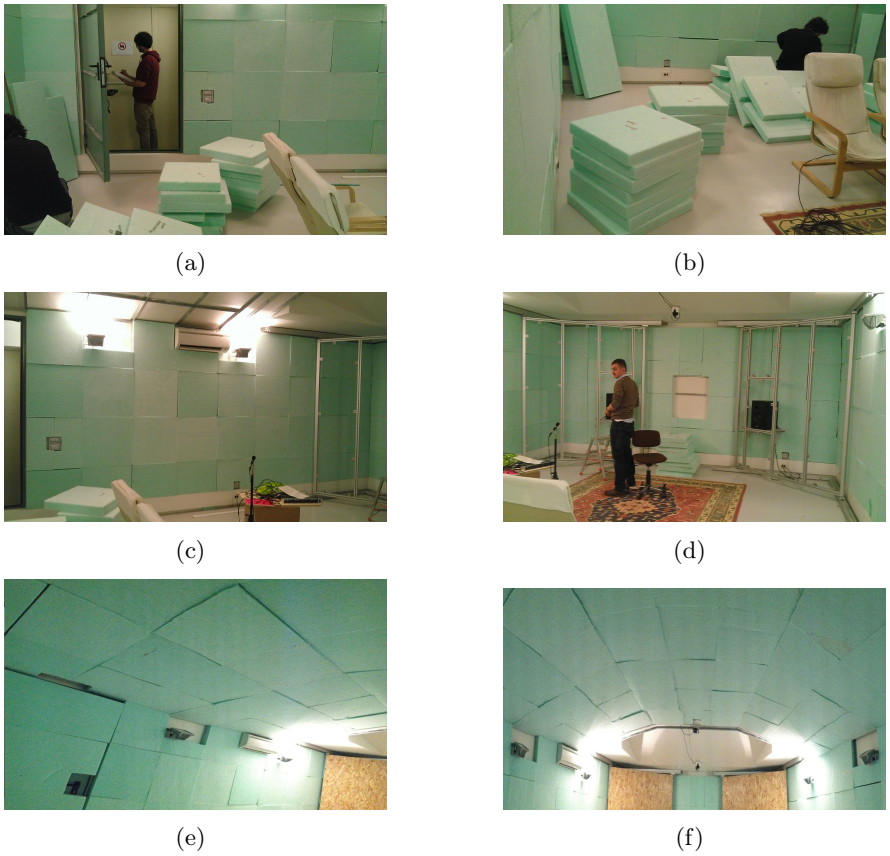

(a) (b) (c) (d) (e) (f)

Figure 3.26: Pictures taken during the cirfiber®mounting process. Picture taken in 03/04/2014.

Figure 3.27: Daikin air conditioning unit placed on the plasterboard wall.

insulation usually works also a good thermal insulation, and given that people, lights and electrical equipment produce considerable amounts of heat, air-conditioning of some sort is more or less a mandatory requirement in all studios. In this case it is used a split air-conditioning. Largely for economic reasons there has been a great increase in the number of 'split' type of air conditioning systems coming into use. Although these are by no means ideal for this purpose, they are many times cheaper than the ducted systems, but as the heat exchanger and their fans are in the studio, with only the compressors remaining outside, there is an attendant noise problem. In control rooms the units can usually be left running in 'quiet' mode, as the noise which really should not be there), but in the studio rooms they usually must be turned off during quiet recordings. Unfortunately this intermittent use can lead to temperature fluctuations which may not be too good for the consistency of the tuning of the instruments. In the room there is a Daikin®RX-JV(GV) inverter unit that is acceptable for control room use when running on low speed, even for critical listening, but it is often required that they should be mounted in front of an absorbing surface [33]. These popular indoor units can virtually be mounted on any type of wall, leaving space free for furniture, decoration and fittings. Wall mounted units are very quiet in operation.

3.3.2 Artificial lights and Electrical plant

The sensation given from the lights is very important for musicians. Light colours, for example, make spaces feel larger then they would do if finished in dark colours. The use of imaginative lighting to create moods can be beneficial to the general ambience of a studio [33]. In the

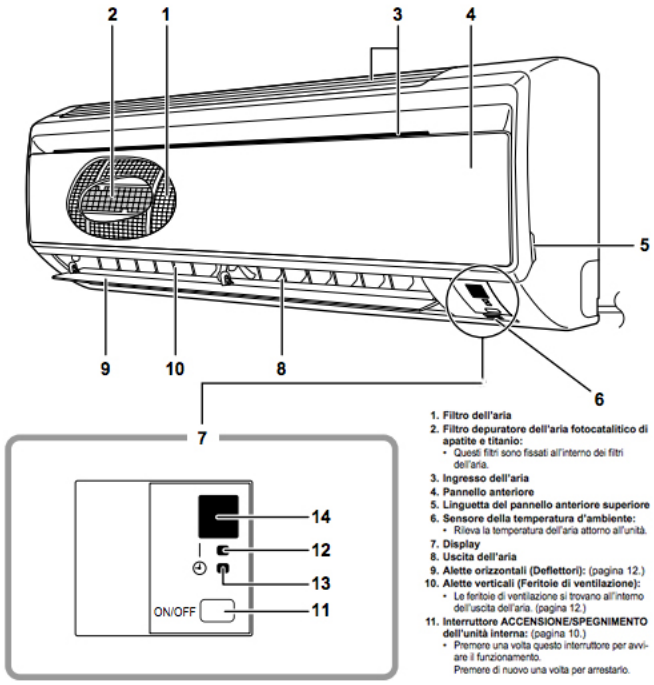

Figure 3.28: Technical detail of the Daikin RX-JV(GV) inverter unit.

room in question, as it is possible to see from the electric scheme, there are six lights Disano®1130 Punto (Max 500 W). The lights are directed against the inclined ceiling in order to give a more diffused light and to avoid a directed light, that can create undesired and annoying shadows.

Since the beginning of the twenty-first century, the pressure has increased on designers to try, where possible, to use lighting of low consumption. The most common types of such bulbs tend to be of the mini-fluorescent type, or LEDs (Light-Emitting Diodes) But the main reason to use a led light is that, by other experiences in different rooms, neon lights produced electric noise that could affect the measurements.

A listening room needs to be as flexible as possible. This means that it should be possible to plug in a lot of sockets and it should be possible to save space. Consequently it is important to decide where to place a big amount of different cables. In fact one should use:

- Data cables
- Power cables

Figure 3.29: Disano®1130 Punto (Max 500 W) placed on the plasterboard wall.

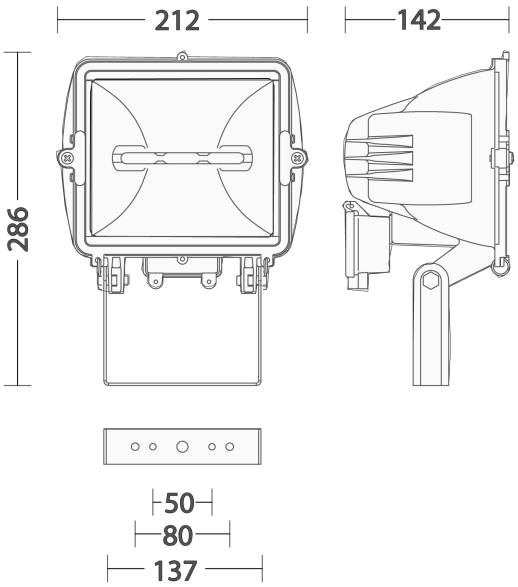

Figure 3.30: Disano®1130 Punto (Max 500 W) technical detail.

Figure 3.31: Picture of the electrical cable over the plasterboard ceiling, made during the manufacturing process.

- Audio cables
- Electrical cables

It was decided to place cables around the perimetric walls using plastic rectangular ducts.

3.3.3 Main monitors

The main monitors are a pair of Dynaudio BM15A. The BM15 is the largest and most powerful speaker within the BM Passive range and is designed for any studio application where higher sound pressure levels and extended low frequency response are required. The Dynaudio Acoustics BM15 is a 2-way, passive studio monitor, featuring a 10" woofer and a 1" dome tweeter, housed in a no-nonsense cabinet with a black matte finish. Dimensions, weight and volume are resumed in the table 3.4. The BM15 cabinet interior has been treated with damping material to minimize aberrant vibration-related distortions. The bass principle used is the Bass reflex, and the bass reflex hole is not placed in the medium axis, as it is possible to see in figure 3.34. The woofer is s molded 10" magnesium silicate impregnated polypropylene (MSP)

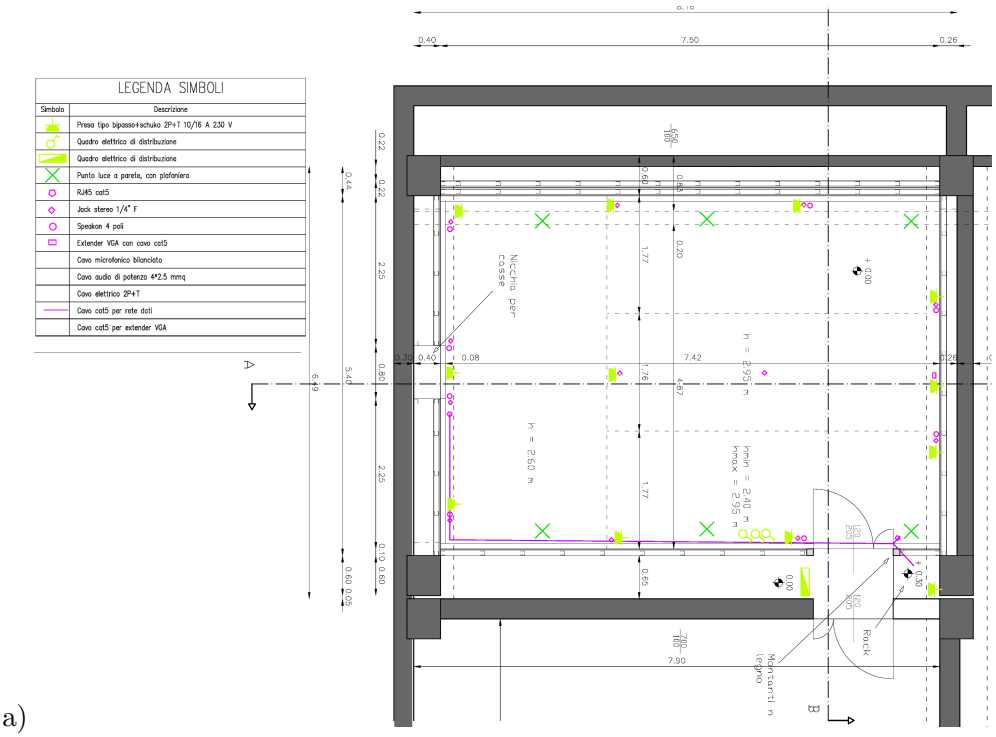

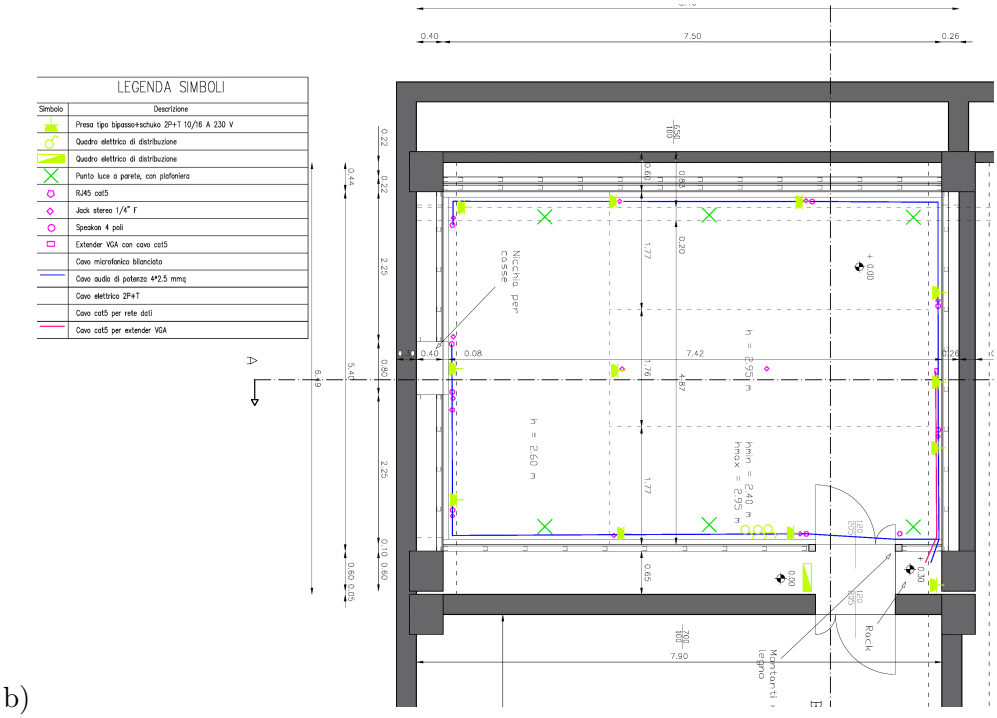

Figure 3.32: Electrical plant. In the plans are described two different kind of electrical plant. a) Data cables b) power cables c) audio cables d)electrical cables

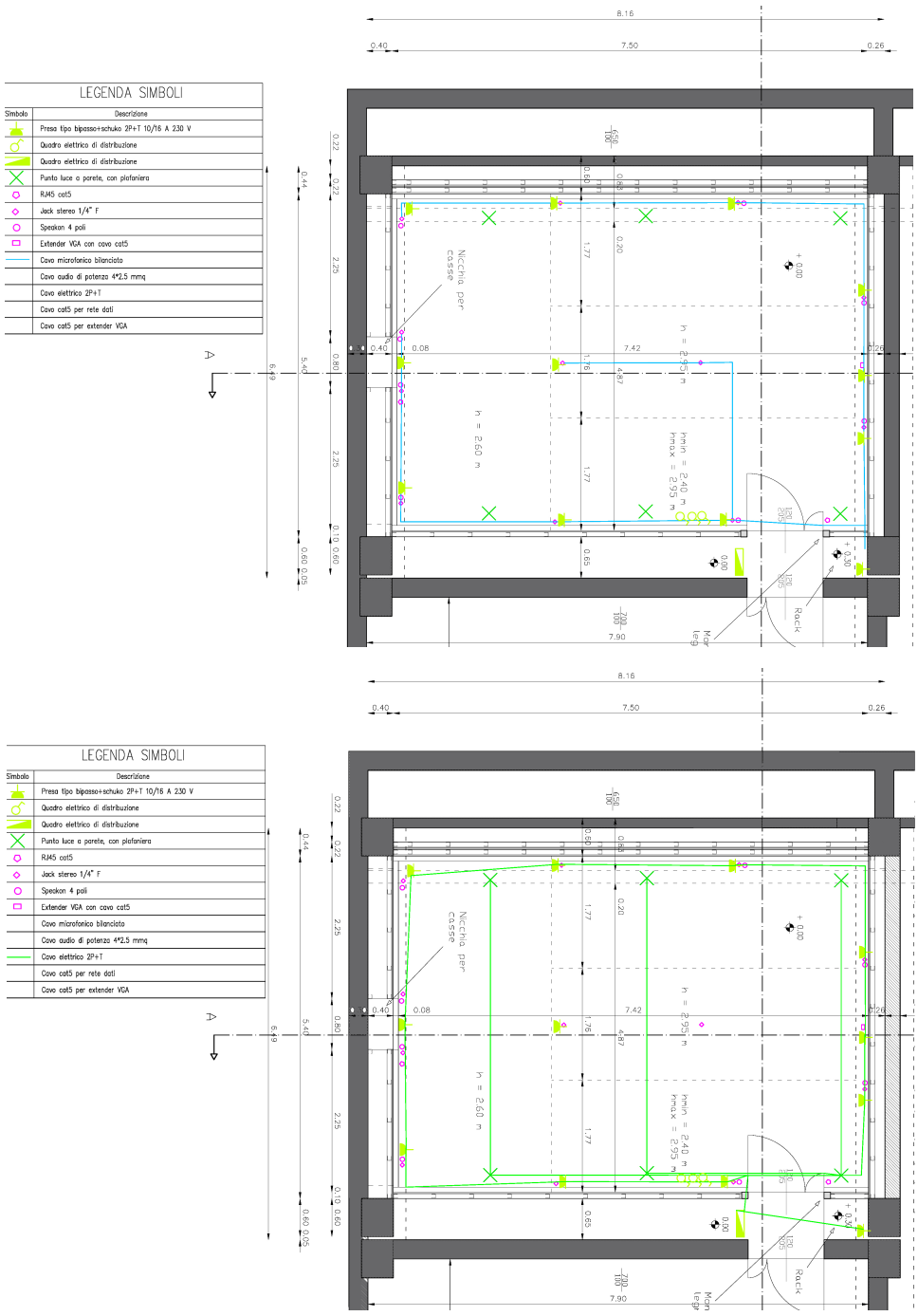

Figure 3.33: Electrical plant. In the plans are described two different kind of electrical plant. a) audio cables b)electrical cables

Table 3.4: Resuming table of the BM15 dimensions, weight and volume.

Width	272 mm
Height	436 mm
Length	321 mm
Weight	12.3 kg
Internal Cabinet Volume	25.8 liters

with 4" pure aluminum voice coil. The tweeter is fluid-protected (a magnetic fluid) and it features a rear acoustic chamber. It is constituted by an esotec 28 mm soft dome, a 4 mm die-cast alu front, a pure aluminium wire voice coil and a protection grille. Finally there are Ported front panel and gold plated binding post. It is possible to find

Figure 3.34: Description of the Dynaudio acoustic BM15.

other technical specifications regarding the acoustic properties of the loudspeaker:

SPL Speaker match : +/-1.5 dB tolerance

Frequency Response: (+/- 3 dB): 43 Hz - 20 kHz

Peak SPL 1m, pair: (IEC Long Term): 127 dB Peak

Peak SPL 2m, 5.1: (IEC Long Term): 128.5 dB Peak

Max SPL 1m: SPL @ 1m (+4/-10): 109 dB RMS

Amplifier Minimum: 50 W (¿ 94 dB SPL @ 2m)

IEC Long term powerhandling: 250W

IEC Short term powerhandling: ¿1000W

Sensitivity: 88 dB

Impedance Nominal: 4 ohm

Impedance HF (200 kHz): 5.9 ohm

Resonance Frequency: 43 Hz

Crossover Frequencies: 2700 Hz

Crossover Slope: Woofer 6 dB/oct; Tweeter 12 dB/oct

Chapter 4

Validation of the room: results and discussions

ITU-R BS 1116-1 [26] and EBU/UER Technical document 3276 [14] were the main guides in the design process of the new listening room. These recommendations, as written before, explain the subjective test prerequisites. It is important to read critically the requirements because they are not all equally important and sometimes other acoustic parameters are to count in the evaluation of the room. In this chapter the room ratio validation will be proposed using the technical documents cited above [26, 14]. In the section 1.3 an in-depth study about the dimension specifications was made. Hence in the next section not only Walker [54] dimension requirements will be used to test the room, but also the Bolt's Blob [6], and the Bonello criterion [7]. It will be discussed about how much prevision about room dimension ratio can influence the real room acoustic performance. The purpose of the discussion regarding the ITU and EBU requirements in the design process is very important. In fact, because of the financial issues, it is important to make the right economical choice, and avoid money wasting. It will be discussed if it is sufficient to satisfy room ratio requirements in order to delate low-frequency problems or if it is necessary to trust in *in situ* measurement during the design/construction process.

Obviously one of the most important requirement that has to be ensured is the sound insulation. It was the first thing that was checked,

before any acoustic treatment. In fact excessive plant noise or external noise can influence negatively any possible activity in the room. If this basic requirements were not satisfied, extra insulation treatment should have been done.

In practice, as explained in chapter 3 the room was designed in order to be as flexible as possible. Every choice in the room acoustic design is not obvious, and also following blindly the most credible room acoustic manuals, the results are not ensured. In order to ensure a good result, it was chosen to design iteratively the room: every acoustic treatment was followed by *in situ* measurement, that were used as check-list that could interrupt or continue the design process. In fact the listening room validation is the result of trials and errors and these *in situ* measurements were not only a check-list, but also a good way to gain experience about the changes, that permits sometimes to make prevision. The *in situ* measurements consists first of all of impulse responses acquisition in order to obtain the reverberation time. Subsequently sound pressure level measurements were performed. The reverberation time tolerance of the room is well described in the technical recommendations, but it is omitted where to take measurements in the room. Measurement positions placement can influence the quality of the results in the detection of spatial singularity. The sound level measurements were analyzed in one-third octave bands differently from the impulse response, in order to find easily hypothetical room modes. The acoustic treatments that have been studied in this room are:

1. Perimetric walls covered by absorptive material

2. Perimetric walls and ceiling covered by absorptive material

3. OSB panels stiffening with wooden rods

Finally, in order to read more critically the spatial distribution of the parameters, sound intensity measurement were performed using the sound room sound source described in the section3.3.3. Indeed the directivity of the sound source could affect the sound pressure level and the reverberation time.

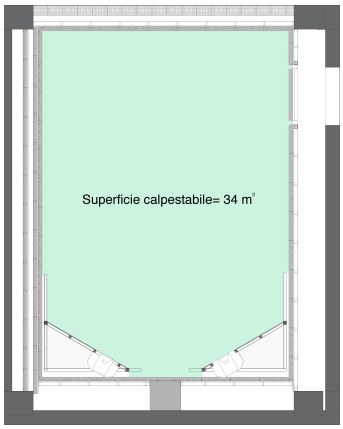

Figure 4.1: Measurement position in the reference case study.

4.1 Room dimension requirements

In order to simplify the modal phenomena and to avoid the worst cases, the ITU 1116 establish suitable net dimensions for a reference listening room. If the test room cannot fulfill these dimensions, the requirements on the sound field conditions and on the loudspeaker arrangements mentioned in the subsequent sections should be fulfilled at least. The floor area should be, in this case study (two-channel stereophonic reproduction) 20-60 m^2.

The room fullfills the recommendation for the floor area because is 34 m^2, so it is in the range. The room should be symmetrical relative to the vertical plane on the mid-perpendicular of the stereo base. The following dimension ratios should be observed to ensure a reasonably uniform distribution of the low-frequency eigentones of the room (obviously considering the room as rectangular):

$$1.1 \cdot \frac{w}{h} \leq \frac{l}{h} \leq 4.5 \cdot \frac{w}{h} - 4 \tag{4.1}$$

where l is the length, w is the width and h is the height. Additionally, the conditions $l/h < 3$ and $w/h < 3$ should apply. Worth mentioning that this optimal room dimension were found by Walker [54] in the theoretical work described before. These equation are fullfilled, so using the ITU 1116 recommendation (*i.e.* the Walker theory), the room it is supposed to ensure a reasonably uniform distribution of its

low-frequency eigentones. For the sake of clarity, here are shown the calculations:

$$1.95 \leq 2.48 \leq 4.79 \quad 2.47 < 3 \quad 1.77 < 3 \tag{4.2}$$

where l= 7.18 m, w= 5.15 m and h=2.90 m.

So far we have shown that there are a few general guidelines for designing small rooms with good distribution of room modes. We know that if two or more modes occupy the same frequency or are bunched up and isolated from neighbors, we are immediately warned of potential coloration problems. Over the years, a number of authors have suggested techniques for the assessment of room modes and methods for predicting the low frequency response of rooms based on the distributions of room modes. Among the most noticeably, Bolt [6], Louden [6], Bonello [7] have all suggested criteria. Possibly the most widely used criterion is that suggested by Bonello. Bonello's criterion is to plot the number of modes (all the modes, axial, tangential, and oblique) in one-third octave bands against frequency and to examine the resulting plot to see if the curve increases monotonically (*i.e.*, if each one-third octave has more modes than the preceding one or, at least, an equal number). Subsequently the criterion consists of the examination of the modal frequencies to make sure there are no coincident modes, or, at least, if there are coincident modes, there should be five or more modes in that one-third octave band. By applying Bonello's method to the equivalent room 5.15m x 7.18m x 2.90 m room, it was obtained the graph in figure 4.2. The conditions of both criteria are met and the calculation modes table is the table 4.1. The monotonic increase of successive one-third octave bands confirms that the distribution of modes is favorable. It is possible that the critical bands of the ear should be used instead of one-third octave bands. Bonello considered critical bands in the early stages of his work but found that one-third octave bands better show subtle effects of small changes in room dimensions. Another question is whether axial, tangential, and oblique modes should be given equal status as Bonello does when their energies are, in fact, quite different. In spite of these questions, the Bonello criterion is used by many

Table 4.1: Table that shows the fist 48 modes, using the rectangular room approximation, *i.e.*, using the given equation 1.34.

#number	n_x	n_y	n_z	Mode type	$f_{Resonance}$
1	1	0	0	Axial	23,90
2	0	1	0	Axial	33,63
3	1	1	0	Tangential	41,26
4	2	0	0	Axial	47,80
5	2	1	0	Tangential	58,45
6	0	0	1	Axial	59,14
7	1	0	1	Tangential	63,79
8	0	2	0	Axial	67,25
9	0	1	1	Tangential	68,03
10	1	2	0	Tangential	71,38
11	3	0	0	Axial	71,71
12	1	1	1	Oblique	72,11
13	2	0	1	Tangential	76,04
14	3	1	0	Tangential	79,20
15	2	2	0	Tangential	82,51
16	2	1	1	Oblique	83,15
17	0	2	1	Tangential	89,56
18	1	2	1	Oblique	92,69
19	3	0	1	Tangential	92,95
20	4	0	0	Axial	95,61
21	3	2	0	Tangential	98,31
22	3	1	1	Oblique	98,84
23	0	3	0	Axial	100,88
24	2	2	1	Oblique	101,52
25	4	1	0	Tangential	101,35
26	1	3	0	Tangential	103,68
27	2	3	0	Tangential	111,64
28	4	0	1	Tangential	112,42
29	3	2	1	Oblique	114,73
30	0	3	1	Tangential	116,94
31	4	2	0	Tangential	116,90
32	4	1	1	Oblique	117,34
33	0	0	2	Axial	118,28
34	1	3	1	Oblique	119,36
35	5	0	0	Axial	119,51
36	1	0	2	Tangential	120,67
37	0	1	2	Tangential	122,96
38	3	3	0	Tangential	123,77
39	5	1	0	Tangential	124,15
40	1	1	2	Oblique	125,26
41	2	3	1	Oblique	126,33
42	2	0	2	Tangential	127,57
43	4	2	1	Oblique	131,00
44	2	1	2	Oblique	131,93
45	0	4	0	Axial	134,51
46	5	0	1	Tangential	133,34
47	1	4	0	Tangential	136,62
48	0	2	2	Tangential	136,06

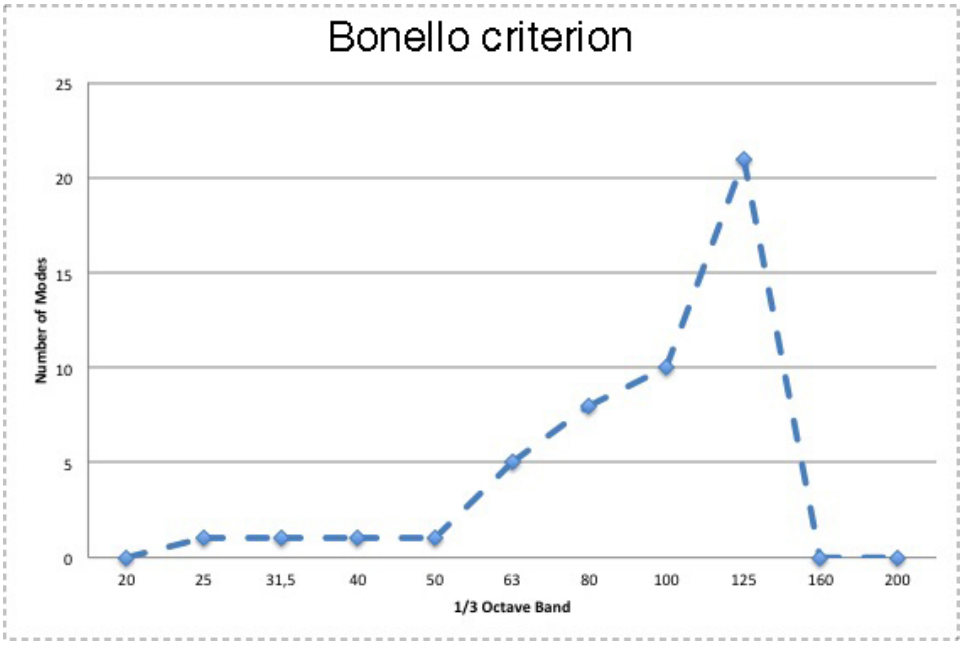

Figure 4.2: Calculation of resonance modes and application of the Bonello criterion for the case study listening room.

designers and a number of computer programs use it in determining the best room mode distributions. Worth mentioning that this theory isn't foolproof though, as some 2:1 room ratios fall into Bolt's area and some perfectly good rooms fall outside it. However it is a useful guide if some care is exercised.

Another tool which historically has been used to help choose room dimensions is the famous Bolt footprint shown in figure 4.3. The ratios of figure 4.3 are all referenced to ceiling height, where, as height, it is considered in this case study only the flat one of 2.90 m. In fact, inclined ceiling does not create modes, because of asymmetry. The Bolt criterion is not satisfied in our case study room. So it is possible that some colorations have to be deleted.

It has long been assumed that a uniform distribution of room modes in the frequency domain is a good thing. Concentrations of modes could cause artificial accentuation of certain frequencies, and gaps in the modal distribution could cause some frequencies to be less audible. Over the years, there have been suggestions of various room dimension ratios that offer superior modal distributions.

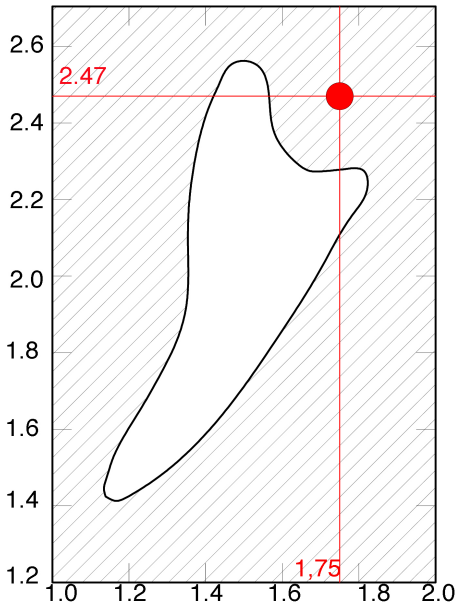

Figure 4.3: Curve domain that encloses dimension ratios given smoothest frequency response at low frequencies in small rectangular room[6]. The red dot represent the position of the case study listening room.

These and other studies have not always acknowledged three problems of real listening spaces that render the predictions unreliable.

1. The calculations assume that the room is perfectly rectangular, and constructed of perfectly flat, perfectly reflecting surfaces. Reality is rarely so simple, since rooms commonly have irregular shapes, large surfaces that absorb sound (they vibrate), furnishings, etc. These departures from the theoretical ideal result in errors in the calculated frequencies.

2. All of the modes are not equally important. In general, the axial modes are the dominant factors. Assessments of rooms should, therefore, incorporate a weighting in which the axial, tangential, and oblique modes are considered in that order of importance.

3. The positions of the sound sources and listeners in practical stereo listening arrangements do not result in uniform acoustical coupling to the room modes. As a result, the loudspeakers do not

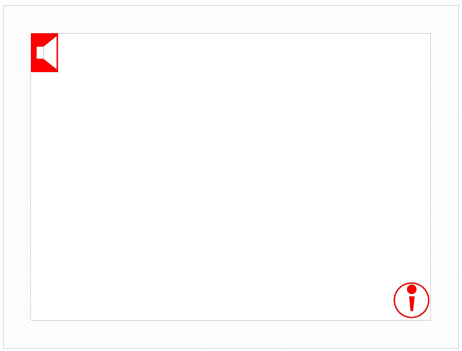

Figure 4.4: Placing a loudspeaker on the floor in a corner will ensure that all of the low-order modes are energized (all modes have a high-pressure region at any intersection of the three room surfaces - wall, floor and ceiling). Placing a microphone at an opposite corner (floor or ceiling) will ensure that it responds to all modes.

supply energy uniformly to all of the existing modes, and the listeners are not in positions to hear the effects of even those modes that are energized.

These complications mean that, in practical situations, predictive schemes may be helpful, but not perfectly satisfying. *In situ* measurements may be the only method for determining exactly what is happening.

4.2 Background and plant noise evaluation

Measurements were made of the background noise in the chamber with the air conditioning system turned off and on. Measurements were performed with an equipment that consisted of:

- 01dB $\frac{1}{2}$ inch microphone;
- 01dB Solo sound level meter;
- 10 m 7 pin midi cable;
- Behringer eurorack UB502;

The microphone positions were 3 and the spatial coordinates are represented in figure 4.5 and in table 4.4.

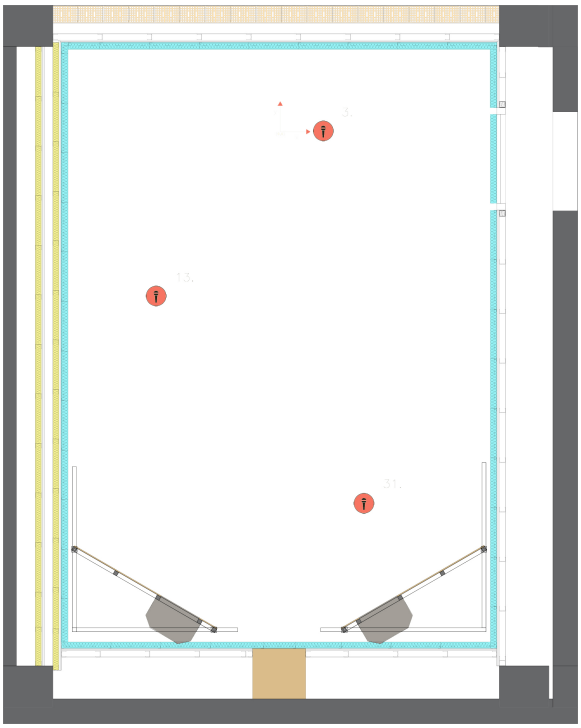

Figure 4.5: Microphone positions for Noise criteria

Table 4.2: Spatial position of the microphones.

Position	x [m]	y [m]	z [m]
3	0.50	0.00	1.20
13	2.00	-1.50	1.20
31	1.00	4.50	1.20

The measurements were taken in three conditions of air conditioning modality:

1. air conditioning at maximum velocity
2. air conditioning at medium velocity
3. air conditioning system turned off

In figure 4.7 are shown mean sound pressure levels (energetic mean on the 3 measurement positions) measured with maximum and medium power of the air conditioning system and with air conditioning turned

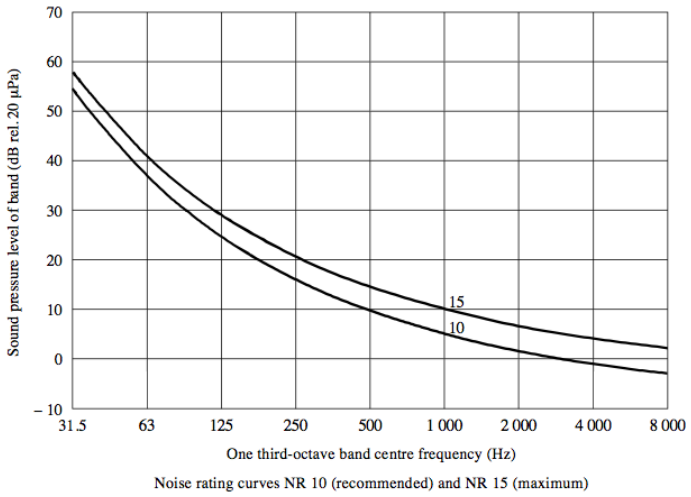

Figure 4.6: One-third octave band background noise level limits noise rating curves, based on the former ISO NR curves. After [25].

Table 4.3: Octave band sound pressure level values in dB.

NR curve	Frequency (Hz)								
	31.5	63	125	250	500	1k	2k	4k	8k
10	62.2	43.4	30.7	21.3	14.5	10.0	6.6	4.2	2.3
15	65.6	47.3	35.0	25.9	19.4	15.0	11.7	9.3	7.4

off. The continuous background noise (produced by the air conditioning system, internal equipment or other external sources) has to be measured in the listening area at a height of 1.2 m above the floor. Hence, the measured curves have to be compared with the NR reference curves, defined in the ISO 1996-1 [49]. They should preferably not exceed NR 10 (see Fig. 4.3) and under no circumstances should the background noise exceed NR 15. The background noise should not be perceptibly impulsive, cyclical or tonal in nature.

The SPL measurements in the octave bands up to the 500 Hz are affected from the background electric noise, due to the measurement chain. Other publications [36] state the happening of this phenomenon. Therefore the sound pressure level in these octave bands will be obviously overestimated. The octave bands lower than 500 Hz show a sonic emission that grows with the air flow rate. It is possible to see that the

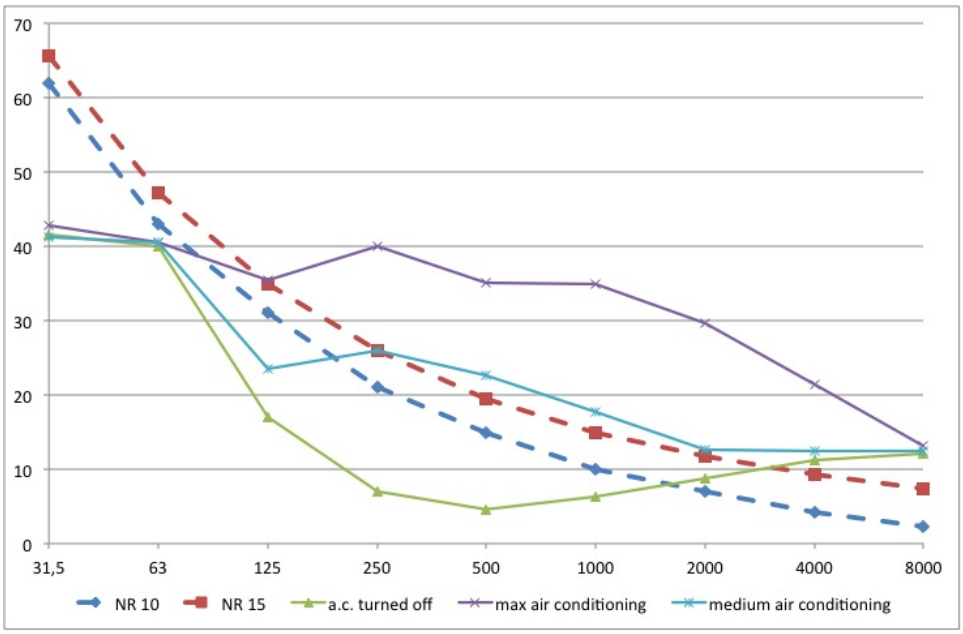

Figure 4.7: The continuous background noise produced by an air conditioning system (in maximum and medium power) and with air conditioning system turned on. The dotted lines are the noise criteria NR10 and NR15 suggested in the ISO 1996-1.

curve, relative to the maximum flow rate, exceeds the NR 15 for octave band higher than 125 Hz. Hence the listening condition will be with air conditioning system mainly turned off or at least with medium air flow rate.

4.3 Reverberation time

Seeking to understand how to proceede in the acoustic validation and design process, the earlier step was to adapt to the technical recommendations ITU-R BS 1116-1 and EBU/UER Tech. doc. 3276, which provide the guidelines to satisfy the requirements for a listening room. In the matter of the reverberation time, the technical recommendations give a time reverberation domain to satisfy as explained in the section **??**. With the aim to identify it, the analytical calculation are outlined below. The average value of reverberation time, T_m, measured over the frequency range from 200 Hz to 4 kHz should be:

$$T_m = 0.25(V/V_0)^{\frac{1}{3}} \tag{4.3}$$

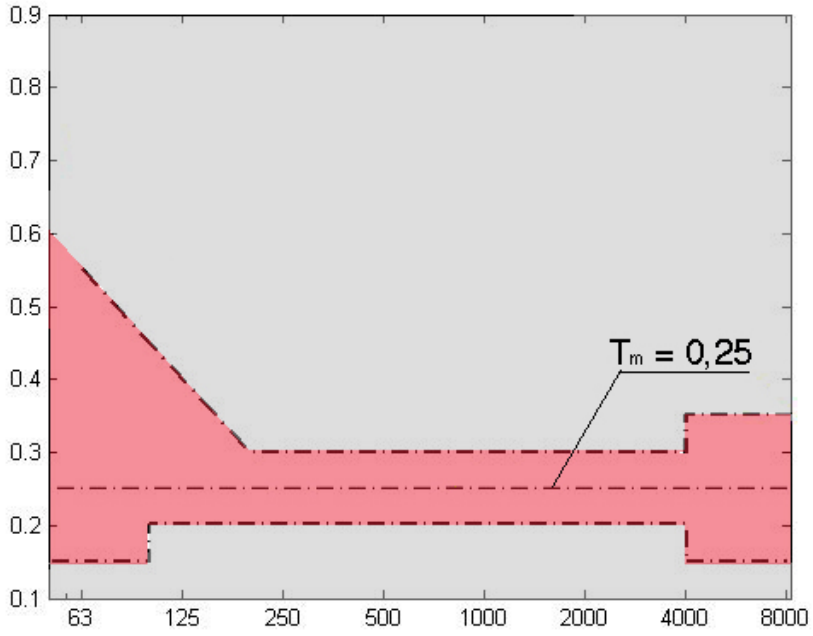

Figure 4.8: ITU 1116 reverberation time criterion applying the measured T_m of the case study room.

where:
V : is the volume of room
V_0 : is the reference volume of 100 m^3.
The tolerances to be applied to T_m over the frequency range from 63 Hz to 8 kHz are given in Fig. 1.22. Using the formula 4.3 the T_m is equal to 0.25 s considering 101 m^3 of total volume. Hence, knowing the T_m=0.25 it is possible to establish the reverberation time domain, using the ITU 1116 shown in 1.22, changing the theoretical T_m with the room one. So the resulting time domain in the figure 4.8 is highlighted in red.

The expected Schroeder frequency depending on the average value of reverberation time, T_m, is 101 Hz. Worth noting that a small listening room is in a transitional sound field, consisting of the direct sound, several strong early reflections, and a much diminished late reflected sound field. What it is heard is dominated by the directional characteristics of the loudspeakers and the acoustic behavior of the room

boundaries at the locations of the strong early reflections. The reverberation time does not reveal anything of this, so it is not useful as an indicator of how reproduced music or films will sound. Nevertheless, excessive reflected sound is undesirable, and a T measurement can tell us that we are "in the ballpark" described in the former recommendation.

4.3.1 IR measurements

Measurements were performed with the integrated Impulse Response (IR) method [50]. A pseudo-random electrical noise was fed into the loudspeaker. The room equipment consisted of:

- Dynaudio acoustic BM15 With 10 inches woofer;
- Bruel & Kjaer 4190 half inch microphone;
- Bruel & Kjaer 2669 pre-amplifier;
- PC providing the MLS and performing the cross-correlation;
- Crawn sound card XLS 1000
- Varicurve Dual Equaliser analyser;
- Monitoring system Dynaudio;
- 30 m mono channel cable

Temperature and humidity were measured same time as measurement, resulting 20.9 C°and 55.4% RH. The decay curve for each octave band was generated by a backward integration of the squared impulse response. The result of a correct T measurement is a number, or a set of numbers for different frequency bands, describing the decay rate over a range of sound levels, typically 20 or 30 dB, and then extended by multiplication to give a number for a 60-dB decay. In the case study it was chosen to use a T_{30}.

Reverberation times were determined by the computation of a linear least-squares fit of the decay curve in the chosen evaluation range. A

statistical analysis was conduced for the T_{30} in the frequency range 63 to 8000 Hz.

IRs were acquired in the whole chamber area with the two sources Dynaudio acoustic BM15. Before carrying out the effective measurements, supposing a very low reverberation time, the MLS length required to obtain a sufficient decay was defined, resulting in 64 K sample that, with a sampling frequency of 48 kHz, returns an impulse response of 1,4 s.

As previously highlighted, it was decided to process an iterative methodology that involves installation, *in situ* measurement and evaluation by the comparison with parameters recommended by the standards mentioned above. The iterative methodology consists of four steps (or configurations) and for each step an installation or a room variation has been implemented.

In every particular configuration, monaural IR measurements were carried out in 64 positions. Worth mentioning that, in order to describe as carefully as possible the spatial behavior of the room, the choice of the positions was carried out considering several factors that could affect the accuracy of the parameters maps. First of all, in order to decide the mesh of measurement positions, it was used as reference a similar case study described in the report of van Munster [53]. In this report measurements are described which were taken in different controlled rooms. Usually positions were set in a 5x3 matrix with an arbitrarily chosen spacing between the positions of 0.5 m, as it is possible to see in figure 4.9. Subsequently an attempt was made to use this mesh in our control room and, because of the dimensions, it was decided to optimize it using a different mesh system as shown in figure 4.10

The main interest, in the reverberation time measurements of this listening room, is to have a maximum accuracy in the listening spaces. Indeed the listening tests are supposed to be conducted in the reference and other recommended listening positions. So it was decided to take more measurements in these area with the purpose to make a more specific study.

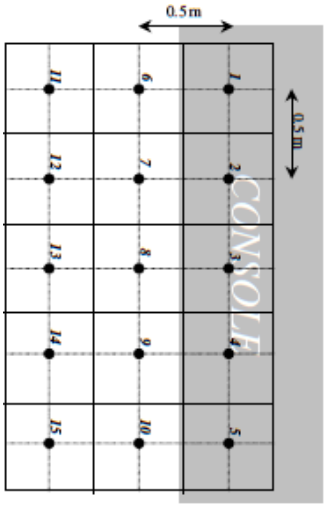

Figure 4.9: Measurement position in the reference case study.

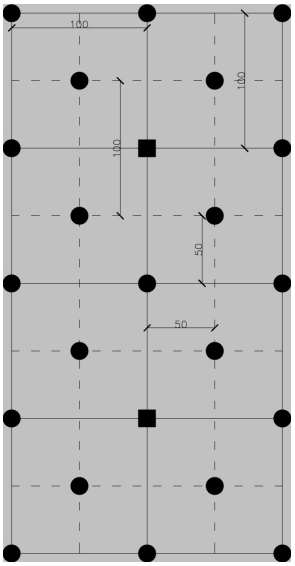

Figure 4.10: Optimised measurement position. The measurement positions are identified by circles and the listening positions are identified by squares.

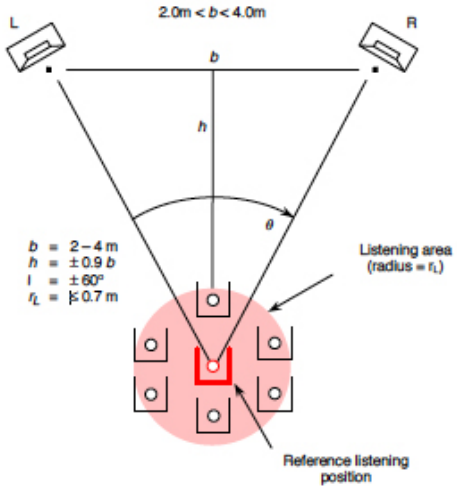

Figure 4.11: Definition of listening area. After [14].

It is to be noticed that EBU Tech. 3276 [14] defines the listening area as the space that is 0.7 m away from the listening point (fig. 4.11).

In figure 4.11 a typical layout is shown of stereo listening arrangement. This instruction is used as an advice for the placement of the microphones during the measurement: in fact 8 measurements were taken in the area directly around the two listening positions. However it is also necessary to evaluate any effects due to significant off-centre listening. The worst case listening positions are included for this reason. It is worth mentioning that the purpose of the measurement was also to realize interpolation maps, so in order to have plausible definition it is important to take dense mesh measurement and to measure also near the walls. In the figure 4.12 the microphone positions for the IR measurements are shown.

4.3.2 Configurations

In the following will be explained all the measured configuration. Seeking to understand every step of the characterization process it is worth mentioning that the panel mounted on the metal tilting frame have two possible inclination, because of the two possible listening position as explained in the section 3.1. The possible θ angle are described in the figure 4.13.

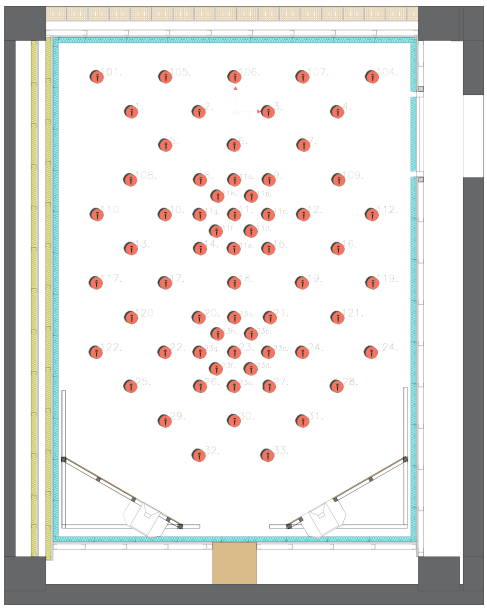

Figure 4.12: IR measurement positions in the listening room.

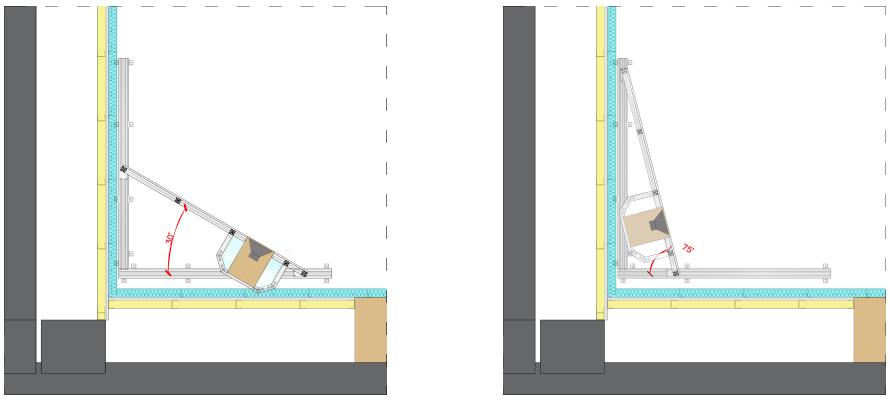

(a) $\theta = 30°$ (b) θ=**75°**

Figure 4.13: The two different set-up of sources position.

Table 4.4: Spatial loudspeaker position and panel angles.

Position	x [m]	y [m]	z [m]	Panel angle [°
S_{1R}	1.28	0.00	1.20	30
S_{1L}	-1.28	5.90	1.20	30
S_{2R}	2.25	5.60	1.20	75
S_{2R}	-2.25	5.60	1.20	75

Using the expression S_1 for the source with the 30°inclined panels and S_2 for the source with 75°inclined panel, in the table 4.4 the spatial position are described using the subscript L for the left loudspeaker and R for the right loudspeaker.

In the first configuration (see fig. 4.14**a**) the perimetric walls were covered with absorptive material. It was avoided to start without absorptive material because the reverberation tolerance, given by the ITU recommendation [26] was known and the plasterboard alone does not supply the necessary absorption. The reflective panels in OSB and MDF were already mounted and inclined at 30°, so that they were coincident with the set-up for the listener in the main listening position (see fig. 4.12). In this configuration there is no absorptive treatment on the ceiling.

In an attempt to find more information about the second listening position the second configuration was settled (see fig. 4.14**b**). It was performed using an inclination of the panels of 75°on the front wall. As in the previous configuration, there is no absorptive treatment on the ceiling.

The third configuration (see fig. 4.14**c**) shows the reflective panels inclined at 30°(settled for the main listening position). In this configuration there is absorptive treatment with porous absorber panels on the ceiling. The choice to design a 'dead'ceiling is an option: sometimes absorptive material is placed on the pavement, but this causes problem because of the dynamic rigidity of the material, that cannot be step on.

The fourth configuration (see fig. 4.14**d**) is an attempt to settle the low frequency problems and avoid modes in the OSB panels due to the

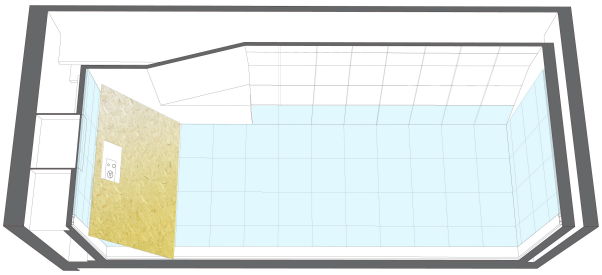
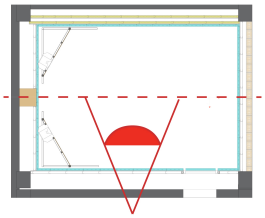

(a) **Configuration 1**

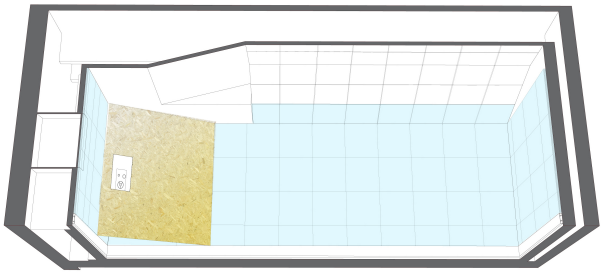
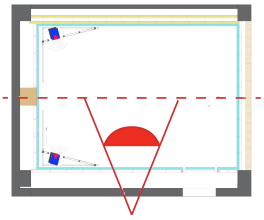

(b) **Configuration 2**

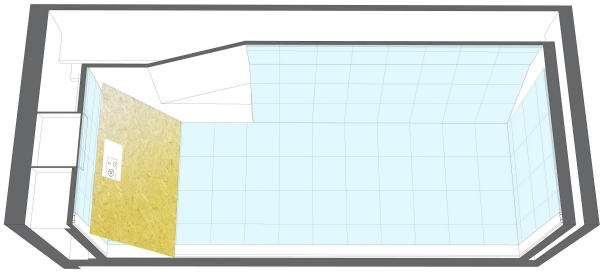
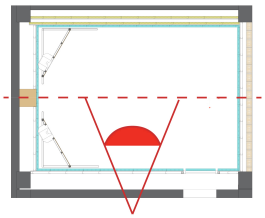

(c) **Configuration 3**

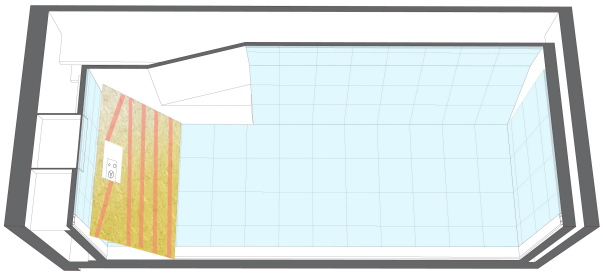
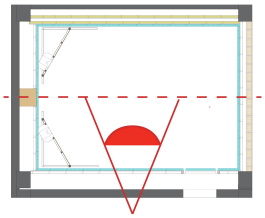

(d) **Configuration 4**

Figure 4.14: Perspective cross-section views representing different set-up analyzed in the IR measurement. Near every perspective cross section view there is the view represented in plan.

Figure 4.15: Panel stiffening manufacturing process.

Figure 4.16: Rods placed in the OSB panel, respecting the metal frame constraint

loudspeaker coupling. As it is possible to see in figure 4.16, the panels were stiffened with OSB strings scrap from the previous OSB panels cutting. The rods were inclined randomly and fixed with screws in order to avoid to create any modularity that risk to accentuate hypothetical mode. This ploy permits to have a random variable thickness that invalids the mode membrane theory. In figure 4.16 is shown the scheme of the rods placed in the OSB panels.

4.3.3 Results

The purpose of taking measurement of these different configurations is mainly to notice how any change influences the T_{30}. Hence it could be possible, through this process, to understand the performance of the materials and to plan future works.

The resulted T_{30} value derived by the *in situ* IR measurement is shown in two different forms:

- Interpolation maps
- Mean values trend as a function of frequency

Subsequently the analysis of the T_{30} will focus on the listening positions, in order to define and charchterize the listening position area.

First of all interpolation maps were realized of T_{30} for different configurations (see fig. 4.14), in order to understand how the T_{30} spatially changes. It was decided to show only the octave bands and not the one-third octave bands because the ITU 1116 [26] shows the reverberation time domain in octave bands. The maps, in every configuration, show a spatially diffuse behavior after the 500 Hz octave band, but for the sake of clarity, the maps between 63 Hz and 8000 Hz octave bands are shown.

The results of the first configuration are shown in the figure 4.19. It is possible to see that in the octave bands of 63 Hz and 125 Hz the T_{30} is definitely higher than the range required by the ITU [26]. In the octave bands of 250 Hz the maps show that there is an area of approximately 6.5 m^2 in the centre of the room where the T_{30} is higher than the nearby locations. In the octave bands higher than 500 Hz this "abnormal" area disappears.

In order to know which phenomena creates these different values of reverberation time, it is possible to analyze deeper the T_{30} of these points, looking at the impulse responses. In the figure 4.17 an impulse response of the position 17 at 250 Hz octave band is shown.

In small rooms, when the sound field is not diffused, the calculation of the reverberation time is often in error. In fact as it is possible to see in figure 4.17 it is not easy to plot the decay of a IR at low

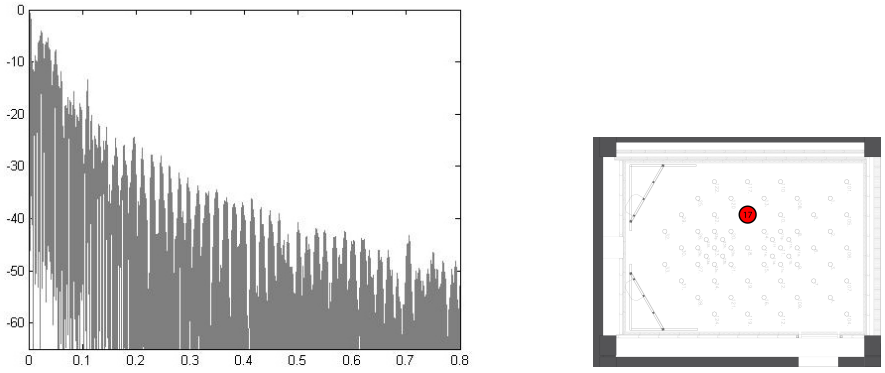

Figure 4.17: Impulse response of the measurment position number 17 (represented in the right plan as a red dot) at 250 Hz in the first configuration.

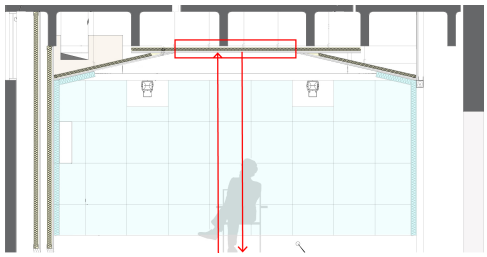

Figure 4.18: Cross-section that show the part of ceiling that as to be considered in order to calculate axial modes.

frequencies, when the sound field is still modal. Hence, considering the low frequencies, the spatial distribution of the reverberation time is potentially affected by mistakes. Phenomena like flutter echoes can compromise the detection of the reverberation time. When occurring between parallel walls, the axial modes normal to the parallel surfaces will constitute the harmonics of a flutter echo with period T and harmonic frequencies 1/T, 2/T *etc*. If the surfaces are hard and smooth, the higher harmonics can be prominent so that discrete tones are being heard. Seeking to understand if there is an uneven distribution of axial modes, the first six z-axis modes were considered (considering the parallel surfaces ceiling-pavement, as represented in figure 4.18). Table 4.5 shows that in the 250 Hz octave band are concentrated 3 modes, *i.e* uneven related with other octave bands. Another evidence of the presence of flutter echoes, in addition to the pair of parallel surfaces, is the fact that absorption is unevenly distributed so that there is less absorption

Table 4.5: Axial modes in z-axis, considering the fist 6 modes.

n_x	n_y	n_z	**Mode type**	$f_{resonance}$
0	0	1	Axial	59 Hz
0	0	2	Axial	118 Hz
0	0	3	Axial	177 Hz
0	0	4	Axial	237 Hz
0	0	5	Axial	296 Hz
0	0	6	Axial	355 Hz

from the parallel ceiling-pavement than from the other surfaces. In terms of modes, this means that tangential modes and oblique modes are more damped than the axial modes in the actual direction, making the latter more prominent. This is also the case study situation; in fact the other modes are damped using the polyester with bonded fibers, that has very high values of absorption coefficient in the 250 Hz octave band (figure 3.23). Furthermore the zone where this flutter echoes is concentrated is only where the ceiling is parallel to the pavement. Worth mentioning that we have almost the same situation in the 500 Hz octave band and the cause is mainly the same. The octave bands higher than 500 Hz have a more homogeneous T_{30} distribution.

The second configuration (see fig. 4.14a) shows the reflective panels inclined at 60°, so it is coincident with the set-up for the listener in the position number 11 (see fig. 4.12). In this configuration there is no absorptive treatment on the ceiling absorptive treatment. It is possible to see that the situation keeps on being almost the same of the configuration number 1, with reflective panels inclined at 30°. In this configuration, in particular at 63 Hz and 125 Hz, the charging of sound in the corner of the rear wall seems to be heavier. In the 250 Hz the "abnormal" area remains in the same point. In 500 Hz octave band the area is expanded in the back part of the room. Flutter echoes keep on being a problem in the second configuration. Mainly two solutions were thought in order to abate them:

- Tilting or inclining the parallel surfaces
- Using porous absorbers

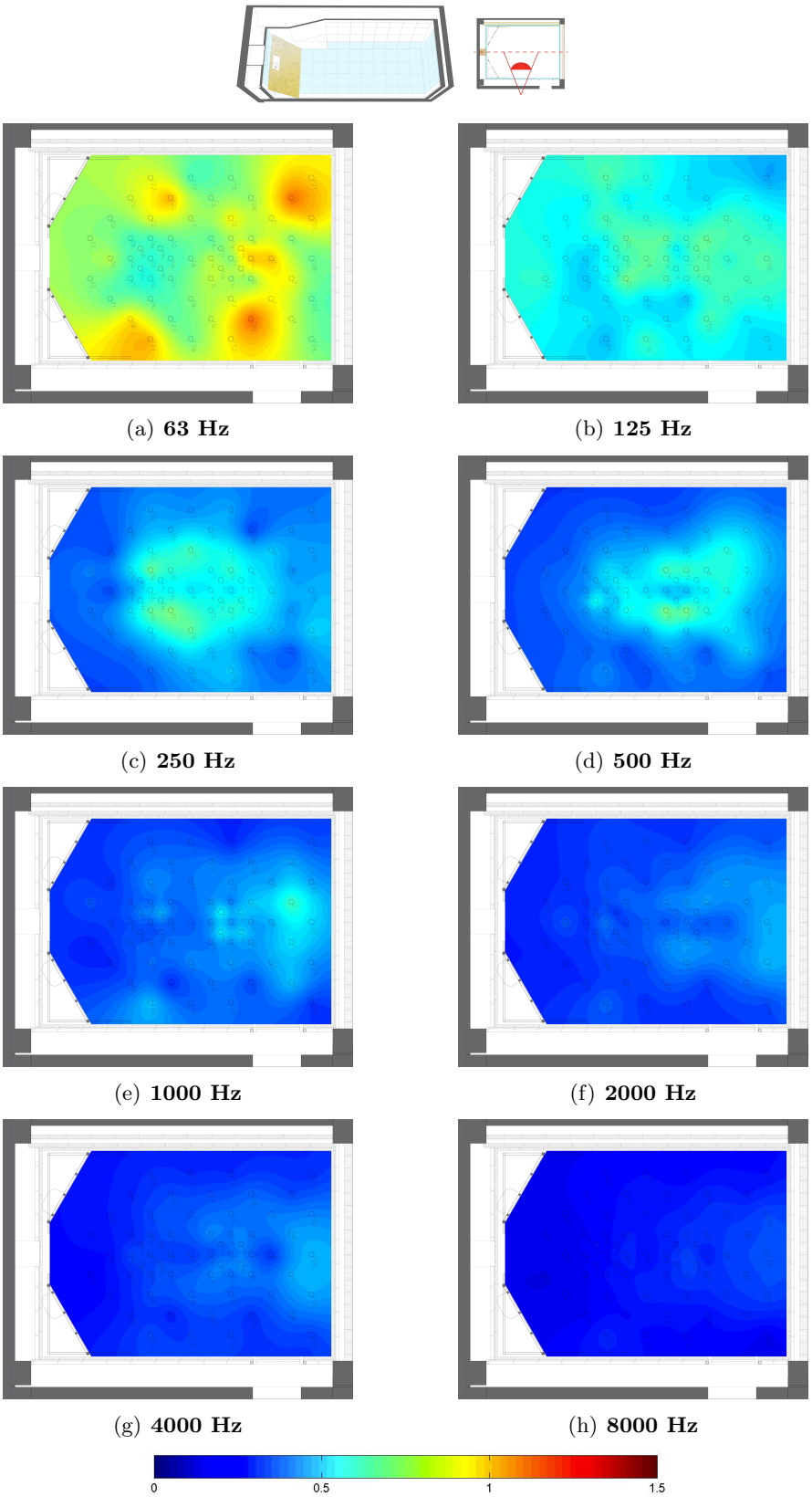

(a) **63 Hz** (b) **125 Hz**

(c) **250 Hz** (d) **500 Hz**

(e) **1000 Hz** (f) **2000 Hz**

(g) **4000 Hz** (h) **8000 Hz**

Figure 4.19: Interpolation maps of T_{30} from the IR. The room is settled in the first configuration.

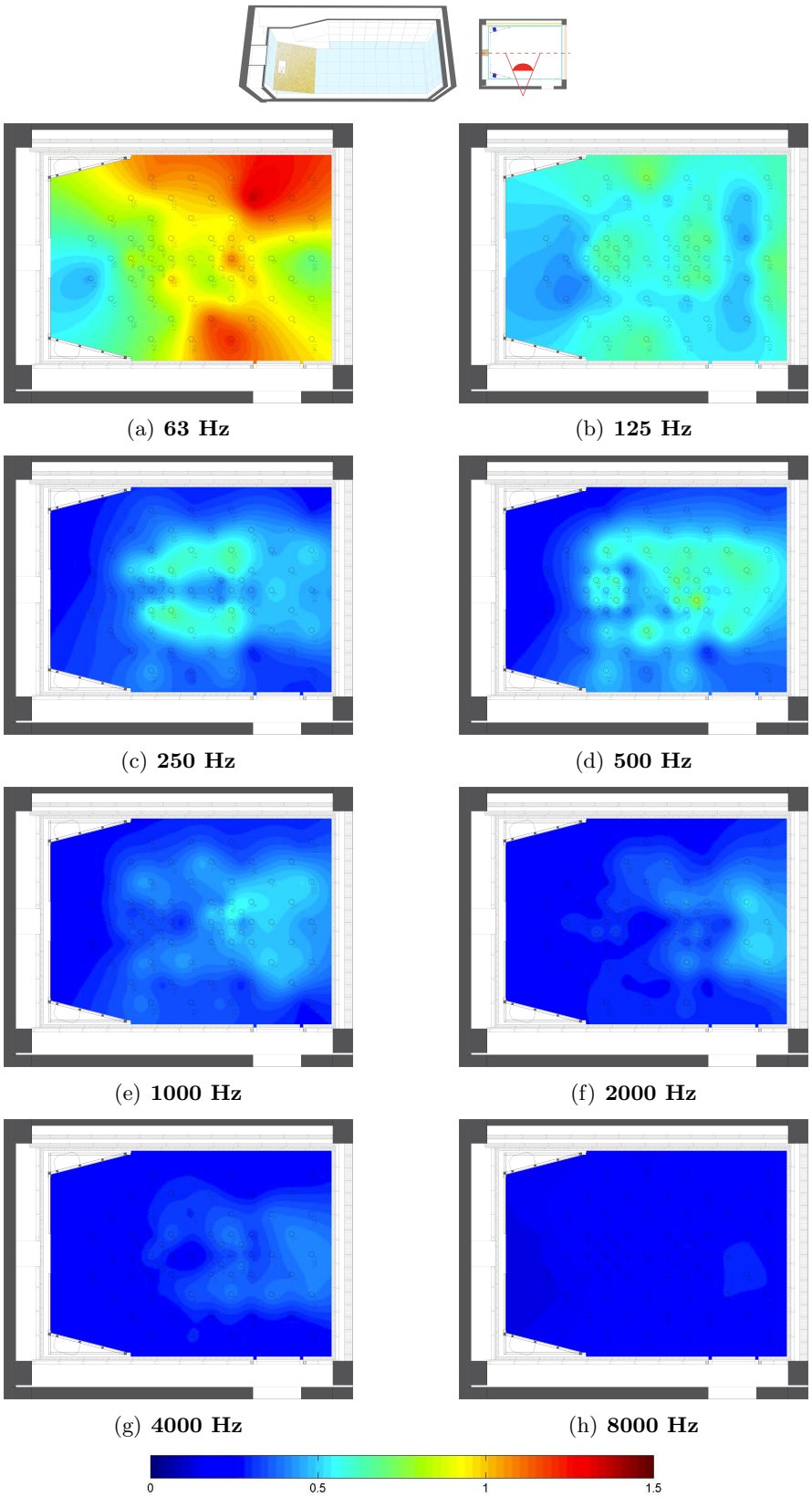

(a) **63 Hz** (b) **125 Hz**

(c) **250 Hz** (d) **500 Hz**

(e) **1000 Hz** (f) **2000 Hz**

(g) **4000 Hz** (h) **8000 Hz**

Figure 4.20: Interpolation maps of T_{30} from the IR. The room is settled in the second configuration.

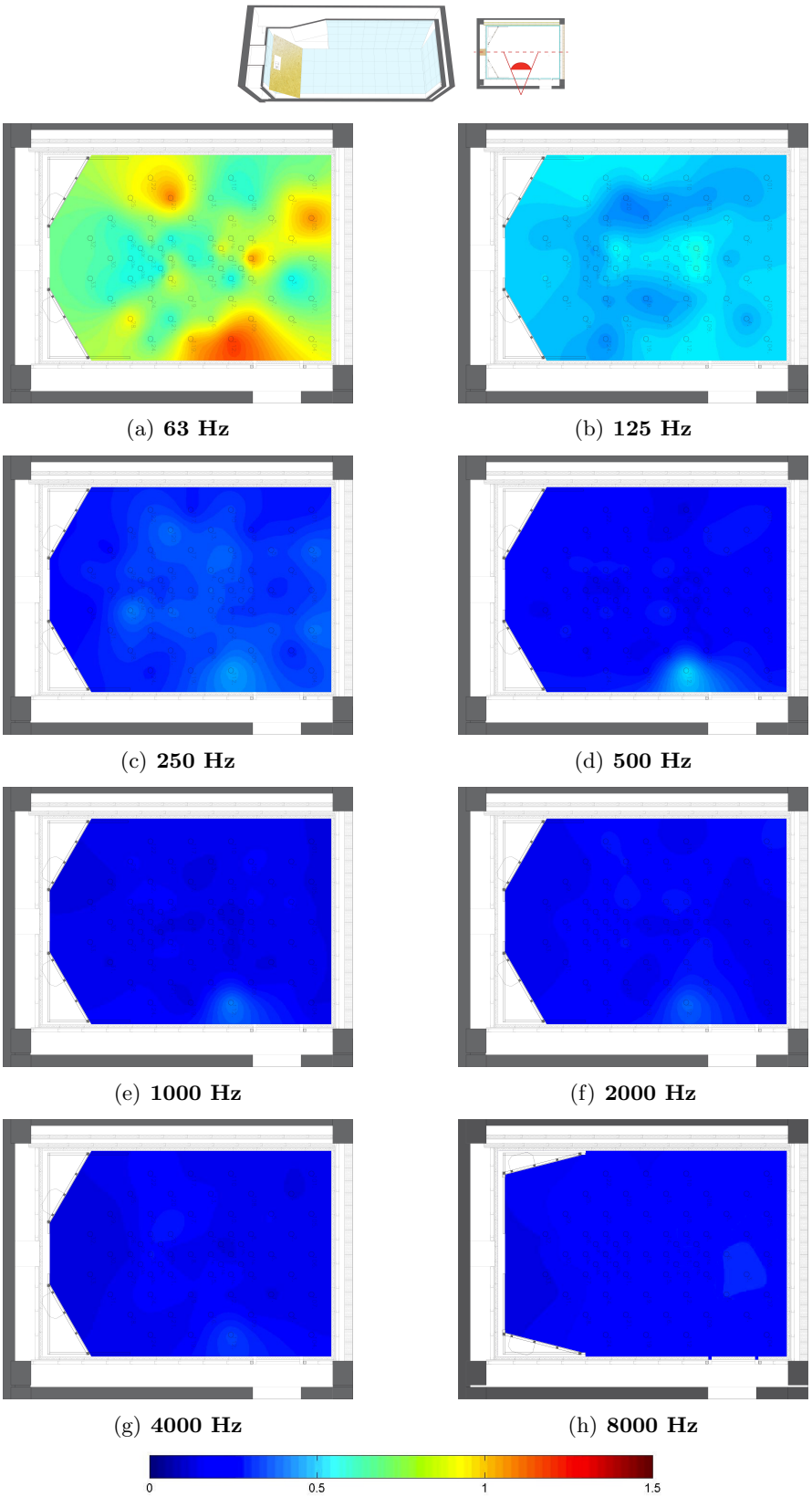

(a) **63 Hz** (b) **125 Hz**

(c) **250 Hz** (d) **500 Hz**

(e) **1000 Hz** (f) **2000 Hz**

(g) **4000 Hz** (h) **8000 Hz**

Figure 4.21: Interpolation maps of T_{30} from the IR. The room is settled in the third configuration.

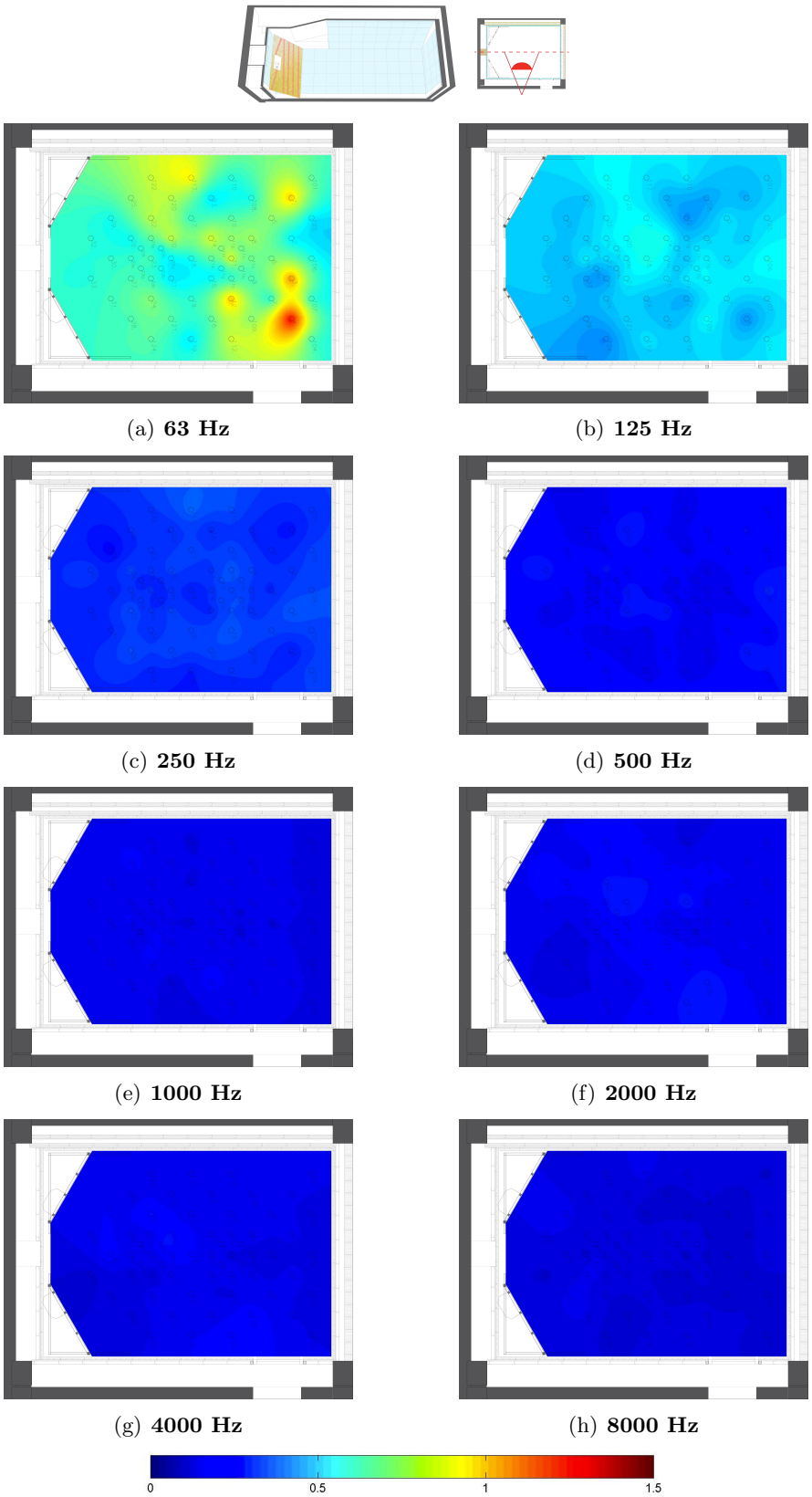

(a) **63 Hz** (b) **125 Hz**

(c) **250 Hz** (d) **500 Hz**

(e) **1000 Hz** (f) **2000 Hz**

(g) **4000 Hz** (h) **8000 Hz**

Figure 4.22: Interpolation maps of T_{30} from the IR. The room is settled in the fourth configuration.

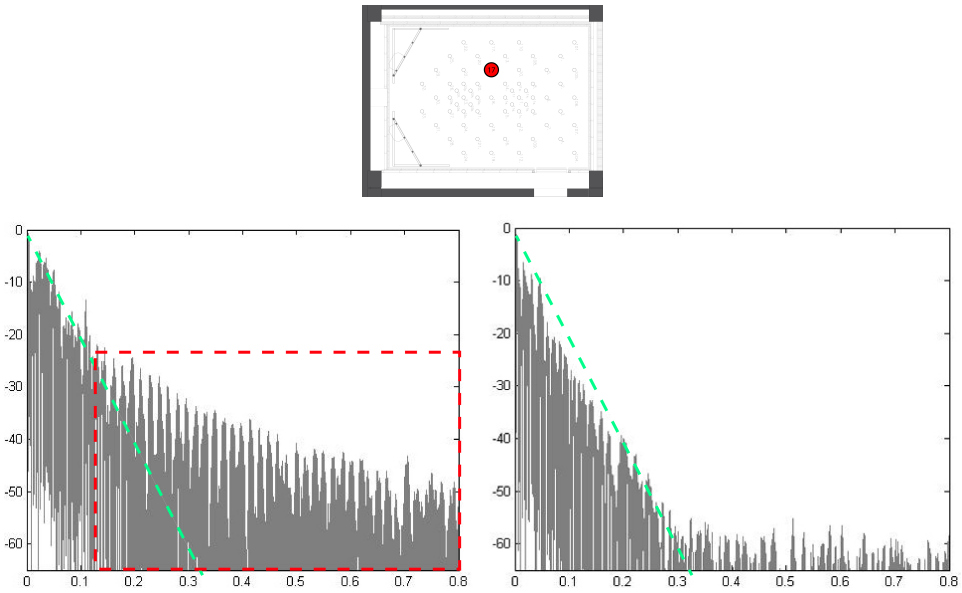

Figure 4.23: Comparison of the impulse response of the measurment position number 17 (represented in the right plan as a red dot) at 250 Hz. The first configuration is on the left, the third is on the right.

The decision was to treat with porous absorber panels the ceiling. Hence the third configuration (see fig. 4.14c) shows the reflective panels inclined at 30°, coincident with the set-up for the listener in the position number 23 (see fig. 4.12) and the ceiling with an absorptive treatment. Looking at the interpolation maps, it is possible to state that the results change massively, in particular in low and mid-frequency range. The critic area in 250 Hz disappears and the T_{30} distribution becomes more homogeneous. In order to compare this configuration to the first and to establish if the flutter echoes create these different values of reverberation time, the impulse responses were analyzed again after the ceiling treatment. In the figure 4.23 the two impulse responses of the point 17 at 250 Hz octave bands are shown. It is possible to see that the IRs slopes have a massive change. In the first case the decay curve has a sort of double slope produced by normal modes of vibration with different decay constants. The part highlighted in red has not a proper slope, but is more constant, because of the flutter echoes. In the third configuration, the part represented in red disappears. That means that the red 'slopes'represented the decay of the modes gener-

ated by the parallelism between the pavement and the ceiling.

In the third configuration the distribution of the T_{30} in the mid-frequencies is quiet homogenous, but at low frequencies it keeps on being inhomogeneous and it is difficult to find porous materials that absorbs at low frequencies. So in the fourth configuration the strategy changed and as explained in the previous section the reflective panels were modified.

The result achieved can be considered positive. The low frequencies band, *i.e.* 63 Hz and 125 Hz, became more homogeneous. Although there are not big changes in the interpolation maps, it is worth noting that it is very difficult to absorb and diffuse the sound at low frequencies.

For the mid and higher frequencies the reverberation time seems to be more volume dependent. As the results show, the smallest control rooms under test have reverberation times below the lower recommended limit, and the rooms with average volume have reverberation times which fall between the recommended limits.

Interpolation maps show whether the T_{30} value is homogenous in the room or not. Instead the trend of the T_{30} mean value compared with the technical recommendation [26] tolerance explains how the mean value is far from the recommendation. In figure 4.24 the mean values of T_{30} and the ITU reverberation time domain [26] are represented. The red line is the trend of the configuration with reflective panel inclined at 30°, while the blue is the trend of configuration with reflective panel inclined at 75°. In this case there is no materials change between this two configurations, so simply using simply the Eyring formula it is possible to know that if there is no room characteristic change of material or volume, the mean reverberation time does not change. Hence in figure 4.24 there are no big difference between red and blue line.

For these configurations, T_{30} falls outside the proposed tolerance band limits of the ITU and EBU recommendations. Hence the room results too reverberant. Once mounted the absorptive material on the ceiling the reverberation time is expected to drastically decrease; this happens in the third configuration. In figure 4.25 it is shown that the trend of the mean parameter T_{30} is still high at low frequency, but

at which frequency it is lower than the ITU 1116 reverberation time domain [26]. This situation is due mainly to the acoustic properties of the absorptive material. The future development of the room involves the design of Schroeder 2-D diffusers built in reflective material. So there is an allowance to reach the reverberation time domain.

The fourth configuration obtains a decrease of 0,1 s in the 63 Hz. The important result of the fourth configuration is that, modifying the reflective panels, a decreasing in low frequencies can be obtained and it is important because the low frequencies reverberation time are very difficult to change.

Finally the analysis of the reverberation time focuses on the listening position. As it is possible to see in figure 4.11 the technical recommendation [26] defines the listening position, but it does not specify which are the requirement that a listening position has to satisfy. In order to understand when the perceived reverberation changes in the listening area, the UNI EN ISO 3382-1 [50] was used as reference. The Annex A introduces an useful value: the Just Noticeable Difference (JND). The JND is the smallest detectable difference at which a change is perceived. It could be applied to a lot of acoustic parameters, *e.g.* the SPL, EDT, C_{80} *etc.*. The UNI EN ISO 3382-1 attributes to the perceived reverberation a JND of 5%. Despite the standard gives a reverberation time range from 1 s to 2 s, in this thesis it will be tried to apply this criterion. The purpose of the graphs in figures 4.28 and 4.28 is to show if the 8 position around the listening positions are or not in the JND range. The first figure 4.28 shows the study of the reverberation time in the listening position number 23. Hence it was proposed a criterion that permits to evaluate the quality of the listening position. It consists of the verification that the standard deviation of the T values, measured in an area with radius 0,7 m around the listening position, fits in the JND range of the reverberation time in the listening position point. If they fit, the listening position could be considered enough homogenous not to give the perception of change of reverberation time. The first and the second configurations have the higher values of T, *i.e.* a higher JND range. The standard deviation are very high in the mid frequency range. Furthermore in the first config-

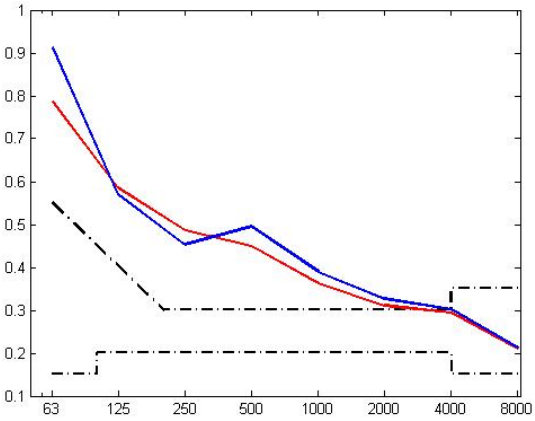

Figure 4.24: Trends of the parameter T_{30} (s). It is represented the mean values, and the ITU's [26] reverberation time domain. The red line is the trend of the first configuration, while the blue is the trend of second configuration.

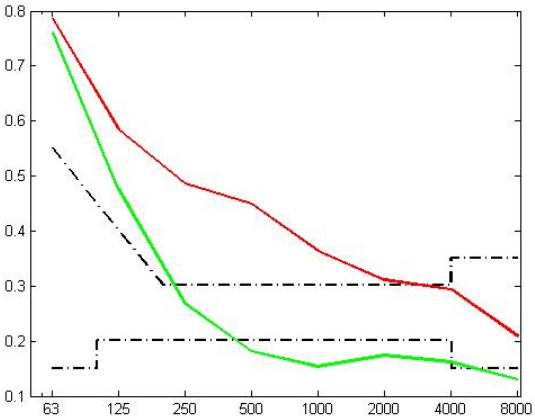

Figure 4.25: Trends of the parameter T_{30} (s. It is represented the mean values, and the ITU's [26] reverberation time domain. The red line is the trend of the first configuration, while the green is the trend of the third configuration.

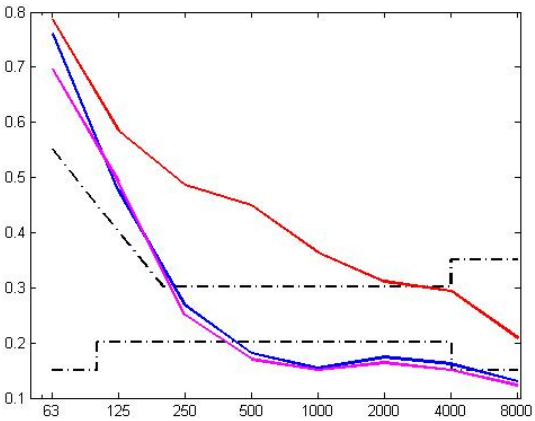

Figure 4.26: Trends of the parameter T_{30} (s). It is represented the mean values, and the ITU's [26] reverberation time domain. The red line is the trend of the first configuration, the blue is the trend of the third configuration and the magenta one is the trend of the fourth configuration.

uration at the 2000 Hz octave band, the JND range and T values are very different, whereas in the second configuration the T mean values of the measurements around the listening position result far from the JND range at 250 Hz and 500 Hz. Hence the second configuration results disadvantegeous compared with the first. Worth remembering that the second configuration is performed for the listening position number 11. In the third configuration the T at mid-frequencies drastically decreases and consequentially the JND range becomes narrower. It could be noted that fortunately also the standard deviations are lower so the standard deviations almost match the just noticeable difference range. At low-frequencies there is still a sensitive difference that is not acceptable. The fourth configuration at mid-frequency range has a lower T, so the JND range is narrower. Hence, it is very difficult that the standard deviation and the JND range completely match, but it is to be considered also that the JND range is not thought for this low value of T. So the JND can be considered acceptable at mid-frequencies. Furthermore the standard deviation in the 63 Hz octave band is halved compared to the standard deviation in the third configuration and it can be defined satisfactory. Worth mentioning that, as written above, in the room development reflective material is going to be used and a percentage of absorbing material will be removed. Hence the JND range in the mid-frequencies octave band will be wider, improving the probability of the standard deviation to match the JND range. The figure 4.28 shows the study of the reverberation time in the listening position number 11. Worth remembering that these configurations except the second one are performed for listening situations in the position number 23, so it is expected that the results will be disadvantageous compared with the results shown in figure 4.28.

Drawing some conclusion, the first configuration the JND range of the T mean values are often misaligned and the standard deviations are wide. Although the second configuration is performed for the listening position number 11, the situation changes compared to the first configuration, but JND range and standard deviation keep on mismatching. In the third configuration the situation gets better, but the mismatching at low frequency keeps on being high because of the high

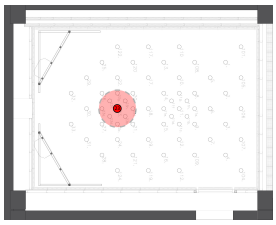

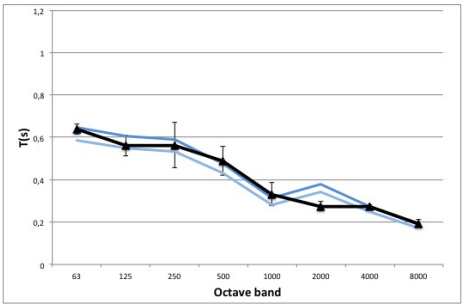

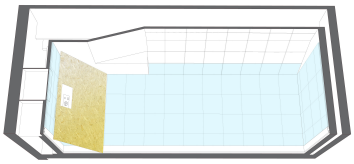

(a) **Configuration 1**

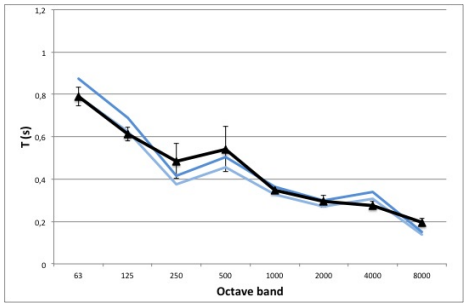

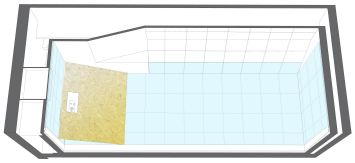

(c) **Configuration 2**

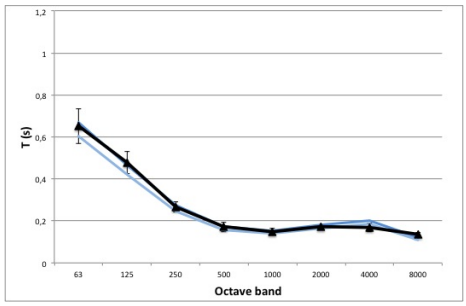

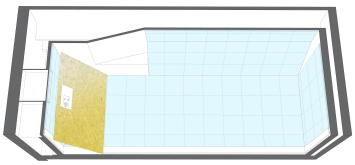

(e) **Configuration 3**

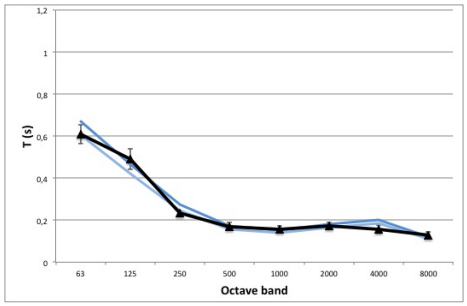

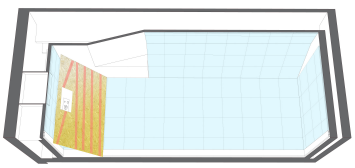

(g) **Configuration 4**

Figure 4.27: Trends of the parameter T_{30} (s) as a function of frequency from IR. It is represented the mean values of the 8 position around the listening position number 23 with the relative standard deviation, the light blue lines defines the JND range of the T_{30} in the listening position 23. All the configuration are shown in chronological order.

standard deviation at 63 Hz. In the fourth configuration an improvement is expected at low frequency, but unlike the listening position 23, the situation gets worse because the JND range and the T mean value completely mismatch.

4.4 Sound pressure level measurements

Sound pressure level measurements were performed in the room. A pink noise was fed into the loudspeaker. The room equipment consisted of:

- Dynaudio acoustic BM15 With 10 inches woofer;
- 01dB $\frac{1}{2}$ inch microphone;
- PC with software generating the pink noise;
- 01dB Solo sound level meter;
- Behringer eurorack UB502;
- 10 m 7 pin midi cable;

The measured temperature and umidity were 21,9 C and 54,4 % RH. The loudspeakers generate 85 dbA of sound pressure level in the listening position at the height of 1.2 m, *i.e.* the main listening position (see fig. 4.9). The sound pressure level is taken in a time window of 10 seconds.

4.4.1 Result and interaction with room modes

The case study listening room is not a rectangular box, as usually. It is known that differences in detailed shape, placement of plants light or furniture ensure that the situation will have its own distinctive problems. At low frequencies it is frequently possible to be quite accurately with the analytical approach about what is happening in a room but the standing wave structure at higher frequencies is usually lost in confusion. There is not only a problem of shape or singularity of the system. Also the measurement position could affect the detection of

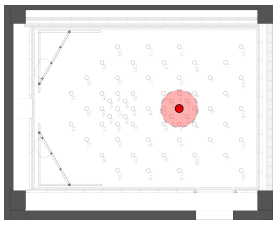

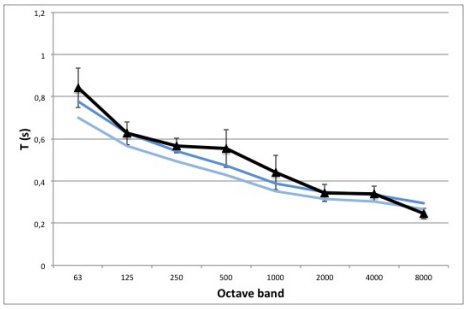

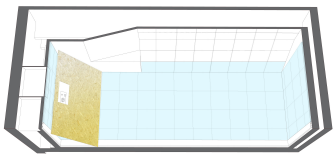

(a) **Configuration 1**

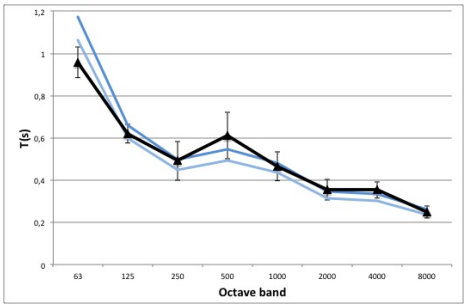

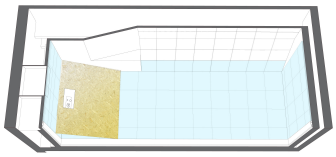

(c) **Configuration 2**

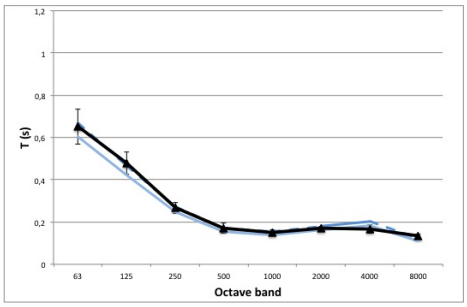

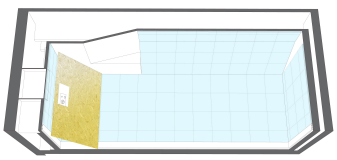

(e) **Configuration 3**

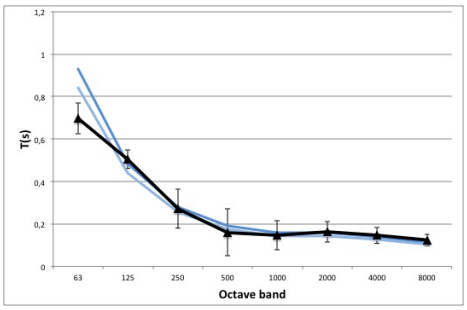

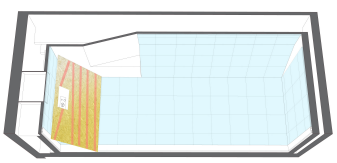

(g) **Configuration 4**

Figure 4.28: Trends of the parameter T_{30} (s) as a function of frequency from IR. It is represented the mean values of the 8 position around the listening position number 11 with the relative standard deviation, the light blue lines defines the JND range of the T_{30} in the listening position 11. All the configuration are shown in chronological order.

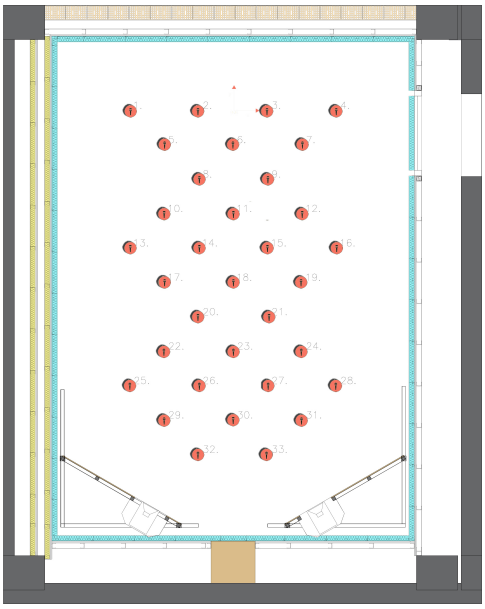

Figure 4.29: Sound pressure level measurement positions in the listening room.

modes. In order to detect room modes, as written in the former section, sound pressure level measurements were carried out, considering that the sound pressure level meter should detect peaks and minimum values of the hypothetical standing wave.

Hence, interpolation maps of SPL were realized. These maps were drawn for the different configurations (see fig. 4.14) described in the section 4.3.2. The purpose of taking measurements of these different configurations is mainly to notice how any change influences the T_{30}. Hence it could be possible, through this process, to understand the performance of the materials and to plan future works.

In this section only low-frequencies maps will be shown, because it is our interest only the detection of the modes and the lack of spatial diffusivity in order to fix it, with a trial and error process as written before. Hence 8 maps representing one-third octave bands will be shown in the range form 50 Hz to 250 Hz.

The first configuration results are shown in the figure 4.30.

Starting from these maps, it is possible to recognize room modes, or simply the lack of diffusivity. So, in order to find a strategy to avoid these colorations, it is possible to make a brief analysis considering the

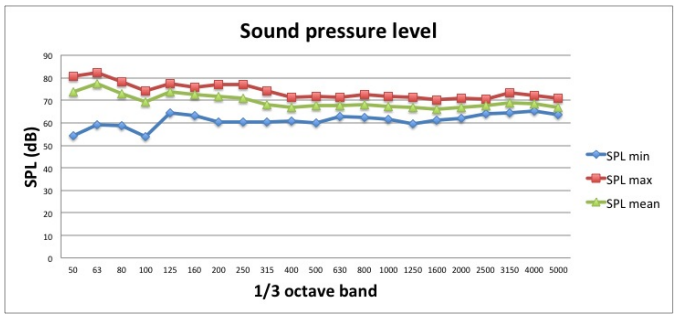

Figure 4.30: Trend of the parameter SPL as function of one-third octave bands; mean values, maximum, minimum. The case study configuration is the first.

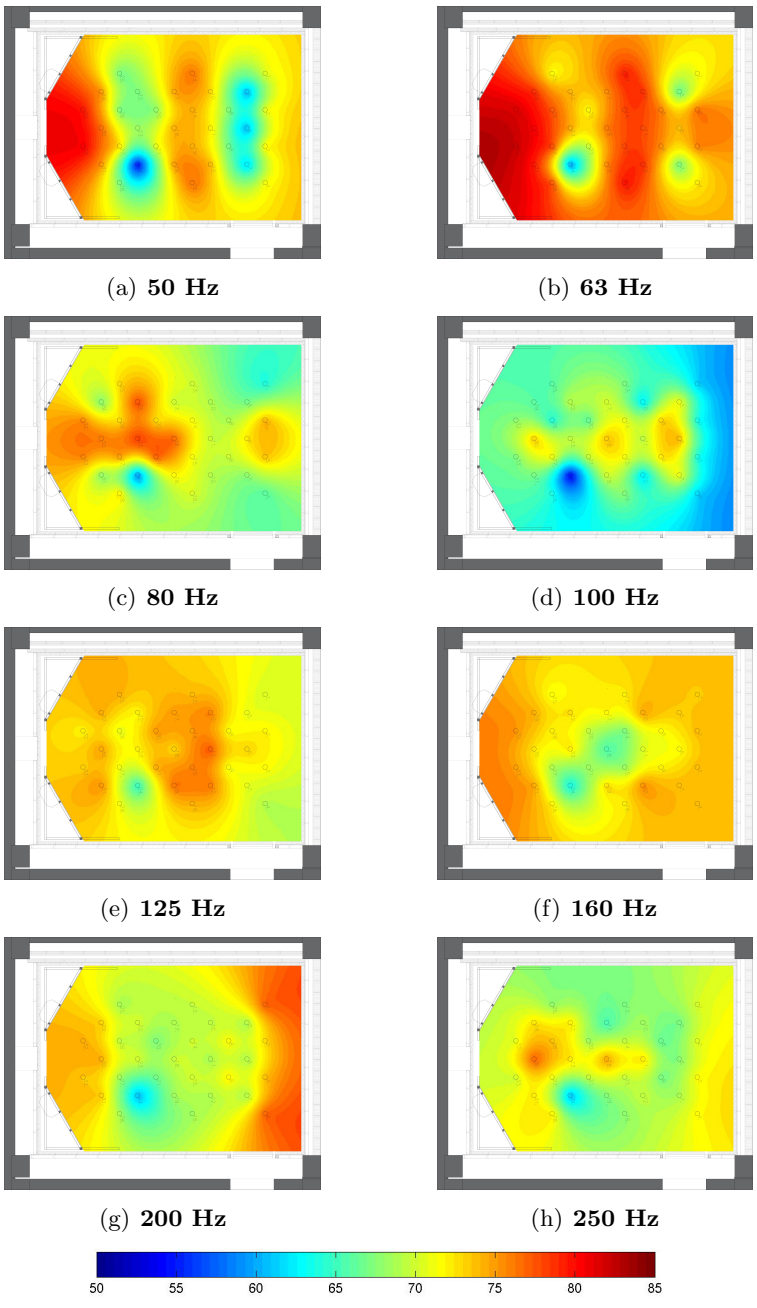

(a) **50 Hz** (b) **63 Hz**

(c) **80 Hz** (d) **100 Hz**

(e) **125 Hz** (f) **160 Hz**

(g) **200 Hz** (h) **250 Hz**

Figure 4.31: Interpolation maps of Sound pressure level. The case study configuration is the first.

only the parallel walls. Considering the length of the room (y-axis) we can find the resonance frequency:

$$f_{RES,y} = \frac{343\,\frac{m}{s}}{2 \cdot 7.18\,m} = 23.9\,Hz \tag{4.4}$$

But this frequency cannot be detected by the sound measurement. In fact the loudspeaker BM15 Dynaudio is supposed to work properly in the frequency range 43 Hz - 20 kHz. So it is possible to find the others resonance frequencies multiplying these by an integer number. Working by progressive number multiplication, $f_{RES,y} \cdot 2 = 47.8\,Hz$, so the energy of this modes is inside the one-third octave band of 50 Hz. It is possible to see in the figure 4.32 the standing wave resulting from this calculation. It is worth noting that the standing wave described is recognizable in the 4.30 **a**, because of the distance between minimum and maximum SPL. Subsequently if it is considered the width of 5,15 m (x-axis), the resonance frequency is 33.3 Hz For the same former purpose, multiplying by two returns $f_{RES,x} \cdot 2 = 66.6\,Hz$ that is in the 63 Hz one-third octave band. Also this standing wave is recognizable in figure 4.33. The standing wave described is not completely recognizable in the 4.30 **a**, but it is still clear. The problem, in this case, is the lack of a measurement position in the near part of the ceiling that hinders the coloration of maximum SPL near the wall. Increasing progressively the integer coefficient of the resonance frequency for the length it is possible to recognize other modes that are still visible in the maps 4.30. In fact $f_{RES,x} \cdot 2 = 99.9\,Hz$, that is in the 63 Hz one-third octave band, should result in a standing wave as plotted on the left of figure 4.34. But in this octave band this is not the only axial modes, in fact the resonance frequency along the y-axis multiplied by 4 gives $f_{RES,y} \cdot 4 = 95.6\,Hz$. So this is also to sum in the SPL pattern.

Trying to observe in practice what happens in the 100 Hz one-third octave band, in figure 4.30 it is possible to see that there are some tracks about this mode summation, but it is still difficult to detect it because of the lack of measurement positions. The plot 4.30 is really only useful for identifying the frequencies of the strongest modes in the room. It is not uncommon to find that the measured frequencies are

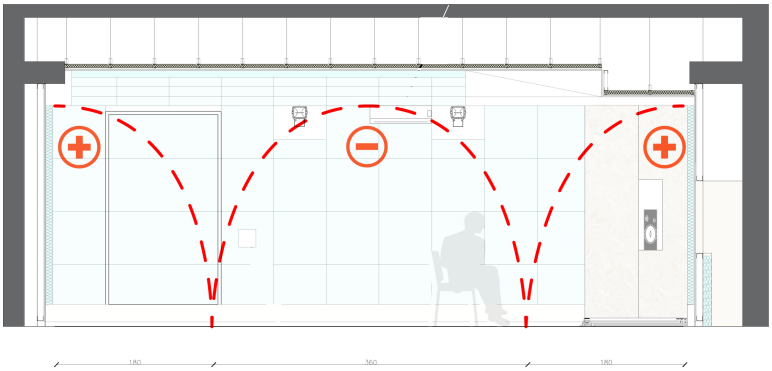

Figure 4.32: Hypothetical standing wave applied to the case study room along the y-axis $n_y = 2$.

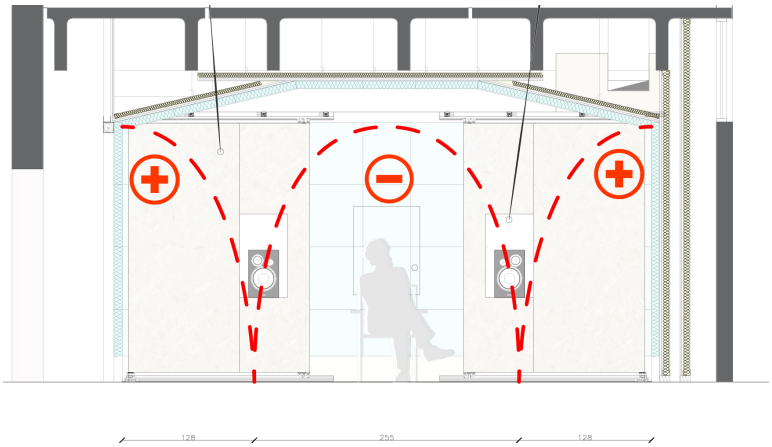

Figure 4.33: Hypothetical standing wave applied to the case study room along the x-axis with $n_x = 2$.

Figure 4.34: Hypothetical standing waves applied to the case study room. The left one is along the x-axis with $n_y = 3$, the right one is along the x-axis with $n_y = 4$

not exactly the same as those that can be calculated. This is because the room is a real one, not an idealized one. It is clear the difference between the modal field and the diffuse one. Indeed the graph shows more energized peaks, that are caused by axial modes, *e.g.* the 63 Hz one-third octave band.

The third configuration is born with the purpose to use the acoustical absorption by the room boundaries in order to remove low frequency energy from the sound field. The loss of energy to room structure reduces sound power that is cointained in the listening room. While this could be viewed as a disadvantage, making the subwoofer work harder, it can also be viewed as a benevolent acoustical factor. This absorption reduces the Q of the room modes, resulting in lower maxima and higher minima tones, described by the stylized curves in figure 4.37. In rooms the nulls are not perfect. Altough the graph 4.35 seems to be flatter than the previous one. It is possible to see spatially the lack of diffusivity is almost the same with the same room modes shown in the maps 4.30. Of course there are clear explanations about that:

- The ceiling can affect the modes on the z-axis, the ones that are not detectable watching these maps, because measurement positions were taken on a plane, *i.e.* at a height of 1.2 m.
- Before every measurement series, the loudspeakers were 'forced'to generate 85 dbA of sound pressure level in the listening position at the height of 1.2 m. That means that every effort to flatten the amplitude of the standing wave is in vain because the loudspeaker is supposed reproduce the same amplitude **??**.

Of course the lack of the ceiling reflection is supposed to evidence the modes along x and y axis, just because subtracting energy to the z axis modes, the SPL pattern become easier to read. Between the measurements test performed, the reverberation time is more influenced by the absorption at low frequencies. In fact with the reverberation time we do not have the problem of the loudspeakers 'forced'to generate 85 dbA, and the main issue is about reflection. In the 200 Hz one-third octave band the SPLs are spatially more diffuse, but in the corner of the rear wall the adjacent measurement position are charged of reflec-

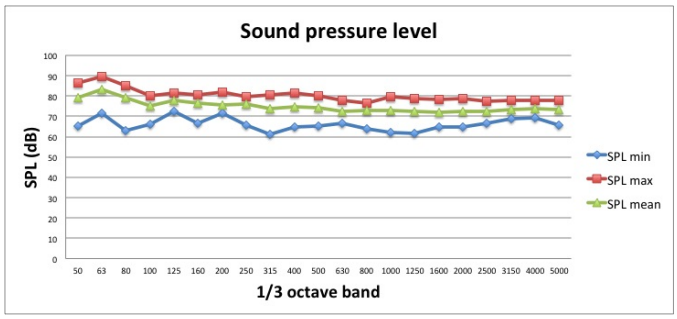

Figure 4.35: Trend of the parameter SPL as function of one-third octave bands; mean values, maximum, minimum. The case study configuration is the third.

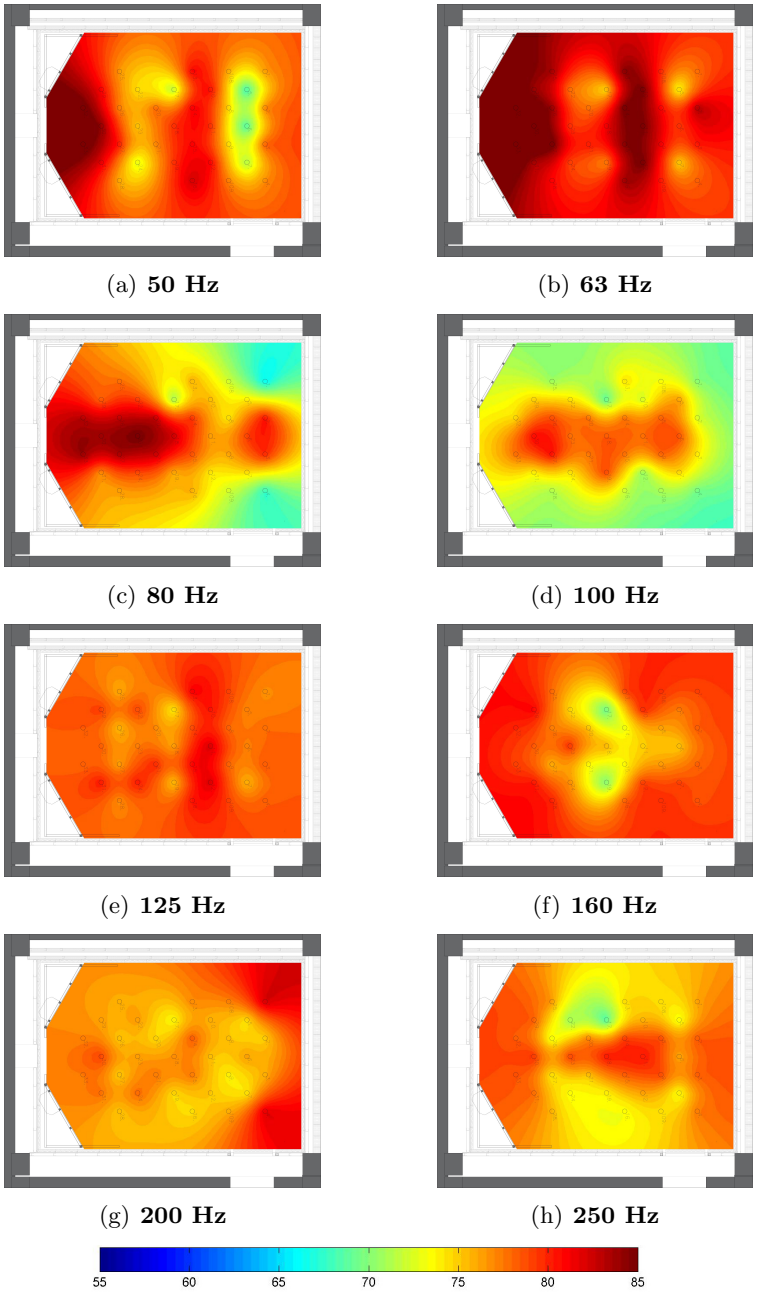

(a) **50 Hz** (b) **63 Hz**

(c) **80 Hz** (d) **100 Hz**

(e) **125 Hz** (f) **160 Hz**

(g) **200 Hz** (h) **250 Hz**

Figure 4.36: Interpolation maps of Ssound pressure level. Third configuration.

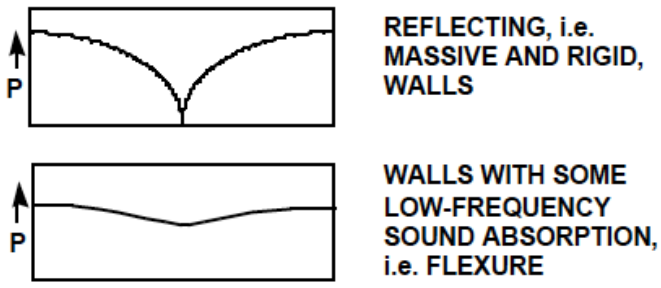

Figure 4.37: An illustration of how room boundaries that have low frequency absorption, *i.e* flexure, can improve the uniformity of sound distribution at the modal frequencies. After [45].

tions that get higher SPL. In the 160 Hz one-third octave band the SPL in the interpolation maps seems to have coloration in two points mainly. It is difficult to say if it is due to the modes coloration or to other phenomena. Indeed in order to recognize resonance in the 160 Hz one-third octave band, the 'resolution'of the maps should be higher, *i.e.* more positions are needed.

Finally the fourth configuration, as it was described in the section 4.3.2, stands out from the others because of the stiffening of the OSB panels. If the panels are described using a membrane approximation, hypothetical modes can born. It is possible that the resonance promotes the emission of sound, coupling with the loudspeakers. It is difficult to establish if it happens or not, but if it would, it could create unwanted and unpleasant coloration, that could alter the original sound. The main goal of this configuration was to reduce the radiation efficiency of the panels, σ. This is defined as the ratio of the radiated power to the power radiated by a large baffled piston ($ka \ll 1$ where a is the piston radius) with a uniform mean-square velocity equal to the temporal and spatial average of the square velocity of the plate:

$$\sigma = \frac{W}{S\rho_0 c\langle v^2\rangle_{t,s}} \tag{4.5}$$

where W is the radiated sound power, and S is the surface area of the plate [21]. Hence reducing S, uncoupling the OSB panels, the σ is reduced. In fact the extra OSB strings have the goal to 'interrupt'the modes, nullifying the hypothesis of uniform and negligible thickness.

Furthermore in order to avoid that the cavities besides the panels generate resonance, every cavity was filled with approximately 1 m^2 of polyester scraps. It is very difficult to deeply understand which installation produce the specific effect on the interpolation maps. It is possible to state that in the 100 Hz one-third octave band the modes are more clear as well as the loudspeaker directivity. Furthermore there is image centralization that is visible also in the maps 4.40. One possible explanation could be that the stiffening of the panel inhibits the lateral panel radiation that modifies the wavefront.

The purpose of the maps in figure 4.40 is to show clearly the difference between the 3rd and the 4th configuration.

4.5 Directivity of the source

Not only the listening room, but also the loudspeakers are a dominant factor in a multichannel sound system. Together, they influence timbre, dynamic range, and directional and spatial effects - in other words almost everything that matters to critical listeners [45]. In order to determine the directivity of the loudspeakers, measurements were performed with a two microphone intensity probe.

A pink noise was fed into the loudspeaker. The room equipement consisted of:

- Dynaudio acoustic BM15 With 10 inches woofer;
- 50GI-R Sound intensity probe;
- 01 dB sound intensity analyzer with two channel input;
- PCs providing the pink noise and performing the cross-correlation with a 01dB software elements;
- 10 m mono channel cable

To cover the frequency range of interest (50 Hz-3150 Hz), the 50 mm spacer was chosen.

The measured temperature and umidity were 22.4 $^{\circ}C$ and 54.9% RH. In order to make the measurement repeatable, the loudspeakers

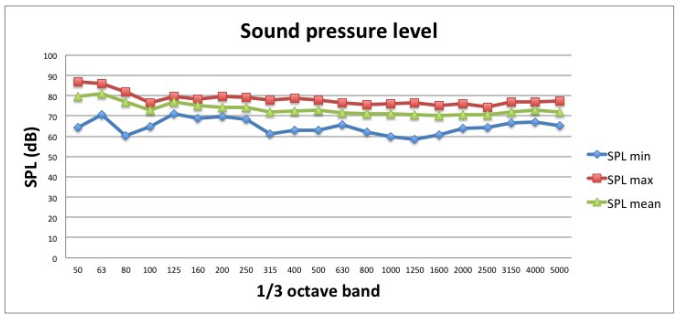

Figure 4.38: Trend of the parameter SPL as function of one-third octave bands; mean values, maximum, minimum. The case study configuration is the fourth.

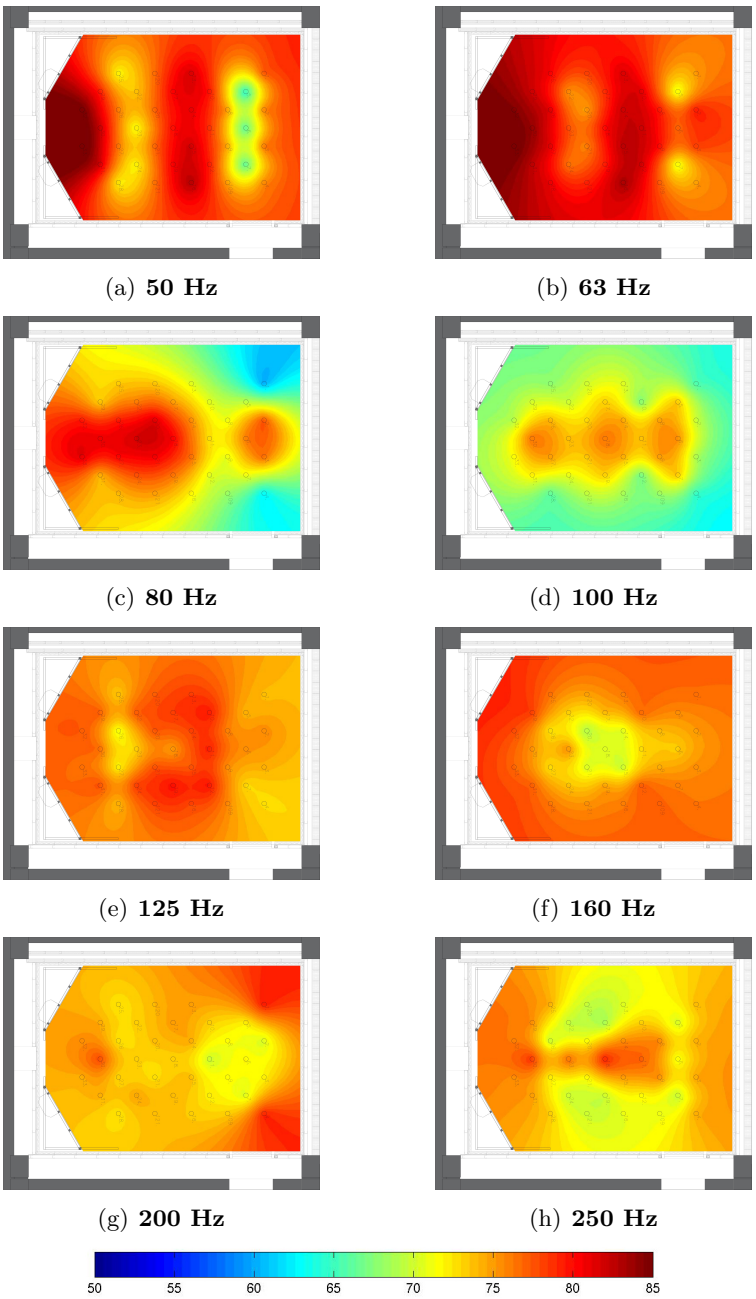

(a) **50 Hz** (b) **63 Hz**

(c) **80 Hz** (d) **100 Hz**

(e) **125 Hz** (f) **160 Hz**

(g) **200 Hz** (h) **250 Hz**

Figure 4.39: Interpolation maps of sound pressure level. Fourth configuration.

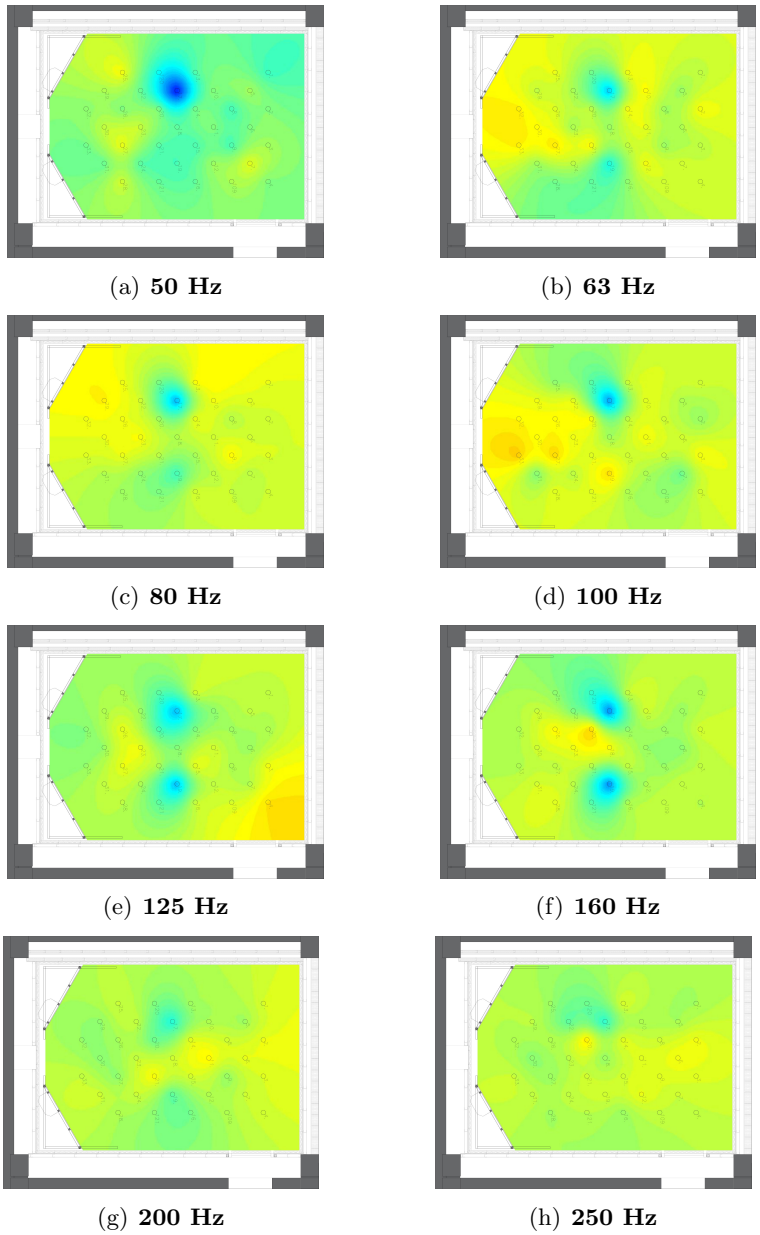

(a) **50 Hz** (b) **63 Hz**

(c) **80 Hz** (d) **100 Hz**

(e) **125 Hz** (f) **160 Hz**

(g) **200 Hz** (h) **250 Hz**

Figure 4.40: Interpolation maps of SPL difference between the third configuration and the fourth configuration.

Figure 4.41: The 50GI-R Sound intensity probe [19].

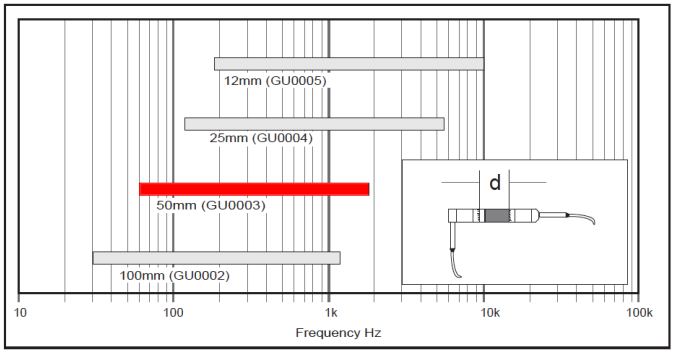

Figure 4.42: Frequency ranges coverd by the various spacer lengths.

were calibrated, measuring the A-weighted sound level in the listening position, at the height of 1.2 m. It was measured for each loudspeaker 85 dBA, whereas both loudspeakers measure 88 dBA.

The *discrete points technique* was used as described in the international standard ISO 9614 part 1 [52]. It requires that the choice of the positions and of the shapes be done avoiding to take measurements on reflective or absorptive surfaces. Since it was more practical, and in order to avoid time wasting, the final shape choice was a cube. In order to get only the information that are useful, during the measurements the source was already placed in the frame with the OSB panels. The mean distance between the measurement surface and the source surface is 0,5 m, as it is required in ISO 9614 part 1 [52]. The chosen surface includes also not absorbing parts, *i.e.* the pavement surface in quartz hardened (with an absorptive coefficient value in diffuse field less than 0,06).

The source that is to be measured is the Dynaudio acoustic BM15 With 10" inches woofer. In order to avoid errors and have a feedback about the measurement, a prevision of the directivity should be made. The tweeter in this loudspeaker is not centered in the same woofer axis. That means that the directivity of one loudspeaker should not be perfectly symmetrical in every frequency band.

Unfortunately, because of the reflective panel installation, it is possible to measure only half part of the loudspeaker directivity, indeed half part of the measurement shape includes absorptive material, so measurements were taken as shown in the figure 4.44. The surface has to be discretized, having at least one position for square meter and at least 10 position in total. 28 position were chosen for each loudspeaker, using a squared mesh 0.25x0.25 (see figure 4.44). Worth mentioning that two microphone stands were used, especially for the points at lower heights, and the measurements were performed aligning the central point between the two microphone on the 50GI-R (see fig. 4.43).

The most important part of the sound intensity measurement procedures is the calibration. Two types of calibration have to be performed: pressure calibration of the microphones and phase calibration

Figure 4.43: Picture of the sound intensity measurement, during the placing of the 50GI-R (left picture) and during the data acquisition with $dBfFA^{©}$ (left picture).

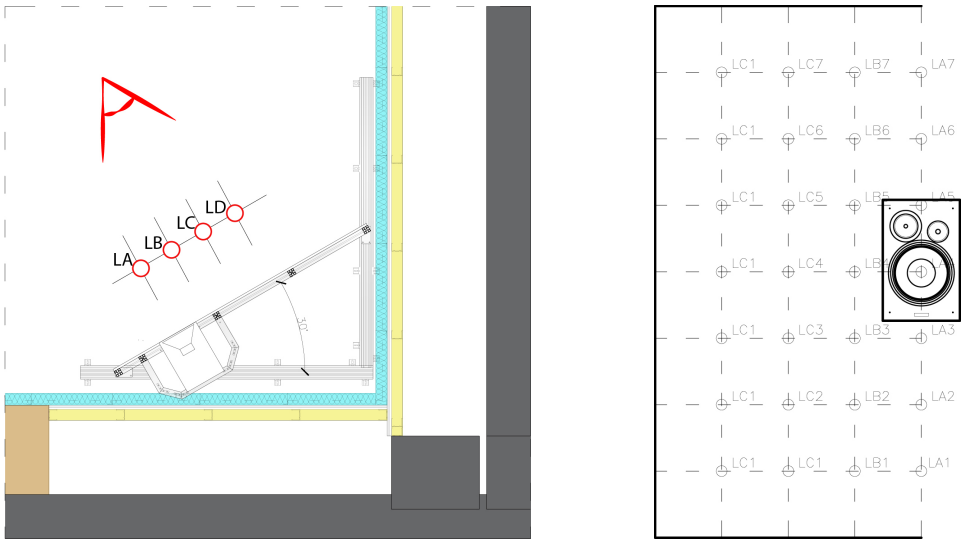

Figure 4.44: Frontal picture of the mesh for the Sound Intensity interpolation maps. Plan with the measurement position.

of the sound intensity probe. The first one is the same of the classic microphone calibration. The phase calibration of the sound intensity probe is the least one. It was performed using dBSOND32© software package that create a phase correction datafile.

4.5.1 Results

Accurate sound reproduction from a loudspeaker is largely dependent on the absence of linear (frequency and phase) response and non-linear (harmonic and intermodulation) distortions, and on maintaining a constant directivity across the frequency range. In a reflection-free environment, directivity would be unimportant, as one would listen to the sound radiated along a single axis, preferably the best one. In real rooms, sounds radiated in most directions from loudspeakers eventually reach the listeners. The directional properties of the loudspeaker, the physical arrangement and the acoustical properties of the listening room determine the spectrum, amplitude, directional and temporal factors of the multitude of sounds arriving at listeners' ears. All of these sounds combine and interact physically, at the entrance to the ears, and perceptually, in the auditory systems and brains of listeners. As a result, virtually every perceptual aspect of stereo reproduction can be affected.

It is a good idea to strive for constant directivity over most of the frequency range, indeed the directivity contains a lot of information. As it is clear from the figure **??**, as sounds increase in frequency (go up in pitch), the higher intensity levels are more concentrated.

Therefore, in order to maintain a uniform dispersion of the sound, the loudspeaker designers progressively reduce the size of the radiating diaphragms as we go up in frequency. How many different sizes of transducers are used in a loudspeaker system is, in part, determined by the requirement for constant directivity. Every transducer becomes progressively more directional, favoring the forward direction as it goes up in frequency.

As it was written above, the low-frequencies have a more omnidirectional directivity, as it is possible to see in figure **??** . Furthermore the higher intensity levels are measured in the woofer area up to the

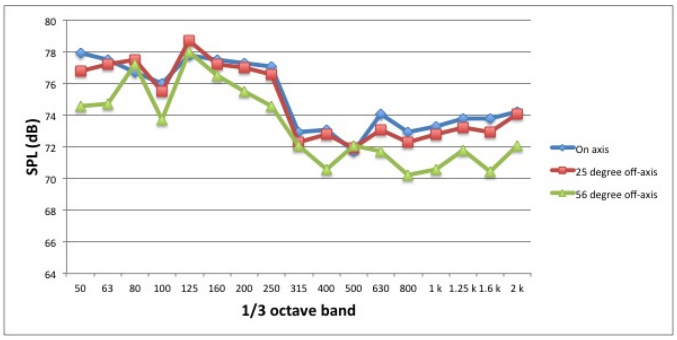

Figure 4.45: Frequency response measurements of a loudspeaker showing (top to bottom) a very smooth and flat on-axis response, and increasingly non-flat behavior at increasing angles off axis.

250 Hz one-third octave band. At 350 Hz one-third octave band, the directivity pattern shows a discontinuity losing density, being more dense in the loudspeaker adjacent zone.

The discontinuity in directivity is what causes the off-axis problems seen in Figure **??**, that shows some measurements, indicating that the design of the directivity for this loudspeaker system was focused on the on-axis performance. In this, it is very smooth and flat, nontheless there is a discontinuty in the flatness at 315 Hz, but the flatness get worse off-axis. In some frequencies the pavement influence is clear. Worth mentioning that at low frequencies it is the room that dominates, but at middle and high frequencies, it is the loudspeaker itself, its frequency response and directivity that dominate sound quality. Indeed in the 2000 Hz one-third octave band the directivity pattern is more concentrated in the zone very near tweeter.

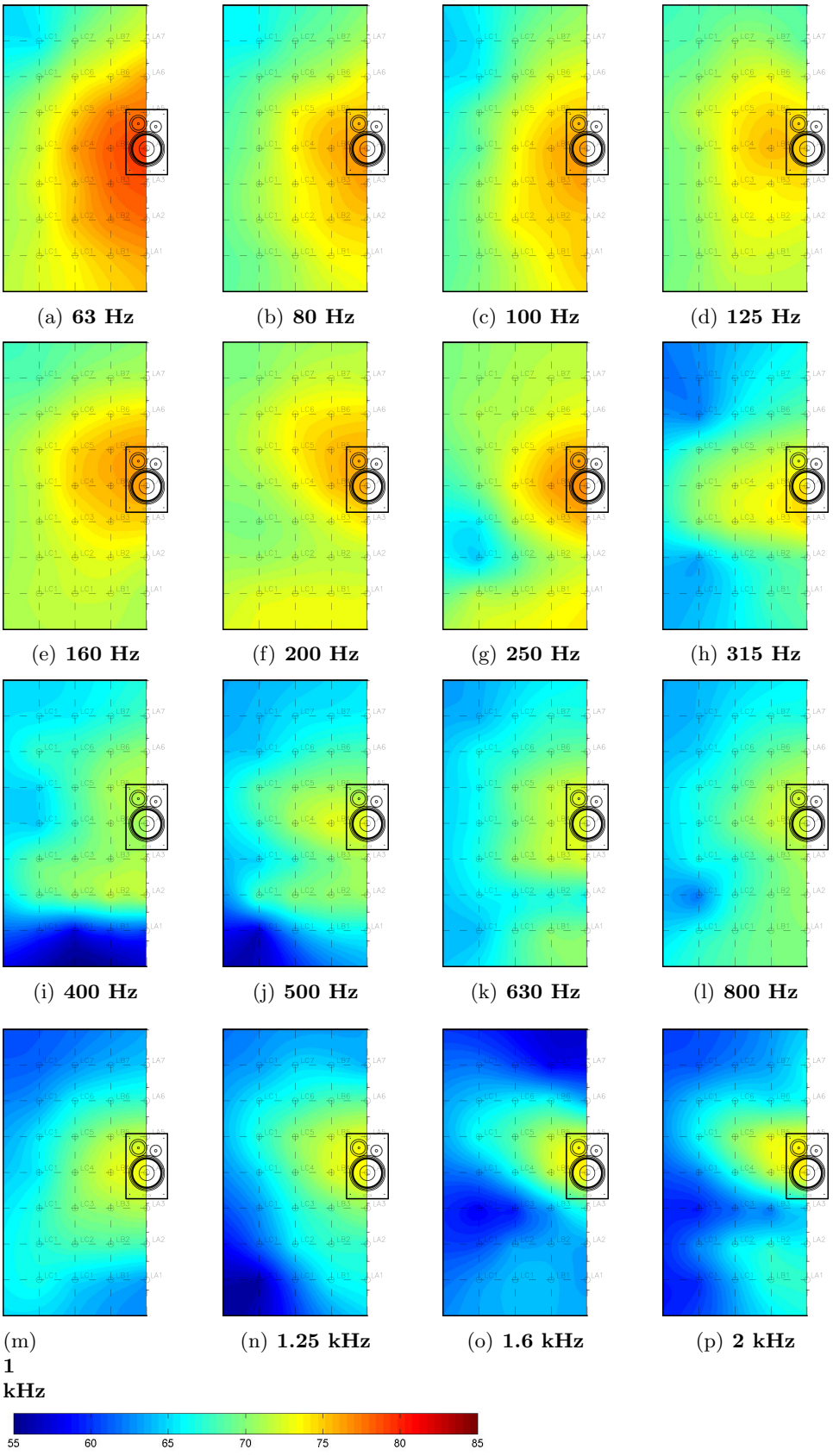

(a) **63 Hz** (b) **80 Hz** (c) **100 Hz** (d) **125 Hz**

(e) **160 Hz** (f) **200 Hz** (g) **250 Hz** (h) **315 Hz**

(i) **400 Hz** (j) **500 Hz** (k) **630 Hz** (l) **800 Hz**

(m) **1 kHz** (n) **1.25 kHz** (o) **1.6 kHz** (p) **2 kHz**

Figure 4.46: Interpolation maps of sound intensity levels. The measurement surface it is 0.5 m toward the Dynaudio BM15 plane.

Chapter 5

Final consideration and conclusion

The present study concerns the design and the acoustic characterization of a new listening room. Designed and then built in a space placed inside the CIRI laboratories. The main goal of the room is to perform acoustic measurement, auralization, psichoacoustic subjective tests and in addition it could be used as recording studio.

Seeking to understand how to procede in the the acoustic validation and design process, the earlier step was to fit to the technical recommendations ITU-R BS 1116-1 and EBU/UER Tech. doc. 3276, which provides guidelines to satisfy the requirements that a listening room should have in order to perform subjective measurements. These recommendation requirements are divided in two typologies: room ratio requisites and specifications based on *in situ* measurement.

The first one mentioned is supposed to ensure a reasonably uniform distribution of the low-frequency eigentones in the room. Among the copious theoretical methods elaborated over the last decades, the technical recommendation employs the Walker theory elaborated in 1993. Other authors have suggested techniques for the assessment of room modes and methods for predicting the low frequency response of rooms based on the distributions of room modes. The most notably criteria developed were proposed by Bolt [6] and Bonello [7]. So these were also applied to the case study room in the earlier steps. While on one side

the Bonello's criteria shows a satisfactory distributions of room modes and the ITU 1116 required ratio range results fullified, on the other the room ratios do not fit in the Bolt's blob. It is important to say that all these criteria make too many assumptions being consequently not completely reliable: indeed the calculation assumes that the room is perfectly rectangular and with entirely flat and reflecting surfaces. Furthermore Bonello adopts another approximation: the modes are considered as equally important being axial, tangential or oblique. Finally, in practice the loudspeakers do not supply energy uniformly to all the existing modes like is assumed in all these theories. Aknowledging the deficiency of those result because of those assumptions, it was decided to process an iterative methodology that involves installation, *in situ* measurements and evaluation by comparison with the parameters recommended in the above mentioned standards.

Concerning the latter typology of requisites, *i.e.* those based on *in situ measurment*, first of all was made a measurement of the background noise in 3 critical positions in order to verify the insulation quality and the noise produced by the air conditioning system. This condition is very strict, as NR 10 curve has to be satisfied. It Resulted that, with the air conditioning system turned off, the background noise curve measured respected the NR 10 curve; therefore it is possible to assume that the insulation technology performance is satisfactory. Consequently it was not needed to apply new layers of material or modify the insulation technology.

Reverberation time (T) and sound pressure level (SPL) were the acoustic parameters involved in the iterative methodology. In this process each parameter has proven to be differently sensible to each changement and has played a different role in the design process. The iterative methodology consists of four steps and for each step an installation or a room variation has been implemented.

Regarding the reverberation time, monoaural impulse responses were aquired in 64 different positions using an appropriate grid. After post-processing the reverberation times were obtained, presented in interpolation maps and plots of the T mean value compared with the technical recommendation values. Then a study about the reverberance

perceveived in the listening positions was made, making a comparisons between the standard deviation and the so-called Just Noticeable Difference (JND).

The result shows that in small rooms, when the sound field is not diffused and standing wave or flutter echoes occur, it is very difficult to uniquely define the reverberation time. Nonetheless, when T assumes anomalous values it is possible to look at the impulse response to see if there are axial modes.

Using this methodology in this case study, flutter echoes can be seen in the first configuration and, in order to delete it, it was made the decision to treat the ceiling with porous absorber panels of CIRFIBER®. Worth mentioning that the choice of this material was the result of a study that evaluated the absorption coefficient through reverberant chamber measurement, following UNI-EN-ISO 354. The reverberation time results confirm that the absorptive treatment successfully deletes the flutter echoes .

An other problem that was detected is the high reverberation time in the 63 Hz octave band, meaning that the chosen fiber material is not effective at low frequencies. With the aim of decreasing the T it was decided to reduce the radiation efficiency uncoupling the reflective panel surface and the loudspeakers. So extra OSB rods were added in order to stiffen the panels. Although the mean T value at 63 Hz remained outside the technical standard recommended range, the results showed that this treatment was effective, because the reverberation time at 63 Hz decreased of 0,1 s. Furthermore the study of the just-noticeable difference (JND) in the listening position showed an improvement. Indeed the standard deviation of the listening area seemed to fit better in the JND range of the reverberation time of the listening position, i.e. the listening area was enough homogenous.

Concerning the sound pressure level, the measurement were performed in 33 positions, in one-third octave bands, in order to detect clearly the existence of axial modes. The goal was to find coloration due to room modes at low frequency, analyzing interpolation maps in order to study the low frequency, *i.e.* to find a correlation between the calculated modes and the real room behavior. On one hand SPL results

not very sensible to the placement of the absorbing material, differently from the reverberation time, on the other hand it is very sensible to the room modes. The results also show that analitically calculated room modes match the real behavior of the room delineated in the interpolation maps. Regarding the SPL changement in the fourth configuration, *i.e.* the stiffening of the reflective panels, it is very difficult to deeply understand the cause of the specific effect on the interpolation maps. Anyway it is possible to state that in the 100 Hz one-third octave band the modes are more clear as well as the loudspeaker directivity and there is image centralization.

In addition it is well known that inside a room, the high frequency response can be considered a function of loudspeaker performance and absorption, whereas the low frequency response is highly related to the room geometry and position of source and receiver. Therefore, in order to characterize completely the listening room, the loudspeaker system was studied and sound intensity measurements were performed. The discrete points technique was used to find the directivity pattern, as described in the international standard ISO 9614 part 1. As sounds increase in frequency (go up in pitch), the higher intensity levels are more concentrated. Furthermore the higher intensity levels are measured in the woofer area up to the 250 Hz one-third octave band. In the 350 Hz one-third octave band the directivity pattern shows a discontinuity losing density, being more dense in the loudspeaker adjacent zone.

In conclusion, this iterative methodology can be considered a succesfull approach: although the reverberation time does not completely fit in the ITU 1116 range, the room results compatible with the strict requirement about noise criteria. Furthermore every phase of this iterative process has produced an improvement in the acoustic parameters. Concerning the future development, is suggested to make Schroeder 3-D diffusers built with reflective material. This would allow to reach the recommended reverberation time range in the mid-frequency and in addition it would improve sound diffusion.

Bibliography

[1] 01dB, *Sound Power determination according to ISO 9614 standard(dBFA32)*, 2001.

[2] ANSI S1-12-1992 *Engineering methods for the determination of sound power levels of noise sources, using sound intensity*, New York, American national standard institute (2002).

[3] Ballou, G.M., *Handbook for sound engineers*, Elsevier, Oxford, 2008.

[4] Beranek, L.L., *Acoustics*, Massachussetts Institute of Technology, 1992

[5] Beranek, L.L., Blazier, W.E., Figwer, J.J., "Preferred noise criterion (PNC) curves and their application to rooms", *J. Acoust. Soc. Am.*, **50**(5), (July 1971).

[6] Bolt, R.H., "Note on Normal Frequency Statistics for Rectangular Rooms", *J. Acoust. Soc. Am.*, **18**(1), 130-133, (May 1946).

[7] Bonello, O.J., "A New Criterion for the Distribution of Normal Room Modes", *J. Audio Eng. Soc.*, **29**(9), 597 606, (September 1981).

[8] Bourke, P.D., "A Contouring Subroutine", *Byte*, **12**(6), 134-150, (June 1987).

[9] Bruel&Kjaer, *Sound Intensity*, 2006, http://www.bksv.com/doc/br0476.pdf

[10] CEI IEC 1045-2-1, *Fixed film resistor networks for use in electronic equipment*, Geneva, International Electrotechnical Commission (1991).

[11] Cox, T.,D'Antonio, P., Avis, M.R., "Room Sizing and Optimization at Low Frequencies", *J. Audio Eng. Soc.*, **52**(6), 640-651, (June 2004).

[12] Draft technical reccomandation N12-A, *Sound control and listening room*,Nordic public Broadcasting corporation, Copenhagen, International Organization for Standardization (1992).

[13] Everest, A., *Master handbook of acoustic*, McGraw-Hill, 1994.

[14] EBU/UER Technical document 3276, *Listening conditions for the assessment of sound program material: monophonic and two channel stereophonic*, Geneva, European broadcasting union (1999).

[15] Fahy, F., *Foundation of Engineering Acoustic*, Academic Press, 2001.

[16] Fazenda, B.,Holland, K.R., Newell, P.R., Castro S.V., "Modulation transfer function as a measure of room low-frequency performace", *IOA Proceedings*, **28**(8), 187-194, (June 2006).

[17] Fazenda, B.M., Davies, W. J., "Views of Control Room Users", *IOA Proceedings*, **23**(8), 1-8, (March 2001).

[18] Garai, M., *L'acustica degli ambienti chiusi*, 2013, http://acustica.ing.unibo.it/aai/21%20Acustica%20Ambienti%20Chiusi.pdf.

[19] G.R.A.S. Sound and Vibration *Instruction Manual:50GI-R Sound Intensity Probe*, 2013, www.gras.dk.

[20] Guidorzi, P., and Barbaresi, L.,and Garai, M. , "La Misura dellAssorbimento Acustico con Diverse Metodologie: Camera Riverberante, Metodi impulsivi e tubo a onde stazionarie), 34o Convegno Naz. AIA, (June 2007).

[21] Hopkins, C., *Sound insulation*, Elsevier, 2007.

[22] Howard, D.M., Angus, J.A.S., Angus, J., *Acoustics and Psychoacoustics*, Taylor & Francis, 2001.

[23] Hunt, F. V., Beranek, L.L., Maa, D.Y., "Analysis of Sound Decay in Rectangular Rooms", , *J. Acoust. Soc. Am.*, **80**(11), 514-517, (June 1939).

[24] ISO 140:1995(E), *Acoustic-Measurement of sound insulation in building and of building elements*, Geneva, International Organization for Standardization (1995).

[25] ISO 9568:1993, *Cinematography - Background acoustic noise levels in theatres, review rooms and dubbing rooms*, Geneva, International Organization for Standardization (1993).

[26] ITU-R BS 1116-1,*Methods for the subjective assessment of Small Impairments in Audio System including Multichannel Sound Systems*, Geneva, International Telecommunication Union (1997).

[27] Knudsen, V., Harris, C., *Acoustical designing in architecture*, American institute of phisics, 1950.

[28] Kuttruff, H., *Room acoustics*, Spoon press, 1991.

[29] Kuttruff, H., *Room acoustics*, Elsevire, 2000.

[30] Louden, M.M., "Dimension-ratios of rectangular rooms with good distribution of eigentones", *Acustica*, **24**(1), 101104, (February 1971)

[31] Millington, G., "A Modified Formula for Reverberation", *J. Acoust. Soc. Amer.*, textbf4(3), 69-82 (June1932)

[32] Morse, P.M., *Vibration and sound*, Mc Graw-Hill, 1948.

[33] Newell, P., *Recording studio design*, Elsevier, 2012.

[34] Olson, H. F., "Field-Type Acoustic Wattmeter", *J. Audio Eng. Soc.*, **22**(5), 321-327, (June 1974).

[35] Olson, H. F., *Music, Physics and Engineering*, Dover publication, 1967.

[36] Prodi, N., Pompoli, F., Pompoli, R., Fausti, P., Bonfiglio, P., Farnetani, A., Fabbri, U., "Caratterizzazione acustica della nuova camera anecoica dell'universitá di Ferrara", *A.I.A. 35°convegno nazionale*, (June 2008).

[37] Sabine, W.C., *Collected papers on acoustics*, Peninsula publishing, 1992.

[38] Schröder, M., "Die statistischen Parameter der Frequenzkurven von groβen Rumen", *Acustica*, **4**(2), 594-600, (January 1954).

[39] Sette, W. H., "A New Reverberation Time Formula", *J. Acoust. Soc. Amer.*, **4**(5), 193-210, (June 1933).

[40] Smirnov, A., *Room sizes compliance with international standards and recommendations*, 2010, http://www.acoustic.ua/forms/rr.en.html

[41] Stephenson, M., *Assessing the Quality of Low Frequency Audio Reproduction in Critical Listening Spaces*, phD Thesys, University of Salford, 2012.

[42] Spagnolo, R., *Manuale di acustica applicata*, De AgostiniScuola, 2008.

[43] Toole, F. E., "Maximizing loudspeaker performance in rooms - Part 1- Why Loudspeakers Sound the Way They Do", *Harman International Industries*, 1-28, (January 2006).

[44] Toole, F. E., "Loudspeakers and Rooms for Sound Reproduction A Scientific Review", *J. Audio Eng. Soc.*, **54**(6), 451-457, (June 2006).

[45] Toole, F. E., "Loudspeakers and Rooms working together", *Infinity*, 1-17, (1997).

[46] Trendelenburg, F., *Einfurung in die akustik*, Springer-Verlag, 1961.

[47] UNI 9177:2008, *Reaction to fire - Combustible products classification*, Geneva, International Organization for Standardization (2008).

[48] UNI EN ISO 10534-2, *Acoustics - Determination of sound absorption coefficient and impedence in impedence tubes*, Geneva, International Organization for Standardization (1998).

[49] UNI ISO 1996-1:2010, *Acoustics - Description, measurement and assessment of environmental noise Basic quantities and assessment procedures*, Geneva, International Organization for Standardization (2010).

[50] UNI EN ISO 3382-1, *Acoustics - Measurement of room acoustic parameters- Part 1: Performance spaces*, Geneva, International Organization for Standardization (2009).

[51] UNI EN ISO 354:2003, *Acoustics - Measurement of sound absorption in a reverberation room*, Geneva, International Organization for Standardization (2003).

[52] UNI EN ISO 9614-1:2009, *Acoustics - Determination of sound power levels of noise sources using sound intensity - Part 1: Measurement at discrete points.*, Geneva, International Organization for Standardization (2009).

[53] Van Munster, B.J.P.M, *Beyond Control: Acoustic of sound recording control rooms- past, present and future*, Master thesis, Eindhoven University of Technology, 2003.

[54] Walker, R., "Optimum dimension ratios for studios control rooms and listening rooms" , *BBC Report*, 1-8, (August 1993).

[55] Walker, R., "Low frequencies room responses - Part 2 - Calculation methods and experimental results", *BBC Report*, 1-9, (August 1993).

Ringraziamenti

Desidero innanzitutto ringraziare il Professor Garai, per avermi dato l'opportunitá di poter compiere un percorso di crescita incredibile e di formazione nel mondo dell'acustica. Lo ringrazio inoltre per avermi sempre sostenuto in tutte le mie idee, compreso l'erasmus in Turchia. Ringrazio poi i miei correlatori che mi hanno assistito durante tutto il mio percorso, durato piú di un anno, in cui ho potuto imparare moltissimo. Li ringrazio per avere condiviso con me non solo le loro conoscenze e la loro incredibile competenza, ma anche loro amicizia. Ringrazio Dario per avermi per primo accolto nel laboratorio di via Terracini e per avermi contagiato con la sua passione per l'acustica e per la birre assieme; Luca, per avermi aiutato a preparare le catene di misure, per aver condiviso con me le sue conoscenze teoriche e pratiche (grazie per avermi insegnato che il trapano ha una frizione, il nome dei cavi e come funzionano gli altoparlanti) e per non esserti mai risparmiato nel darmi spiegazioni e per non avere mai perso la pazienza con me anche quando forse avresti dovuto. Grazie Simona per le interrogazioni che mi hanno insegnato tantissimo, per avermi saputo spronare e consigliare, non solo sulla tesi ma su ogni cosa, ti ringrazio per essermi stata dietro, avermi dato i compiti da consegnare, per i briefing e le pause sigarette. Infine per completare l'ufficio UL 10 ringrazio Lisa, per le chiacchiere, la disponibilitá e per essere stata compagna di tesi e poi dottoranda e per avere condiviso con me la passione, l'amicizia e parte di un percorso. Ringrazio infine Federica per aver avuto la pazienza di rileggere la tesi (e ci vuole una gran pazienza), per essere stata disponibile al consiglio e per avermi aiutato con le misure sul tubo di Kundt. Scrivere questa tesi é stato come vivere per un anno

con una famiglia, la famiglia del Lazzaretto. Ringrazio quindi i tecnici Maurizio e Fabrizio, i professori, i dottorandi del piano di sopra, i miei compagni di tesi (e sono stati tanti) Elisa, Alessandra P., Stefania, Lidia, Alessandra T. e Davide e infine ringrazio la responsabile di questa grande famiglia, Stefania che ha saputo creare un ambiente ideale per la ricerca, se penso a posti come il Lazzaretto mi viene da pensare che nel campo della ricerca in Italia c'é ancora speranza.

Questo é la conclusione non solo di sei anni e mezzo incredibili, ma di un percorso che dura una vita e la dedica e i ringraziamenti vanno tutti ai miei genitori, che mi hanno dato appoggio incondizionato su tutto senza eccezioni. Vi ringrazio per avermi spinto a non mollare mai, per avermi trasmesso la vostra tenacia nei confronti della vita. Se penso ai vostri sacrifici per permettermi tutto questo mi sento davvero piccolo. Senza non sarebbe stato possibile e questa laurea é tanto vostra quanto mia. Grazie per essere stati sempre li dalla scelta piu banale come quella del vestito della laurea fino alle chiamate all'ambasciata turca per il permesso di soggiorno.

Sei anni e mezzo di ingegneria sono volati e se potessi tornare indietro li rifarei tutti da capo, perché ho avuto la fortuna di farli con gli amici migliori. Tra tutti ovviamente ringrazio Tommi, mio compagno di tutti i laboratori e mio migliore amico, senza di te non mi sarei laureato oggi e magari a luglio potrai dire la stessa cosa tu. Grazie per avermi aiutato in tutto e non esserti mai risparmiato, grazie per avere litigato con me senza mai risentimento ne rancore e per aver capito che anche se sono il piú matto di tutti alla fine, forse non sono cosí male. Grazie per avermi aiutato col tuo carattere a sconfiggere l'ansia per gli esami.

I momenti di studio e di divertimento non sarebbero stati gli stessi senza Giovanna e Francesca, le mie prime amiche di universitá, con cui condivido gioie e momenti meno belli. Grazie per il supporto, per avermi portato in Croazia e per non smettere mai di cercarmi anche se ormai siete delle donne in carriera e per esserci sempre.

Grazie a CANDY MOUNTAIN questo melting pot di gruppi che si é unito e mi tempesta di notifiche, grazie per avermi fatto sorridere e per non avermi fatto mai sentire solo e per essere cosí social.

Grazie a Giuva per avermi accolto per 6 mesi a casa sua, per essere stato compagno di studio e di festa incredibile #sangriaparty. Grazie a Paas, per la Croazia e perché anche se ci vediamo raramente non cambia mai nulla e siamo sempre amici #Parigiinpillole. Grazie ad andre, padrone di Los Angeles, miglior disegnatore di Candy mountain, ottimo padrone di casa e grande amico #pagliaagogo. Grazie a Salvatore per aver studiato con me mille esami#XD. Grazie a Ervis per essere un mastodonte e per avermi fatto battere il #recorddichistameglio. Grazie al capitano per le sue mazzanight invincibili #mazzanight. Grazie a Minu che ha studiato con me estimo e altri esami e per tutte le volte che mi dice #staisereno. Grazie a Charlie perché la tua forza di volontá é di ispirazione per tutti noi #mammacharlie. Grazie alla Chia per le notti edili di restauro, per i pomeriggi alla certosa, il caffé shackerato, le feste assieme e per i consigli sentimentali #iononmangio. Grazie alla Meggie per avere creato il primo embrione di Candy mountain e per aver condiviso anche lei con noi l'esperienza mistica di restauro #dormomasoloduеminuti. Grazie alla Shimi, grande compagna di avventure Milanesi e sulla riviera #Melissa. Nonostante siano arrivate alla fine in questo gruppo ringrazio altri due componenti nuovi. Prima Beatrice bomberona Scardovi, con cui ultimamente piú che mai sto condividendo questo periodo in cui le nostre vite stanno cambiando ma tocca pure fare la tesi #luglio2014. Poi c'é Sonia, new entry del gruppo, la mia poledancer preferita, dispensatrice di aforismi sulla vita, grazie per l'aiuto nell'introduzione, abstract e conclusioni e per essere stata un grande appoggio nella volata finale #esclusiva.

Grazie a quel collage di persone che é stato via dei mille, 11 come una squadra di calcio. Tra tutti, grazie a Bingo, che anche se mi rubava le merendine, gli voglio sempre un gran bene e grazie Tiarossi per esserci sempre quando torno a Cesena da figliolprodico.

Grazie alla Turchia, per avermi insegnato tanto, non solo di universitá ma anche sull'importanza della libertá. Grazie a Koen e Dennis per avermi insegnato l'inglese e avermi sempre incluso nel gruppo dei Theguys, grazie a Lukas per quel matto viaggio assieme in giro per la Turchia e per avermi insegnato con che atteggiamento bisogna affrontare i drammi della vita. Grazie a Ozge per avermifatto da tradut-

trice nella mia epopea alla stazione di polizia turca.

Grazie a tutti quelli che non ho citato, troppi, che hanno attraversato anche solo per un momento la mia vita e ci hanno portato qualcosa di buono.